Bernhard Berg, BSc

Design and Synthesis of Transition-State based Inhibitors of DPP3

MASTER'S THESIS

to achieve the university degree of

Diplom-Ingenieur (Dipl. Ing.)

Master's degree program: Technical Chemistry

submitted to

Graz University of Technology

Supervisor

Univ.-Prof. Dipl.-Ing. Dr.rer.nat. Rolf Breinbauer

Institute of Organic Chemistry

Graz, July 2017

AFFIDAVIT

I declare that I have authored this thesis independently, that I have not used other than the declared sources/resources, and that I have explicitly indicated all material which has been quoted either literally or by content from the sources used. The text document uploaded to TUGRAZonline is identical to the present master‘s thesis.

Date

Signature

The following thesis was completed under supervision of Univ. Prof. Dipl.-Ing. Dr. rer. nat. Rolf Breinbauer between September 2016 and July 2017 at the Institute of Organic Chemistry at the Graz University of Technology.

Meiner Familie

"Auch eine Enttäuschung, wenn sie nur gründlich und endgültig ist, bedeutet einen Schritt vorwärts, und die mit der Resignation verbundenen Opfer würden reichlich aufgewogen werden durch den Gewinn an Schätzen neuer Erkenntnis."

Max Planck

Table of contents

Abstract **1**
Kurzfassung **2**
1 Introduction **3**
2 Theoretical background **6**
2.1 Metalloproteases 6
2.1.1 Dipeptidyl-peptidase 3 (DPP3) 7
2.1.2 Substrate binding mode and catalytic mechanism 8
2.1.3 Inhibitors of DPP3 9
2.2 Transition-state analogue concept of enzyme inhibition 10
2.2.1 Design of angiotensin-converting enzyme (ACE) inhibitors 11
2.2.2 Synthesis of α-aminophosphonic acids and α aminophosphonates 12
2.2.3 Phosphonamidates as transition-state analogue inhibitors 14
3 Aims of this thesis **15**
4 Results and discussion **17**
4.1 Synthetic approach towards phosphonamidate Inhibitors of hDPP3 17
4.1.1 Asymmetric synthetic sequence towards (*R*)-α-aminophosphonic acid isostere 11 18
4.1.2 Synthesis of Cbz- and monoallyl phosphonate building blocks 20
4.1.3 Preparation of L-phenylalanine methylester 21
4.1.4 Initial phosphonamide coupling attempts 21
4.1.5 Synthesis of protected phenylalanine building blocks 22
4.1.6 Synthesis of functionalized phosphonamidate dipeptides 23
4.1.7 Attempt of selective TMSE-deprotection of dipeptide fragment 25
4.1.8 Synthesis of Boc-Phe-Pro-Trp-OMe tripeptide 26
4.1.9 Assembly of phosphonamidate tetrapeptide 27
4.2.0 Final deallylation of phosphonamidate dipeptide and tetrapeptide 27
5 Summary and outlook **29**
6 Experimental section **32**
6.1 General aspects 32
6.1.1 Solvents 33
6.1.2 Reagents 34
6.2 Analytical Methods and Instruments 34
6.2.1 Thin layer chromatography (TLC) 34

6.2.2 Flash chromatography 34
6.2.3 Gas chromatography with selective mass detection (GC-MS) 35
6.2.4 High performance liquid chromatography (HPLC) 35
6.2.4.1 Preparative High performance liquid chromatography (prep. HPLC) 36
6.2.5 Nuclear magnetic resonance spectroscopy (NMR) 37
6.2.6 Determination of the melting point 37
6.2.7 High resolution mass spectrometry (HRMS) 38
6.2.8 Specific optical rotation 38
6.3 Biological assay 39
6.3.1 Fluorescence-based inhibition assay 39
6.4 Experimental procedures and analytical data 40
6.4.1 Dimethyl (2*R*,3*R*)-2,3-dihydroxysuccinate (1) 40
6.4.2 Dimethyl (4*R*,5*R*)-2,2-dimethyl-1,3-dioxolane-4,5-dicarboxylate (2) 41
6.4.3 (*S*,*E*)-2-Methyl-*N*-(2-methylpropylidene)propane-2-sulfinamide (3) 42
6.4.4 ((4*R*,5*R*)-2,2-Dimethyl-1,3-dioxolane-4,5-diyl)bis(diphenylmethanol) (4) 43
6.4.5 (3a*R*,8a*R*)-2,2-Dimethyl-4,4,8,8-tetraphenyltetrahydro-[1,3]dioxolo[4,5-e][1,3,2]dioxaphosphepine 6-oxide (5) 45
6.4.6 (*S*)-1-Methoxy-1-oxo-3-phenylpropan-2-aminium hydrochloride (6) 47
6.4.7 (*S*)-2-(Trimethylsilyl)ethyl (tert-butoxycarbonyl)-L-phenylalaninate (7) 48
6.4.8 (*S*)-1-Oxo-3-phenyl-1-(2-(trimethylsilyl)ethoxy)propan-2-aminium hydrochloride (8) 49
6.4.9 (9*H*-Fluoren-9-yl)methyl (tert-butoxycarbonyl)-L-phenylalaninate (9) 50
6.4.10 (*S*)-*N*-((1*R*)-1-((3a*R*,8a*S*)-2,2-Dimethyl-6-oxido-4,4,8,8-tetraphenylpentahydro-[1,3]dioxolo[4,5-e][1,2]oxaphosphepin-6-yl)-2-methylpropyl)-2-methylpropane-2-sulfinamide (10) 52
6.4.11 (*R*)-1-Amino-2-methylpropyl)phosphonic acid (11) 54
6.4.12 (*R*)-(1-(((benzyloxy)carbonyl)amino)-2-methylpropyl)phosphonic acid (12) 55
6.4.13 Benzyl ((1*R*)-1-((allyloxy)(hydroxy)phosphoryl)-2-methylpropyl)carbamate (13) 57
6.4.14 Methyl ((allyloxy)((*R*)-1-(((benzyloxy)carbonyl)amino)-2-methylpropyl)phosphoryl)-L-phenylalaninate (14) 59
6.4.15 2-(Trimethylsilyl)ethyl ((allyloxy)((*R*)-1-(((benzyloxy)carbonyl)amino)-2-methylpropyl)phosphoryl)-L-phenylalaninate (15) 62
6.4.16 Methyl (tert-butoxycarbonyl)-L-phenylalanyl-L-prolyl-L-tryptophanate (16) 63
6.4.17 Methyl ((allyloxy)((*R*)-1-(((benzyloxy)carbonyl)amino)-2-methylpropyl)phosphoryl)-L-phenylalanyl-L-prolyl-L-tryptophanate (17) 65

6.4.18 *P*-((*R*)-1-(((benzyloxy)carbonyl)amino)-2-methylpropyl)-*N*-((*S*)-1-oxo-3-phenyl-1-(2-(trimethylsilyl)ethoxy)propan-2-yl)phosphonamidate diethylammonium (18) 67

7 References 69

8 Abbreviations 73

9 Danksagung 79

10 Appendix: NMR Spectra 80

Abstract

In this thesis novel phosphonamidate-based compounds as transition-state analogue inhibitors of endogenous DPP3 enzyme were synthesized and investigated. The DPP3 enzyme is a zinc-dependent metallopeptidase with the functionality to selectively cut dipeptide fragments from the *N*-termini of physiologically active peptides. DPP3 is thought to be involved in various physiological processes such as nociception, regulation of blood pressure, protein turnover and immune functions. A specific and potent inhibitor of DPP3 would be desired as a valuable tool to elucidate the exact function of the enzyme. Previously developed inhibitor molecules "HER" and "SHE" were used as lead structures and a synthetic route towards dipeptides and tetrapeptides, containing a phosphonamidate moiety was established. Selected compounds were tested in a fluorescence-based inhibition assay, however a desired inhibitory activity was not observed.

Kurzfassung

Im Zuge dieser Arbeit wurden neue Phosphonamidatverbindungen als Übergangszustand-analoge Inhibitoren des körpereigenen DPP3 Enzyms synthetisiert und untersucht. Das DPP3 Enzym ist eine Zink-abhängige Metallopeptidase, welche Dipeptide selektiv am *N*-Terminus von physiologisch relevanten Peptiden abspaltet. Forschungsergebnissen zufolge, scheint das DPP3 Enzym in einer Vielzahl von physiologischen Prozessen involviert zu sein, vor allem, Schmerzleitung, Regulierung des Blutdrucks, Proteinumsatz und immunologische Funktionen. Ein spezifischer und potenter Inhibitor des DPP3 Enzyms könnte als Werkzeug dienen, um die genaue Funktion des Enzyms aufzuklären. Die zuvor entwickelten DDP3 hemmenden Moleküle „HER“ und „SHE“ wurden als Leitstrukturen benutzt und eine Syntheseroute für Dipeptide und Tetrapeptide mit einer geschützten Phosphonamidat-gruppe wurde etabliert. Ausgewählte Verbindungen wurden in einem Fluoreszenz-basierenden Assay untersucht, allerdings konnte eine gewünschte Enzymhemmungsaktivität nicht beobachtet werden.

1 Introduction

One of the central subjects of Chemical Biology and Biochemistry is to understand the interactions of enzymes and their substrates in detail. Enzymes are an essential component to life, speeding up metabolic processes to sustain the host cell and enable cell division. Remarkably one quarter of genes in the human genome is dedicated to code enzymes exhibiting the importance of these almost exclusively protein-based molecular devices.[1] Enzymes catalyze reactions by decreasing the energy difference from substrate to transition state through stabilization of the latter. This difference in reaction time can be very extreme. The carbonic anhydrase enzyme for instance is capable to accelerate the hydration reaction of CO_2 10^7-fold compared to the uncatalyzed transformation.[1] The activity of an enzyme can be reduced or even completely halted when an inhibitor is bound to it. This can be used as an effective strategy to eradicate hostile cells in an organism or correct metabolic disparities and therefore, inhibitors of enzymes are often used as medicinal drugs. Furthermore, specific enzyme inhibition via small functionalized molecules can give interesting insights into the substrate binding mechanism of the enzyme as well as the involved functional residues of the substrate compound during the binding process.

Structure-based design of enzyme inhibitors is state of the art in nowadays drug development. This strategy builds upon the three-dimensional data of biological components relevant in diseases, such as enzyme-inhibitor structures, which have been characterized by X-ray crystallography or NMR-spectroscopy. With this data in hand the specific inhibitor binding mechanism and fragment affinities towards the binding pocket of the target enzyme can be predicted and combined with powerful synthetic methodology, such as protecting group strategy, catalytic reaction cascades and multi-step synthesis, the design and synthesis of novel bioactive molecules is feasible in a creative manner. Structure-based drug design can be divided into various subcategories. Virtual screening is an approach were comprehensive small molecule structure databases are mined for potential molecules, dock-able to an enzyme binding pocket. With the use of a scoring function rankings of the database compounds can be created. Another strategy is establishing the framework of a small molecule inhibitor stepwise inside a 3D-structure model of the receptor active site. The advantage of this method is that novel molecular fragments which were not thought about initially or are not present in structure databases, can be considered for further inhibitor design.[2,3,4]

The generation of non-nucleoside HIV-reverse transcriptase inhibitors for the treatment of HIV/AIDS at the pharmaceutical company Tibotec was accomplished by a structure-based approach. The electronic environment, the involved intermolecular interactions upon binding and the shape of the binding site of the target protein are important parameters which need to be determined, prior to ligand-design. The HIV-reverse transcriptase is necessary for the virus to translate its genomic RNA into double-stranded DNA, which then is transferred into the genome of the infected cell.[2] Without the activity of this enzyme the virus is not able to replicate itself and consequently this reverse-transcriptase poses a drug target. Non-nucleoside reverse transcriptase inhibitors act by a unique mechanism known as allosteric inhibition, where the inhibitor molecule binds to a lipophilic cavity site close to the polymerase active site of the enzyme resulting in conformational changes, which ultimately lead to the blockage of activity.[2]

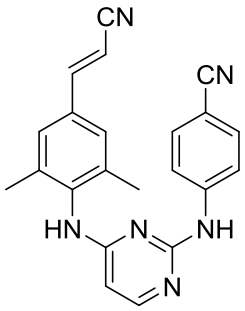

Rilpivirine

IC_{50} = 0.4 nM

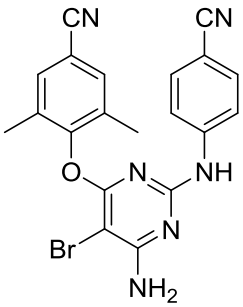

Etravirine

IC_{50} = 1.4 nM

Figure 1: Molecular structures of current non-nucleoside reverse-transcriptase inhibitors applied in HIV/AIDS treatment.[2]

The molecules depicted in Figure 1 show strong antiviral activities and were designed to be resistant to mutated HIV-1 strains due to their conformational flexibility and their ability to interact in binding to the amino acid residues in the binding pocket and even to their mutated deviations. Both compounds were approved by the FDA for medical treatment of AIDS.[2]

For many enzymes, their specific physiological role is not yet known and potent inhibitors as molecular tools could lead to the discovery of their function. The human dipeptidyl-peptidase III (hDPP3) enzyme, also known as enkephalinase B, is a zinc-dependent metallopeptidase capable of cleaving off dipeptides from oligopeptides at the *N*-terminus. The DPP3 enzyme is not only found in various human cells for instance kidney, brain, liver, and small intestine, but also in other mammals and insects such as the death's head cockroach, *B. craniifer*.[5]

Enkephalinase B is associated with the degradation of Leu-and Met-enkephalin, two opioid pentapeptides responsible for nociception control in the human body. Moreover hDPP3 could have a potential role in blood-pressure regulation, endogenous defence against oxidative stress and is strongly linked to certain forms of cancer, such as ovarian carcinoma.[5] This research suggests that the enzyme may be involved in a wide variety of physiological reactions, however the exact role of the enzyme is still unknown.[5]

In order to obtain further insight into the enzyme's specific purpose, a specific inhibitor molecule would be desired, which should be non-toxic, stable in the physiological environment, and selective for DPP3. This thesis will focus on the design and synthesis of novel phosphonamidate-based inhibitors for DPP3.

2 Theoretical background

2.1 Metalloproteases

The enzyme family of metalloproteases or metalloproteinases is involved in various physiological functions, such as regulation of immune cell development, cell migration, ligand-receptor interplay, and restructuring/degradation of the extracellular matrix (ECM). The zinc atom is used predominantly in various metalloproteases for peptide cleavage because of its Lewis acidity, fast ligand exchange, intermediate polarizability, and adaptable coordination geometry among other reasons. Zinc-dependent metalloproteases can be classified in groups, containing a specific catalytic motif. Examples are the metzincins, featuring a HEXXH+H motif with three histidine units coordinated to the zinc ion and the thermolysin group (HEXXH+E) consisting of two histidines and one glutamate residue.[8,9]

Matrix metalloproteinases (MMPs) and membrane-anchored disintegrin metalloproteinases (ADAMs) are found in microtissue environments and these enzymes are capable of amending membrane-bound or extracellular soluble proteins post-translationally to either enhance their delivery process or deactivating these proteins. As a result, the immunological processes are either initiated or shut down. In general enzymes fall into the category of MMPs if three conditions are fulfilled, namely their dependence on a zinc-ion binding motif to hydrolyze substrates, a cysteine switch located inside the pro-peptide domain, and if their sequence is homologous to matrix metalloproteinase 1 (MMP1).[8]

In terms of structure MMPs possess four main domains: the pro-peptide domain incorporating a cysteine-switch motif with approximately 80 amino acids and thereafter the catalytic domain containing the zinc-binding motif HEXXHXXGXXH with coordination to two distinct zinc ions, one purposed for catalytic processes and one structural zinc ion. This catalytic domain possesses a length of approximately 170 amino acids and is connected to a propeller-shaped haemopexin domain by a subunit linker region. Endogenous tissue inhibitors of metalloproteases (TIMPs) are composed of 184-194 amino acids and regulate the activity of MMPs through selective inhibition. Certain factors such as the interleukin-6 receptor and the tumor necrosis factor receptor are involved in inflammatory responses and their signaling transduction is controlled by MMPs and TIMPs. These unique features indicate an important function of metalloproteases in immune cell reactions.[8]

2.1.1 Dipeptidyl-peptidase 3 (DPP3)

The dipeptidyl peptidase 3 enzyme has been characterized as a zinc-dependent metallopeptidase with the function of removing dipeptide fragments of the *N*-terminus from biologically relevant oligopeptides in an iterative manner. The enzyme belongs to the M49 family, which is distinguished by a HEXXGH catalytic motif and exhibits a strong preference to split so called opioid peptides such as endomorphins and enkephalins, examples are depicted in Figure 2. These opioid peptides are a vital component of the endogenous opioid system alongside their associated opioid receptors and together they govern nociception, drug addiction, immune function, stress response, and reward mediating food-intake, among others.[5,7,10,11]

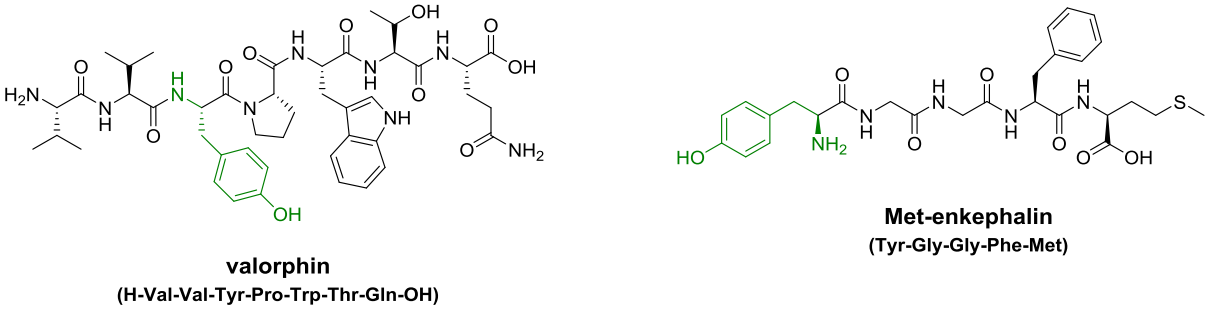

Figure 2: Structures of endomorphin compound valorphin and Met-enkephalin, which show binding affinity towards DPP3 enzyme (the green colored molecule fragment resembles the opiate core structure).[5,7,10,11]

Moreover, DPP3 has been associated with various mechanisms of cancer cells, with literature reports highlighting for instance overexpression in endometrial carcinoma and ovarian malignant tissues.[10] In squamous cell lung carcinoma it is reported that DPP3 induces competing interference with NF-E2-related Factor 2 (NRF2), which subsequently triggers uncontrolled transcriptional activation in these cells.[10]

Other research mentions the functionality of DPP3 in the process of protein turnover. In the cytosol compartment selected ubiquitinated proteins are broken down by cytosolic peptidases into smaller fragment peptides with variable amino acid lengths and DPP3 could play a potential role in degradation of peptides constituted by four to eight amino acids, due to matching substrate length and a non-specific catalytic behavior as suggested by Prajapati *et al.*[5]

The DPP3 enzyme was found expressed in different anatomical regions in mammals such as the spinal cord, liver, brain, erythrocytes, and skin tissue. It was also detected in the human central proteome, alongside a vast number of different ubiquitous proteins. This broad distribution over various cell types and the ability to dock and cleave a wide spectrum of

peptides, contribute to the assumption that DPP3 is involved in not one but many different physiological processes in the host cell.[10]

2.1.2 Substrate binding mode and catalytic mechanism

The crystal structure of hDPP3 reveals two lobe-shaped domains which are divided by a large cleft (Figure 3).[7,10]

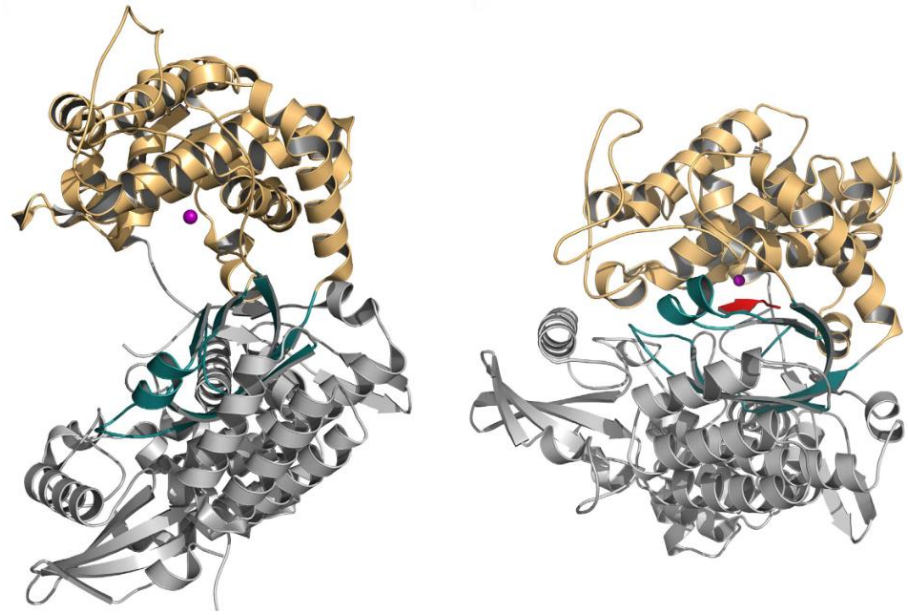

Figure 3: Structural representation of hDPP3 in the open conformation (left) and closed conformation (right). The catalytic zinc ion is depicted as a magenta sphere, the upper lobe is presented in orange, the five-stranded β-core in teal and the lower lobe in grey. The red arrow depicts a bound peptide. Figure taken from Kumar *et al*.[10]

The zinc binding site is located in the α-helical upper domain and is composed of one glutamate (Glu-508), two histidine (His-455 and His-450) residues, and a water molecule. These four units are forming a tetrahedral coordination sphere to the zinc ion. The lower lobe is assembled by a central five-stranded β-barrel unit as well as mixed α- and β-folds and is linked to the upper lobe by flexible loop regions. An additional glutamate (Glu-451) unit is positioned in close proximity to the catalytic active site of the enzyme and up to now two distinct mechanisms of substrate activation are proposed depending on the substrate. In a water-promoted mechanism Glu-451 supposedly activates the water molecule by deprotonation and the resulting hydroxy anion species acts as a nucleophile and attacks the amide bond of the substrate. A tetrahedral transition state is formed, which is stabilized by intermolecular interaction of the His-568 residue and subsequently collapses and the disintegrated peptide bond fragments are produced (Scheme 1).[7,10]

Contrary to these findings, in the complex of hDPP3 with synthetic opioid pseudopeptide IVYPW, a water molecule was not found in the active site but rather a carbonyl group coordinating to the zinc ion. It is hypothesized that the Glu-451 residue is itself the nucleophile which attacks the peptide bond forming an anhydride like structure. Based upon the findings of Kumar *et al*. hDPP3 inhibitor peptides are likely processed via the anhydride mechanism where the water molecule is pushed out of the active site whereas in other substrates, such as Met- or Leu-enkephalin the water-promoted mechanism is prevailing.[7,10]

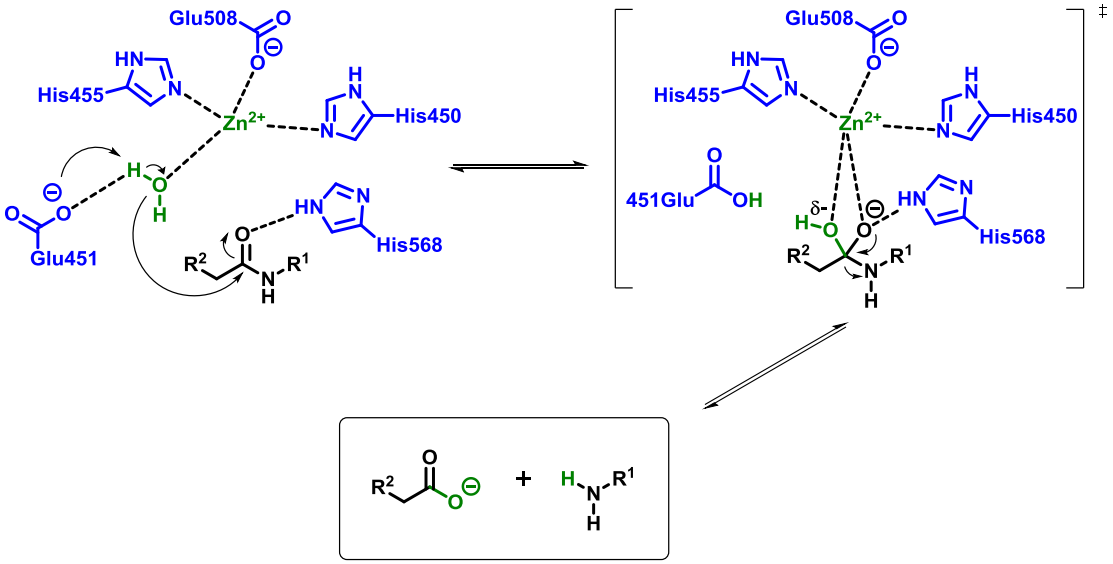

Scheme 1: Water-promoted mechanism of substrate hydrolysis in the catalytic active site of hDPP3.[10]

2.1.3 Inhibitors of DPP3

Various compounds achieve inhibition of the DPP3 enzyme, however most of them are either non-selective (metal chelating compounds, mercury derivatives), or are slowly degraded by the enzyme (tynorphin). Examples of DPP3 inhibitors are presented in Figure 4. Interestingly serine protease inhibitors such as 3,4-dichloroisocoumarin and the chemical weapon agent diisopropylfluorophosphate exhibited inhibitory activity against DPP3, although no serine residue has been shown to participate in substrate catalysis.[5,7]

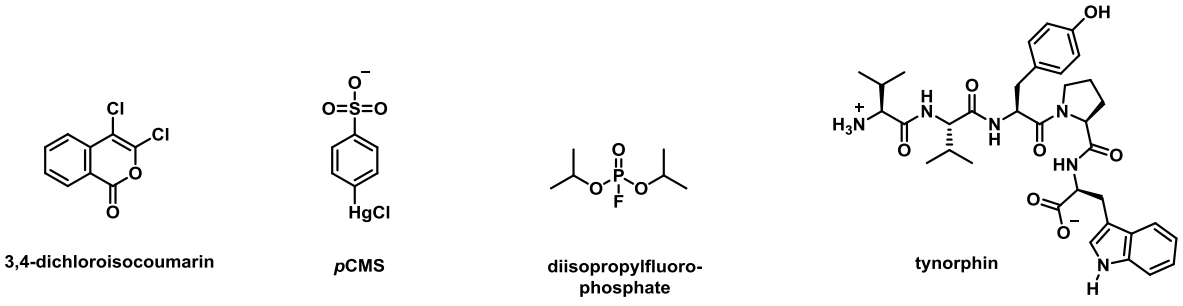

Figure 4: Selected DPP3 inhibitors.[5,7]

The opioid pentapeptide tynorphin was reported as a slowly converted substrate of DPP3, with a high affinity towards the enzyme and did not show as much potency versus other enkephalin degrading enzymes. The crystal structure of tynorphin in complex with DPP3 reveals formation of a β-strand by three amino acid moieties of the peptide which is bound to a five-stranded β-core of DPP3. Furthermore, the *C*-terminus of bound tynorphin is hypothesized to initiate a large domain motion of DPP3 upper and lower lobes, which positions the catalytically important zinc ion in close proximity to the carbonyl moiety of the amide bond. Tynorphin was chosen as a lead structure for inhibitor design by J. Ivković[12] and C. Lembacher-Fadum[13] due to these detailed interaction studies.[5,7,12,13]

2.2 Transition state analogue concept of enzyme inhibition

Chemical transformations from starting materials to the final products are proceeding through a high energy condition called the transition state. The transition state can be characterized as a structure with bonds halfway formed or broken displaying the movement of electrons from one atom to another. It is in such a critical high energy state, that external changes trigger a spontaneous collapse of the transition state and more stable products are formed. In 1948 Linus Pauling claimed that the immense reaction rate increase by enzymes is attributed to strong binding of the enzyme to the labile transition state. A method for examination of the transition state structure is to employ isotope-labelled substrates in an enzyme catalyzed reaction and subsequently compare the reactivity with a non-labelled natural substrate. This strategy is called the kinetic isotope effect approach, which measures the ratio of labeled ($k_{labeled}$) and unlabeled ($k_{unlabeled}$) reaction rates (Figure 5).[14,15]

$$KIE = \frac{k_{unlabeled}}{k_{labeled}}$$

Figure 5: Kinetic isotope effect.[14,15]

Exchange of isotopes in a substrate is advantageous since it represents a minimal modification of the molecule in contrast to exchanging functional groups. By monitoring the conversion of these labelled substrates via techniques such as NMR-spectroscopy the connection and disconnection of bonds during the reaction can be determined. Transition state analogue compounds are designed to resemble the transition state structure in order to bind tightly to the enzyme and thus block the binding site for future substrates. Sophisticated inhibitor design can be commenced with the knowledge of the precise transition state architecture as well as information about the catalytic residues in the binding pocket of the target enzyme.[14,15]

2.2.1 Design of angiotensin-converting enzyme (ACE) inhibitors

The treatment of hypertension, a medical condition with increased arterial blood pressure, became possible through the discovery of Captopril, the first specific inhibitor for the angiotensin-converting enzyme (ACE). Blood pressure regulation of the body is controlled by the renin-angiotensin-aldosterone system, where decreased blood pressures trigger renin protease production in the kidneys. Angiotensinogen is cut by renin, releasing the decapeptide angiotensin I, which is subsequently processed to the octapeptide angiotensin II by removal of a dipeptide from the *C*-terminus via ACE. Angiotensin II in turn is responsible for tightening of blood vessels (vasoconstriction) and the generation of the hormone aldosterone, which contributes also to an increase of blood pressure by increasing absorption of sodium ions in the kidney. ACE is also involved in the degradation of bradykinin, a peptide known for extending blood vessels, thus increasing blood pressure even further. Inhibiting the enzymatic functionality of ACE prevents the proteolytic cleavage of angiotensin I to angiotensin II and thus stops an increase in blood pressure.[2,16]

Before 2003 no crystal structure of ACE had been available, nevertheless the potent inhibitor Captopril was developed much earlier by David Cushman and Miguel Ondetti.[16] The catalytic mechanism of the ACE was thought to be similar to the carboxypeptidase A (both are zinc-depending enzymes), with the difference that ACE removes dipeptides and carboxypeptidase A cuts single amino acid fragments. Another important fruitful discovery was the isolation of peptides from the snake venom of *Bothrops jararaca*, which exhibited antihypertensive properties and inhibition towards ACE. The carboxypeptidase A enzyme structure had already been characterized by X-Ray crystallography and L-benzylsuccinic acid had been found to be a potent inhibitor of carboxypeptidase A presumably by mimicking the cleaved by-products of the enzyme. L-Benzylsuccinic acid was taken as a lead structure for the design of ACE inhibitors. By using a proline moiety, which has been identified in the snake venom peptides, the first template molecule **A** was created (Figure 6). The ethylene linker region of the **A** molecule (depicted in red) deemed crucial in hydrogen bonding interactions and an increase in inhibitory activity was observed by incrementing the region until a huge loss of activity was observed as seen by the IC_{50}-value in molecule **B**. The introduction of a (*R*)-configured methyl unit in α-position to the amide bond in compound **C**, as well as installing a more potent metal chelating thiol group in compound **D** could further enhance the binding affinity towards ACE. Finally, a combination of both moieties implemented in a single molecule, gave the compound **Captopril** which exhibits nanomolar inhibitory activity towards ACE.[2, 16, 17]

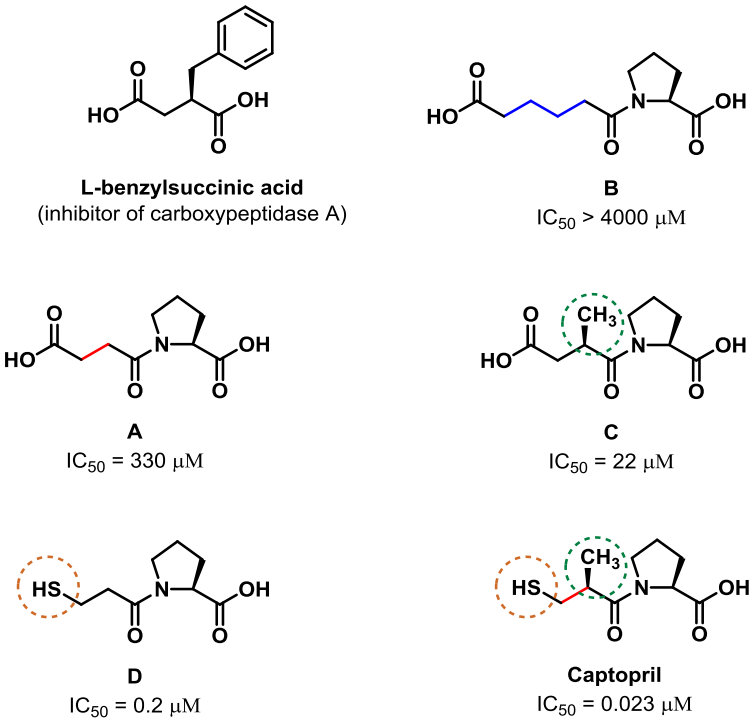

Figure 6: Selected lead-compound structures and the final designed thiol-containing Captopril inhibitor of ACE.[2,16,17]

2.2.2 Synthesis of α-aminophosphonic acids and α-aminophosphonates

α-Aminophosphonic acids and their derivatives are known for applications as enzyme inhibitors (HIV-protease, thermolysin, renin, tyrosine phosphatase), metal extraction in hydrometallurgy, anticancer-, antifungal-agents, and medical screening agents in complexed form with actinides and lanthanides. α-Aminophosphonic acids can be viewed as carboxylic acid isosteres, where the steric, tetrahedral phosphonic acid moiety mimics the transition state of proteolytic amide-bond cleavage by certain enzymes. The stereo configuration of α-carbon is reported to have an impact on the biological potency of these compounds. The PUDOVIK-reaction is a well-established method to generate α-aminophosphonic acids, which commences by nucleophilic attack of a phosphorous species at the electrophilic carbon of imines forming the C-P bond. Stereoselective versions of this reaction have been developed using chiral auxiliary groups attached to the imine or chiral *H*-phosphonate derivatives (Scheme 2).[18]

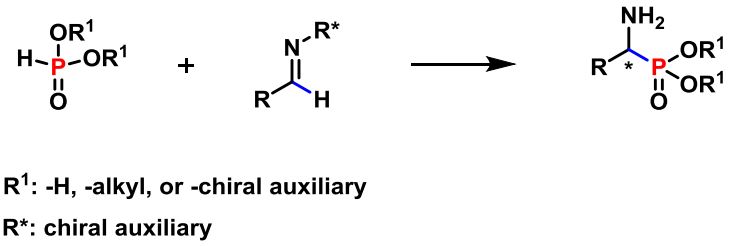

Scheme 2: General scheme of the Pudovik-reaction.[18]

In the publication of Vovk *et al*. reaction of sodium diethyl phosphite with (*S*)-functionalized imine derivatives **E** furnished α-aminophosphonates **F** in excellent 98 % yield and a diastereomeric excess of 95 %. Catalytic hydrogenation followed by TMSBr-mediated hydrolysis gave free α-functionalized aminophosphonic acid **G** (Scheme 3).[18,19]

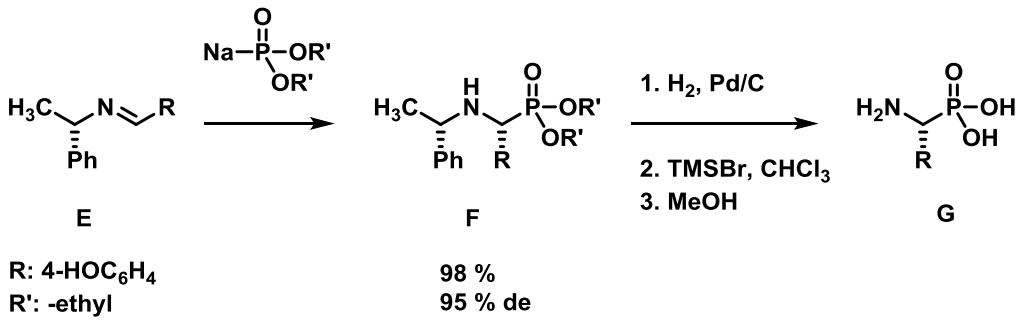

Scheme 3: Nucleophilic attack of sodium-phosphonate followed by catalytic hydrogenation towards α-aminophosphonates.[18,19]

This protocol was applied in the synthesis of porcine kidney alkaline phosphatase inhibitors, which contain a calix[4]arene moiety attached at α-aminophosphonic acids.[19] Another convenient approach towards α-aminophosphonates can be achieved by reaction of phosphites with amines and aldehydes or ketones in a three-component reaction also known as KABACHNIK-FIELDS reaction. Yu *et al*. demonstrated the feasibility of this reaction when using DABCO quaternary ammonium chloride salt as solvent and derivatized anilines, aromatic or heterocyclic aldehydes and triethyl phosphite as essential ingredients for the multicomponent reaction. The authors of this study suggest an initial imine formation, which is promoted by aldehyde activation via DABCO and subsequent nucleophilic attack of the aniline derivative. In the following step triethyl phosphite attacks the imine, forming a phosphonium intermediate, which is reacting with water to yield the corresponding α-aminophosphonates. The DABCO compound was recycled after the reaction and reported to be reused up to 7 times (Scheme 4).[20]

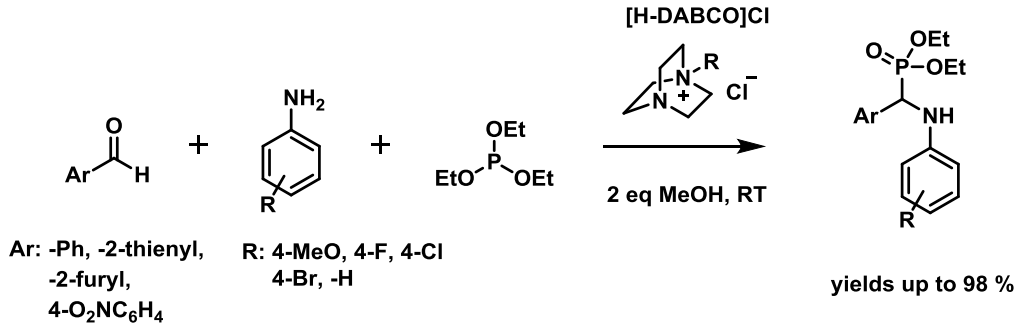

Scheme 4: One-pot three component Kabachnik-Fields reaction with [H-DABCO]Cl as described by Yu *et al*.[20]

2.2.3 Phosphonamidates as transition state analogue inhibitors

The application of phosphonamidate containing molecules as enzyme-inhibitors was demonstrated by compound phosphoramidon (Figure 7), which was found to be a competitive inhibitor of the zinc-dependent metalloprotease thermolysin. This enzyme is known for cleaving amide bonds of several hydrophobic amino acids incorporated in peptides, for instance phenylalanine, leucine, iso-leucine and valine.[2,21]

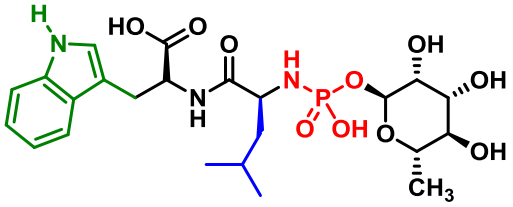

Figure 7: Structure of phosphoramidon, the tryptophan unit in green and the leucine moiety in blue are essential for binding affinity to the enzyme.[2,21]

Phosphoramidon displays a unique combination of a rhamnose entity connected to a central phosphonamidate functional group, which is linked to Leu-Trp dipeptide. The phosphoryl-leucyl-tryptophan fragment of the molecule was shown to be responsible for high affinity towards thermolysin, with the phosphonamidate group replacing the scissile peptide bond.[2,21]

A further example of a phosphorous-containing inhibitor is fosinopril developed against ACE. The molecule was derived from the potent captopril inhibitor by exchanging the thiol group with a phosphonamidate moiety, furnishing compound **H** as lead structure (Figure 8). Because of instability of the free phosphonamidate compound, esters and subsequently phosphinic acid derivatives were prepared and tested. The elongation of the distance between the phenyl group and the phosphinic moiety by four methylene units led to a desired interaction with the S_1 subsite of the enzyme (compound **I**). Final adjustments at the proline moiety by attachment of a lipophilic cyclohexyl fragment gave very potent fosinoprilate, which was further modified into the prodrug ester fosinopril.[2,22,23]

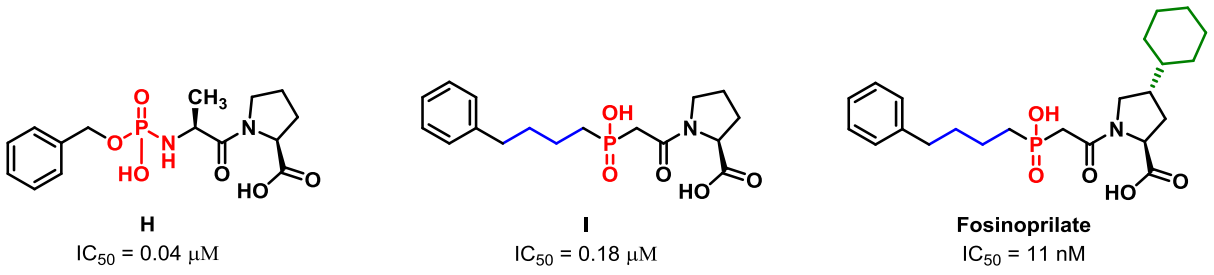

Figure 8: Phosphorous based ACE inhibitors, were optimized towards fosinoprilate.[2,22,23]

3 Aims of this thesis

Tynorphin, a presumed inhibitor for DPP3, was synthesized by Yamamoto *et al.* and a X-ray crystal structure of tynorphin in complex with hDPP 3 had been described by Bezerra *et al* featuring significant domain-motion upon binding. The binding mode itself was investigated by isothermal titration calorimetry (ITC) experiments with the result of an entropy-driven process assumed due to the release of water molecules from the binding cleft of the unbound enzyme.[7] However over time the molecule was slowly degraded by DPP3. Tynorphin consists of the amino acid sequence Val-Val-Tyr-Pro-Trp[7] and was used as a lead structure template by Jakov Ivković[12] and Christian Lembacher-Fadum[13] for the development of novel hydroxyethylene transition state mimetic compounds ***SHE***, (*S*)-hydroxyethylene pseudopeptide and ***HER*** (*R*)-hydroxyethylene pseudopeptide (Figure 9). Compared to the structure of tynorphin the amide bond between Val-Val had been replaced by a hydroxyethylene moiety with the intention that the enzyme is not able to dissociate the molecule at this specific position.[12,13]

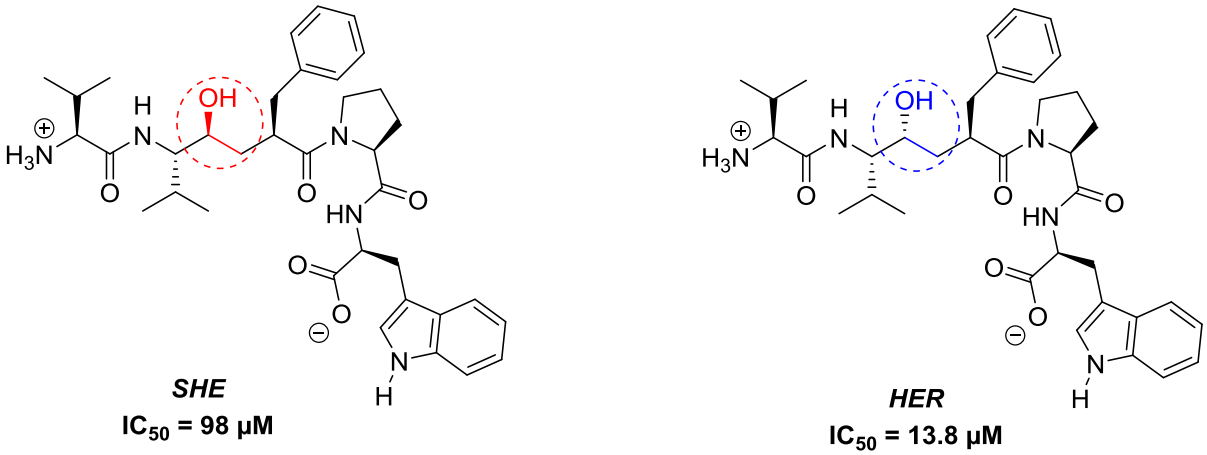

Figure 9: Chemical structure of ***SHE*** and ***HER*** pseudopeptide inhibitors of hDPP3, designed and synthesized by J. Ivković and C. Lembacher-Fadum.[12,13]

The compounds ***SHE*** and ***HER*** were evaluated for inhibition of hDPP3 via fluorescence-based inhibition assay and ITC experiments. Pseudopeptide ***HER*** exhibited an endothermal binding profile similar to tynorphin and an IC_{50}-value of 13.8 µM. With these promising results in hand further improvements of inhibitor specificity and potency towards the nM range were desired and this work shall aim at designing and synthesizing novel transition-state analogue inhibitors based on a phosphonamidate moiety instead of a

hydroxyethylene group placed between the amino acids valine and phenylalanine in the peptide sequence as illustrated in Figure 10.

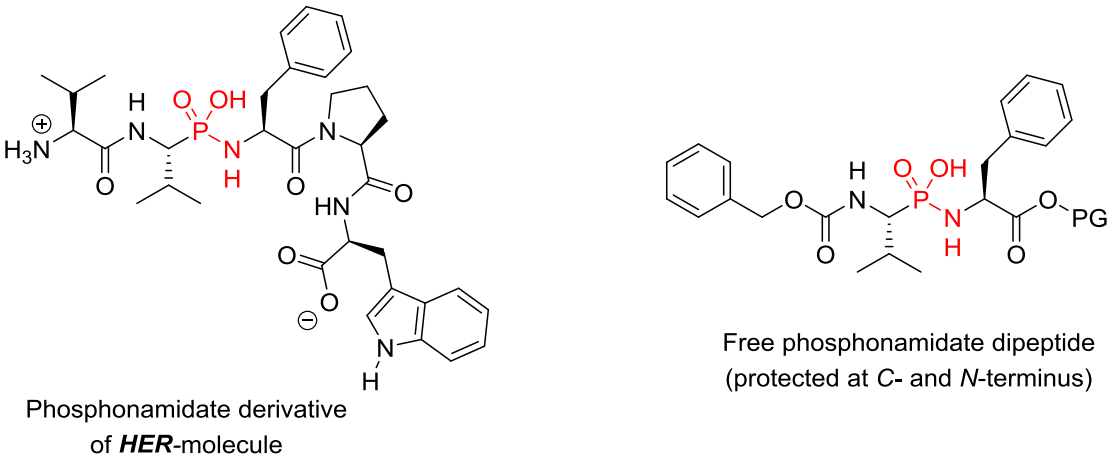

Figure 10: Potential phosphonamidate-based inhibitors of hDPP3 based upon the lead compound ***HER*** developed by J. Ivković and C. Lembacher Fadum.[12,13]

The phosphoramidate moiety could provide useful inhibition properties towards hDPP3 due to its tetrahedral geometry with the objective to mimic the peptide hydrolysis transition state of the enzyme and bind closely to the catalytic zinc ion. Subsequently the binding site for the peptide-bond of potential substrates would be occupied resulting in a decreae of the enzyme's catalytic activity of the enzyme. The phosphonamidate-based compound phosphoramidon proved to be a successful inhibitor of thermolysin, a zinc-dependent metalloprotease with a similar water-promoted catalytic mechanism as the one described in hDPP3.[10,21]

4 Results and discussion

4.1 Synthetic approach towards phosphonamidate Inhibitors of hDPP3

The overall goal was to exchange the second amide bond from the *N*-terminus of the template molecule tynorphin using the bulky tetrahedral phosphonamidate group as a transition-state isoster. A first retrosynthetic analysis suggests an initial disconnection at the Val-Val peptide bond from the *N*-terminal side followed by a second disconnection at the Phe-Pro peptide bond as seen in Scheme 5. These peptide fragment couplings were considered to be realized by known reliable protocols in a sequential manner, however the third disconnection at the phosphonamidate moiety deemed the major challenge of this project. A critical step would be the isolation of the free phosphonamidate due to a major change in polarity of the molecule as well as instability of unprotected phosphonamidate compounds.

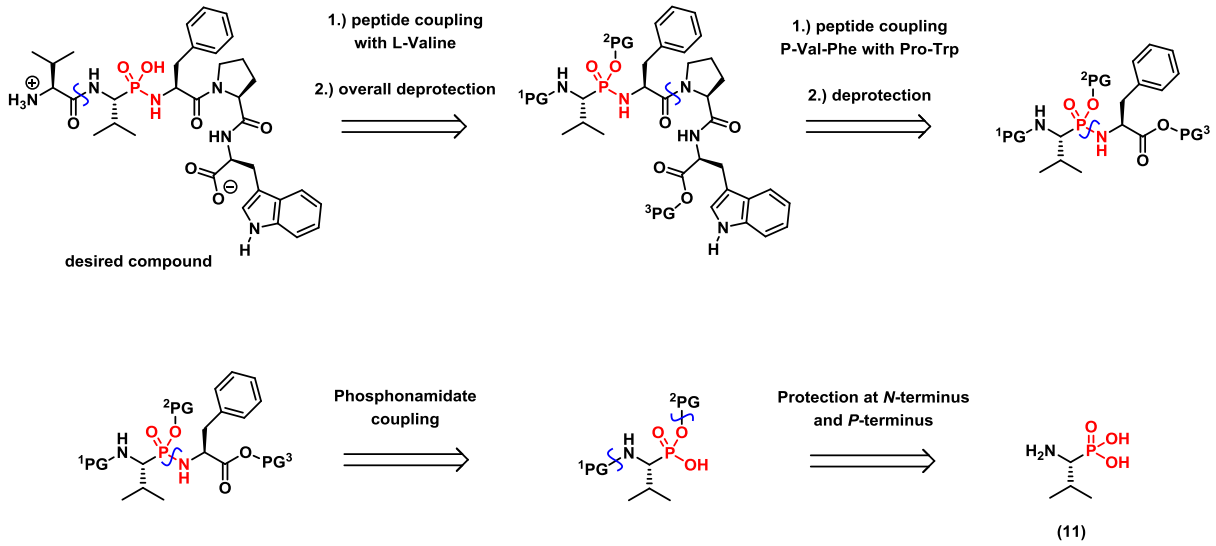

Scheme 5: Retrosysnthetic analysis of the target phosphonamidate linked pseudo pentapeptide.

In the previous steps protection groups should be attachted at the *N*-terminus and at one of the hydroxyl groups of **11** to maintain chemoselective control of the peptide coupling. The starting compound of the sequential peptide synthesis would be the (*R*)-α-aminophosphonic acid isoster of valine, (*R*)-(1-amino-2-methylpropyl)phosphonic acid (**11**).

4.1.1 Asymmetric synthetic sequence towards (*R*)-α-aminophosphonic acid isostere 11

For the synthesis of **11** a method published by Olszewski *et al*. in 2015 was chosen, where nucleophilic attack of chiral *H*-phosphonate **5** to (*S*)-*N*-*tert*-butylsulfinyl aldimines **J** yielded the respective alkyl, aryl or heteroaryl α-aminophosphonates **K** in high diastereomeric ratio towards (*R*)-configuration (Scheme 6). The two chiral auxiliaries were cleaved in the following step by treatment with 4 M HCl in toluene, heating the reaction to 100 °C and free (*R*)-α-aminophosphonic acids **L** were obtained. In the publication the generation of desired building block (**11**) was reported in 92 % yield and high diastereoselectivity, dr = >95:5.[24]

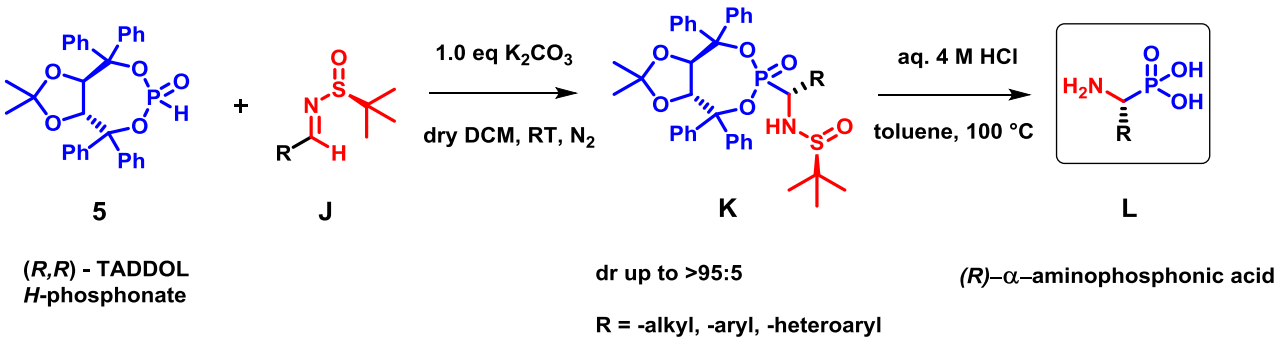

Scheme 6: Reaction sequence towards unprotected (*R*)-α-aminophosphonic acids published by Olszewski *et al*.[24]

The compound **5** could be produced by using a robust and reliable protocol by Beck *et al*. towards the ligand (*R*,*R*)-TADDOL, which carried the function of a chiral auxiliary and could be synthesized starting from readily available L-dimethyl tartraric acid (**1**).[25] Protection of **1** using acetone as solvent and reagent in the presence of $BF_3{\cdot}Et_2O$ gave protected 1,2-diol **2** in good yield after purification via flash chromatography. The following transformation resulting in chiral (*R*,*R*)-TADDOL **4** was carried out using freshly prepared phenylmagnesium bromide solution, produced via GRIGNARD-reaction of phenylbromide and magnesium turnings in dry THF. Efficient cooling and temperature-monitoring by thermometer was necessary to retain control of the exothermic reaction when adding the GRIGNARD-solution dropwise to a solution of protected 1,2-diol **2** in dry THF. After extractive workup and purification via recrystallization from toluene/n-heptane, ligand **4** was obtained in 68 % yield. In the next step preparation of (*R*,*R*)-TADDOL-*H*-phosphonate **5** was carried out by reaction of PCl_3 with **5** in the presence of Et_3N, proceeded with addition of stoichiometric amount of H_2O with the intent to cleave the intermediate P-Cl bond by hydrolysis. The pure *H*-phosphonate **5** was isolated in 77 % yield (Scheme 7).[25,26]

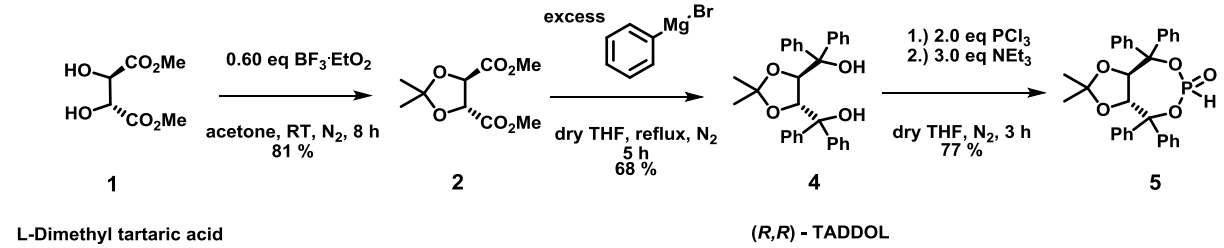

Scheme 7: Synthesis of (*R*,*R*)-TADDOL-*H*-phosphonate **5**.[25,26]

The second chiral building block **3** was prepared using a procedure by Chen *et al*. via dropwise addition of titanium isopropoxide as Lewis acid to a solution of isobutyraldehyde and (*S*)-2-methylpropane-2-sulfinamide in dry THF followed by extractive workup (Scheme 8).[27] Carefully drying the volatile crude product on a rotary evaporator (20 mbar, 40 °C) for 1.5 h furnished (*S*)-*N*-*tert*-butylsulfinyl imine **3** in 98 % yield.

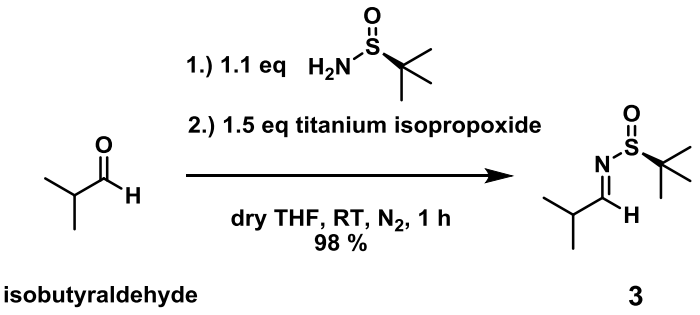

Scheme 8: Synthesis of chiral (*S*)-*N*-tert-butylsulfinyl imine **3**.[27]

With the chiral auxiliaries in hand a hydrophosphonylation reaction between **3** and **5** was performed using K_2CO_3 as activating base. The major (*R*)-diastereomer of α-aminophosphonate **10** could be obtained via recrystallization from Et_2O and combined with a second fraction of product, isolated from the mother liquor, a yield of 77 % was achieved. A single peak at 20.6 ppm in the ^{31}P-NMR spectrum was in accordance with the reported data by Olszewski *et al*.[24] Simultaneous cleavage of both chiral auxiliaries was realized by addition of 4 M HCl to a solution of **10** in toluene and heating the reaction to 100 °C for 2.5 h. The aqueous phase was separated, concentrated in vacuum, and the pure (*R*)-α-aminophosphonic acid **11** was isolated in 72 % yield via crystallization from dry EtOH and stoichiometric amounts of propylene oxide. The (*R*)-configuration at the α-carbon stereo center was confirmed by measurements of the specific optical rotation in 2 M NaOH, which was in agreement with the literature.[24]

In summary, (*R*)-(1-amino-2-methylpropyl)phosphonic acid (**11**) was synthesized with an acceptable overall yield of 23 % in a 6-step convergent synthesis (see Scheme 7, 8 and 9).[24,25,26,27]

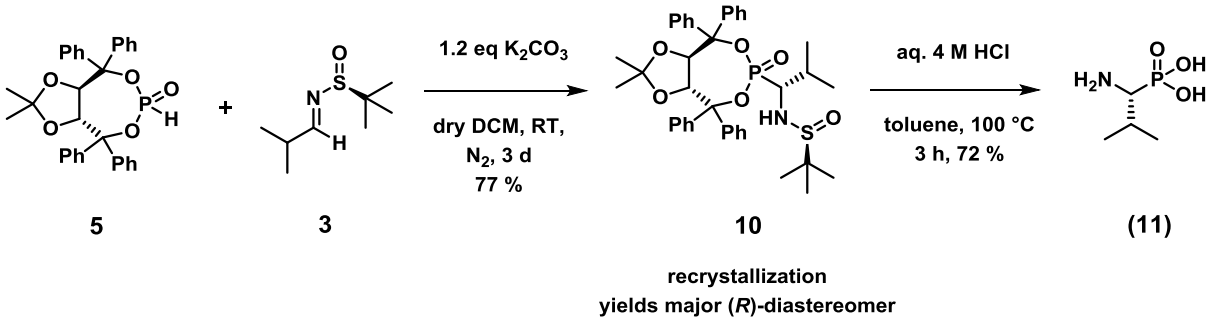

Scheme 9: Hydrophosphonylation of *H*-phosphonate **5** with imine **3** and subsequent removal of both chiral auxiliaries by treatment with 4 M HCl.[24]

A drawback of this synthetic approach is the major loss of 534.7 atomic mass units in the final auxiliary cleavage step, resulting in poor atom economy and repeated synthesis cycles were necessary for sufficient supply of compound **11** to perform further synthetic experiments.

4.1.2 Synthesis of Cbz- and monoallyl phosphonate building blocks

It deemed obligatory to install protecting groups at the *N*- and *P*-terminus of (*R*)-α-aminophosphonic acid **11** to perform with the initial phosphonamidate coupling attempts. The Cbz-protecting group was chosen for the *N*-terminus primarily because of the stability of this protecting group towards basic and moderate acidic conditions, the convenient preparation and removal methods of Cbz-protected amino acids,[28] and the possible utility as a hydrophobic fragment of the inhibitor scaffold.[29] Introduction of the benzyloxycarbonyl (Cbz) group was performed by acylation of the amino functionality of substrate **11** using benzyl chloroformate (Cbz-Cl) in the presence of Na_2CO_3 and $NaHCO_3$ in a mixture of H_2O/acetone (Scheme 10).[30]

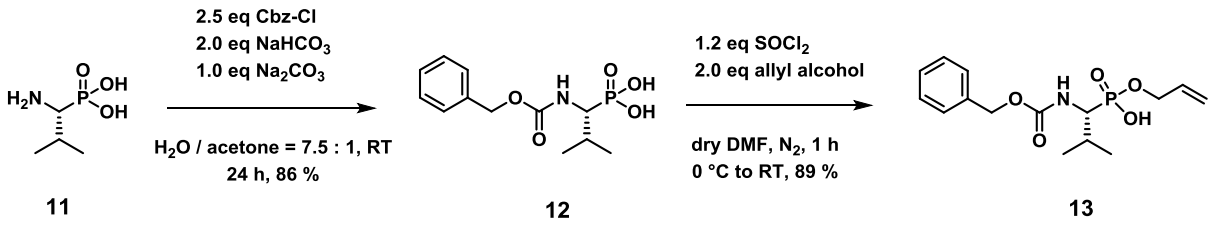

Scheme 10: Acylation of (*R*)-α-aminophosphonic acid **11** followed by selective monoallylation of substrate **12**.[30,31]

During the reaction the pH was kept constant at 8-9 via monitoring and further addition of Na_2CO_3 if it was necessary. This action was crucial, since Cbz-Cl is prone to decompose below a pH of 8 and racemization issues of the amino acid could occur at high pH.[14] Satisfactorily pure Cbz-protected product **12** was obtained after extractive workup in 72 % yield, successfully avoiding further purification steps. Mono-protection at the phosphonate moiety was achieved by adapting a protocol from Hoffmann, converting the free phosphonate to a phosphonochloridate with stoichiometric addition of $SOCl_2$.[31] Allylation of this reactive species with allyl alcohol furnished monoallyl ester **13** in 80 % yield (Scheme 10). Pure product was obtained after extractive workup, which was confirmed by NMR-interpretation.

4.1.3 Preparation of L-phenylalaine methylester

L-Phenylalaine methylester hydrochloride **6** was chosen as the first coupling partner with Cbz-protected P-Valine **12** and produced via esterification of L-phenylalanine. The carboxylic acid was converted into methylester **6** using $SOCl_2$ in MeOH. Moderate 56 % yield of **6** were obtained (Scheme 11).[32]

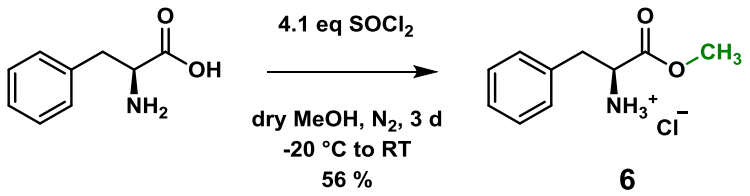

Scheme 11: Esterification of L-phenylalanine by activation with $SOCl_2$ in neat MeOH.[32]

4.1.4 Initial phosphonamide coupling attempts

Phosphonamidate couplings trials were performed first without protection group at the phosphonic acid moiety, following a protocol from colleague Mario Leypold.[33] In a dry Schlenk flask Cbz-protected P-valine **12** and methyl ester protected L-phenylalanine were dissolved in a dry 1,2-DCE/DMF mixture and activated with Hünig's base reagent alongside 4-DMAP. After cooling to 0 °C the coupling reagent EDC·HCl was added. After 2 h full conversion of starting material to a major diphosphate product **N** and small amounts of desired free phosphonamidate **M** was observed via HPLC-MS control as detailed in Scheme 12 (corresponding masses for **M** and **N** were found). Unfortunately, isolation attempts of product **M** via preparative RP-HPLC failed and only decomposition into the starting materials **12** and phenylalanine methyl ester was observed.

After consulting the literature about this phenomenon various resources were found describing the instability of free phosphonamidates in acidic or even neutral conditions due to favored hydrolysis of the P-N bond.[2,29,34] The coupling conditions depicted in Scheme 12 were also investigated with monoallyl protected substrate **13**, using 3.0 eq Hünig's base instead of 1.0 eq. The major product in this reaction could be identified as the EDC-adduct **O** using HPLC-MS and only traces of desired phosphonamidate coupling product **15** was formed.

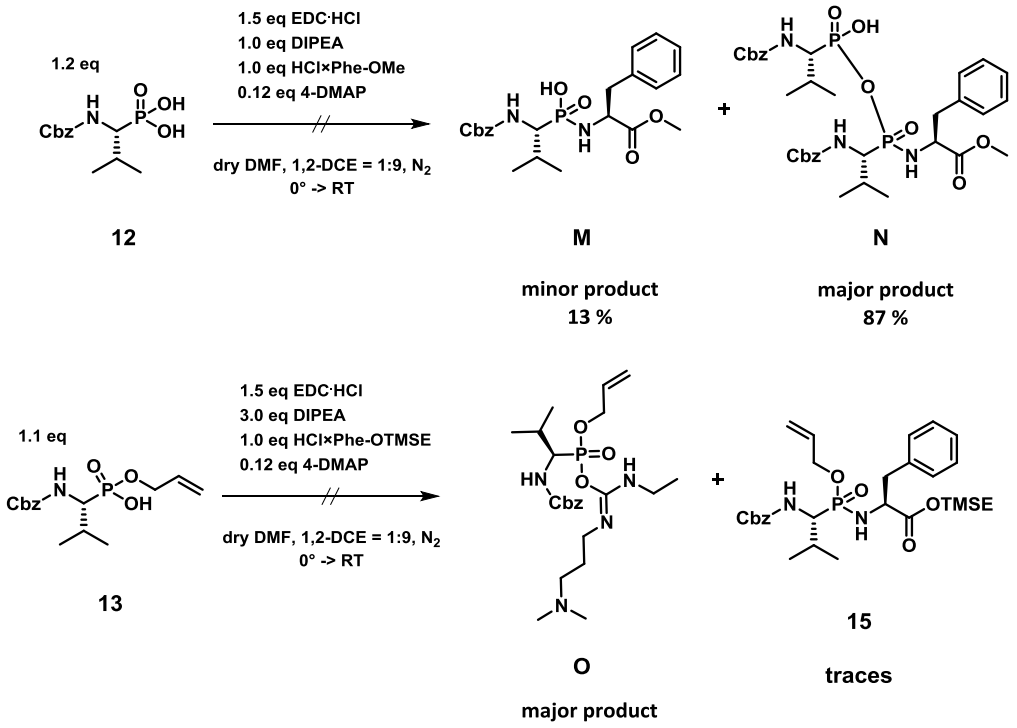

Scheme 12: Failed attempts of phosphonamidate coupling with EDC·HCl reagent.[33]
The product distribution percentages were derived by integration of HPLC-MS chromatograms.
(UV-detection at 210 nm)

The hydrolysis of **M** during preparative RP-HPLC isolation attempts was attributed to the component HCOOH (0.01 %) in the H_2O/MeCN solvent mixtures used in HPLC-separation problems. Consequently, the protection and deprotection strategy had to be revised with the goal to avoid acidic reaction-, workup- and purification conditions.

4.1.5 Synthesis of protected phenylalanine building blocks

Phenylalanine derivatives with 2-(trimethylsilyl)ethyl (TMSE) ester attached at the carboxylic function posed an attractive target due to the stability towards oxidative and reductive ester

cleavage protocols, as well as hydrogenolysis.[28,35] Boc-Phe-OH was coupled with 2-(trimethylsilyl)ethanol employing carbodiimide EDC·HCl conditions in 79 % yield.

Selective Boc-deprotection was carried out by dissolving protected phenylalanine **7** in 4 M HCl in 1,4-dioxane and stirring for 1 h. The TMSE protection group was stable under these conditions and *C*-terminal TMSE-protected phenylalanine **8** was isolated in 96 % yield.

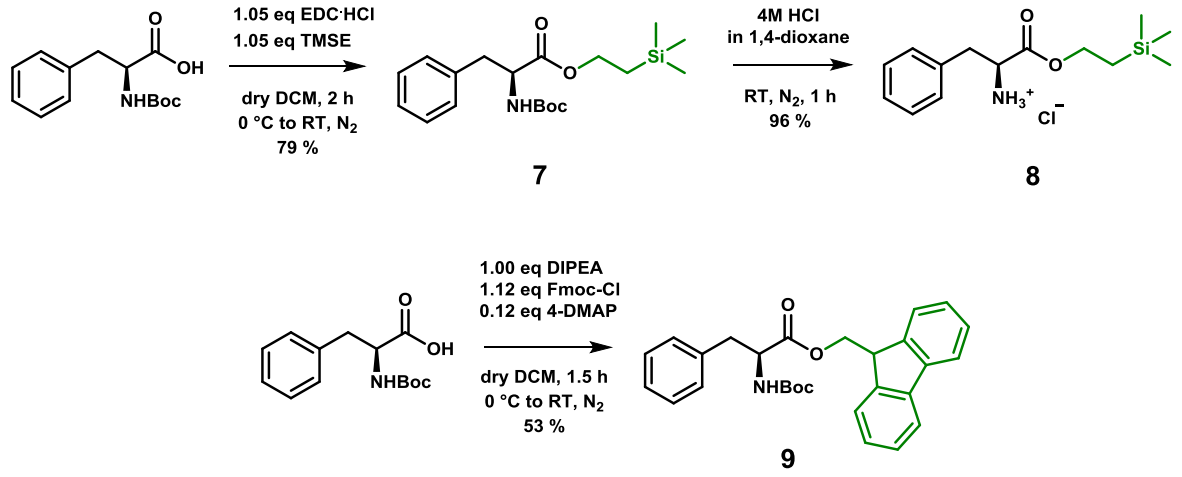

Scheme 13: Synthesis of Phe-OTMSE building block **8** and Boc-Phe-Fmoc building block **9**.[36,37]

Another potentially useful building block for sequential peptide coupling was thought to be the fluorenylmethyl ester of *N*-protected phenylalanine for the reason that the Fmoc group is known to be removed in basic conditions using secondary amines.[20] Boc-Phe-OFmoc compound **9** could be generated by reaction of Hünig's base activated Boc-Phe-OH with Fmoc-Cl and 4-DMAP in 53 % yield after flash chromatography.

4.1.6 Synthesis of functionalized phosphonamidate dipeptides

Very recently a promising strategy was published by Cramer *et al* (Scheme 14).[29] First a synthesis of monoallyl ester protected phosphonate building block **P** was described, which was subsequently connected with functionalized Boc-deprotected dipeptides **Q** via a phosphonamidate coupling protocol. The scope of this coupling procedure ranges from short to long alkyl side chain substituents attached at the dipeptide up to functionalized piperazines. The phosphonamidate products **R** were obtained as a mixture of diastereomers, with a stereogenic phosphorous atom featuring four unique attached functional groups.[29]

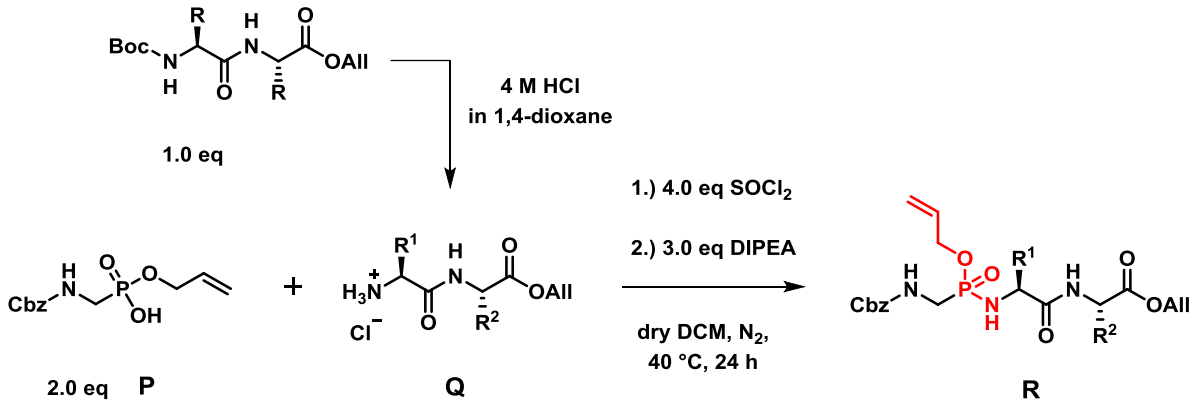

Scheme S14: Phosphonamidate coupling method by Cramer *et al*.[29]

The procedure features an activation sequence with generation of a phosphonochloridate entity via treatment of **P** with $SOCl_2$. Prior to addition of coupling fragment **Q** the phosphonochloridate was allowed to react with Hünig's base forming an electrophilic phosphonylammonium intermediate, which is more susceptible towards nucleophilic attack. The outcome of the reaction was dependent on the creation of this reactive species as mentioned by Hirschmann *et al*. in their extensive publication on phosphonamidate and phosphonate synthesis (Scheme 15).[38]

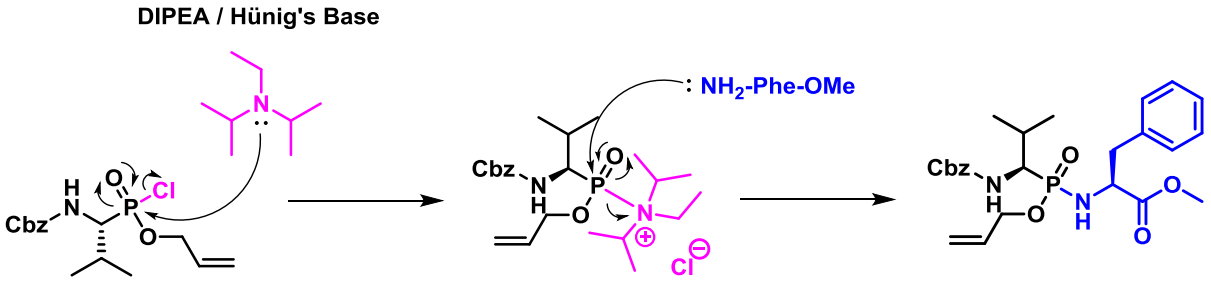

Scheme 15: Suggested mechanism of P-N bond formation by Hirschmann *et al*.[38]

The monoallyl ester substrate **13** was attempted to be combined with the protected phenylalanine derivatives **6** and **8** employing the coupling protocol developed by Cramer *et al*.[29] Delightfully the fragment coupling was successful and allyl protected phosphonamidate dipeptides **14** and **15** could be isolated in moderate yields after purification via flash chromatography (Scheme 16). The lower yields may be attributed to the steric bulkiness of the propyl group attached to the α-carbon atom of substrate **13** resulting in possible reactivity decrease in contrast to monoallyl ester **P** used by Cramer *et al*.[29]

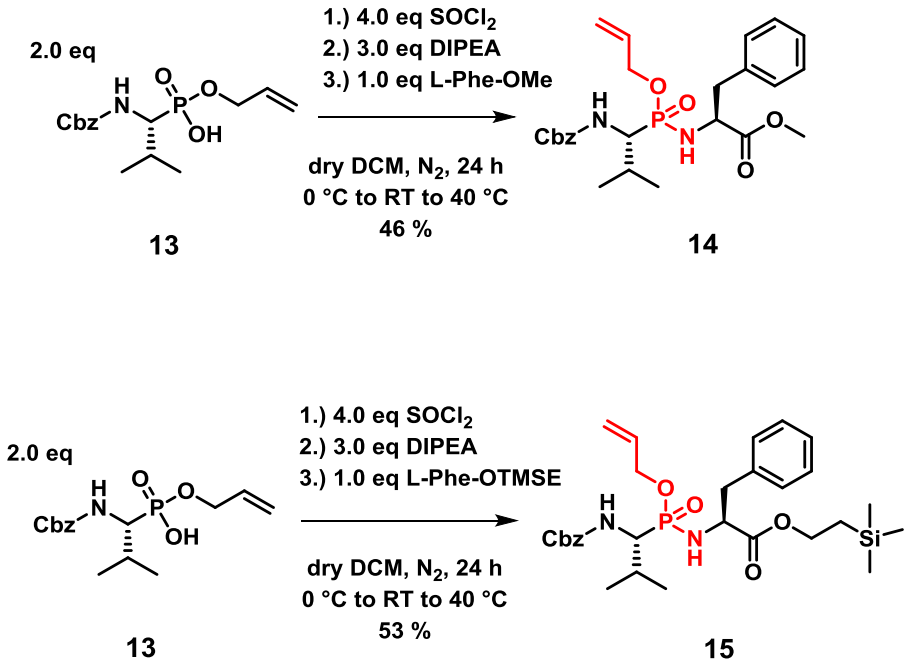

Scheme 16: Phosphonamidate coupling of monoallyl ester **13** with *C*-protected phenylalanine building blocks.[29]

4.1.7 Attempt of selective TMSE-deprotection of dipeptide fragment

A reliable TMSE-deprotection protocol was desired to perform consecutive peptide coupling towards the desired phosphonamidate pentapeptide scaffold. According to the literature, the TMSE protection group is commonly cleaved with fluoride-containing quaternary ammonium fluoride salts, for instance TBAF·3H$_2$O or potassium fluoride dihydrate.[28,35,39]

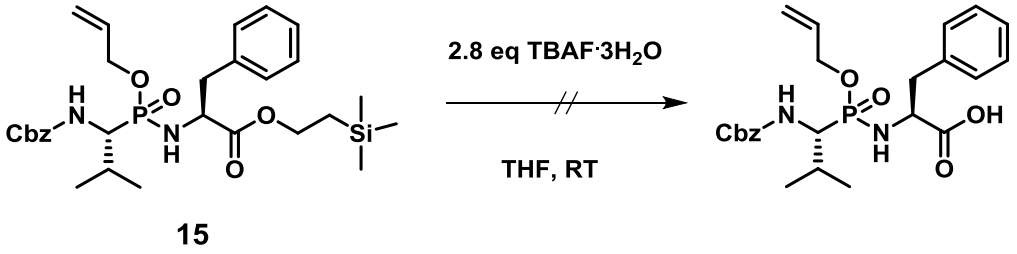

Scheme 17: Unsuccessful attempt of TMSE deprotection using TBAF·3H$_2$O.[40,41]

A procedure taken from Bartholomäus *et al.* was examined were TMSE-protected phosphonamidate **15** was dissolved in THF and treated with TBAF·3H$_2$O.[40] Full conversion of starting material was observed after 3 h via HPLC-MS control and the mass corresponding to TMSE-deprotected phosphonamidate **15** could be observed. After addition of 1 M NH_4Cl-solution and extraction with $CHCl_3$ unfortunately decomposition of product was detected by HPLC-MS (Scheme 17). In a second attempt, the workup was omitted and the

reaction solvent THF was simply removed in vacuum. The polar mixture was subjected to purification by loading the sample onto a reversed-phase Thermoscientific HyperSep C18 cartridge (500 mg, 3 mL) and using H_2O/MeCN mixtures as eluting solvents. However, only unidentified by-products were eluted and no desired TMSE-deprotected phosphonamidat product could be obtained.

4.1.8 Synthesis of Boc-Phe-Pro-Trp-OMe tripeptide

Simultaneously, we wanted to further examine the scope of the phosphonamidate coupling method by Cramer *et al.* and decided to synthesize tripeptide **16** and attempt to connect this building block directly to the monoallyl phosphonamidate fragment **13**. The dipeptide Boc-Pro-Trp-OMe was previously synthesized by J. Ivković (synthesis described in the PhD thesis of J. Ivković) and could be used for this project.[12] Boc-deprotection of this pseudodipeptide was performed using neat TFA and EtSH as carbocation scavenger. After stirring for 1 h full conversion was observed and after extractive work-up the crude H-Pro-Trp-OMe was dried in oil pump vacuum to constant mass. Boc-Phe-OH was activated with coupling reagent HBTU to avoid racemization and freshly Boc-deprotected H-Pro-Trp-OMe was added. Tripeptide **16** could be isolated in 71 % yield after flash chromatography and washing with H_2O and brine to remove remaining tetramethylurea.

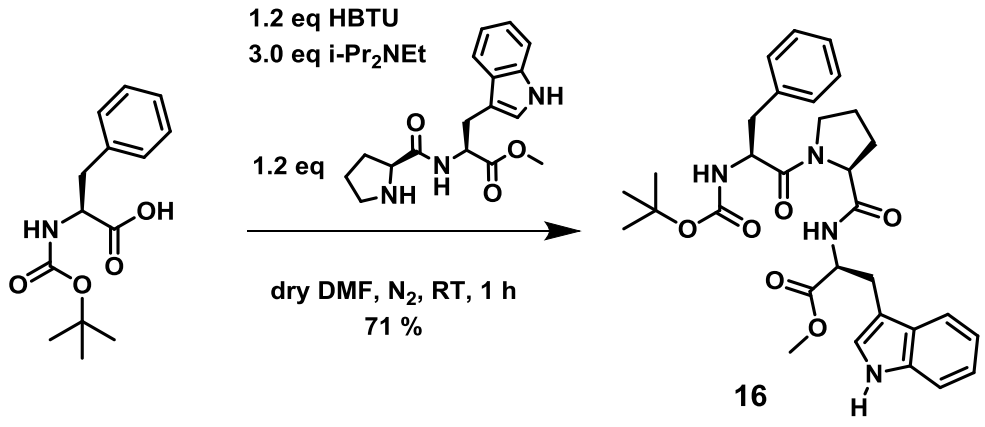

Scheme 18: Peptide coupling of Boc-Phe-OH with dipeptide H-Pro-Trp-OMe employing HBTU as coupling reagent.[12]

4.1.9 Assembly of phosphonamidate tetrapeptide

With the Boc-Phe-Pro-Trp-OMe tripeptide in hands a successful phosphonamidate coupling could be achieved using monoallyl protected phosphonate **13** following the method by Cramer *et al.* (see Scheme 19).[29] Prior to phosphonamidate coupling the Boc-deprotection of **16** was carried out by stirring in 4 M HCl in 1,4-dioxane. Full conversion was indicated after 1 h by TLC and subsequently all volatile components were removed in vacuum. Phosphonamidate coupling was performed by first adding $SOCl_2$ to convert **13** into the phosphonochloridate, which was subsequently transformed into the reactive phosphonylammonium intermediate by nucleophilic attack of added Hünig's base. Finally, freshly Boc-deprotected H-Phe-Pro-Trp-OMe tripeptide was added and the reaction was stirred overnight at 40 °C. After extractive work-up and purification via flash chromatography the phosphonamidate pseudotetrapeptide **17** was obtained as a mixture of diastereomers in low 39 % yield and contained small amounts of impurities indicated by ^{31}P-NMR measurements.

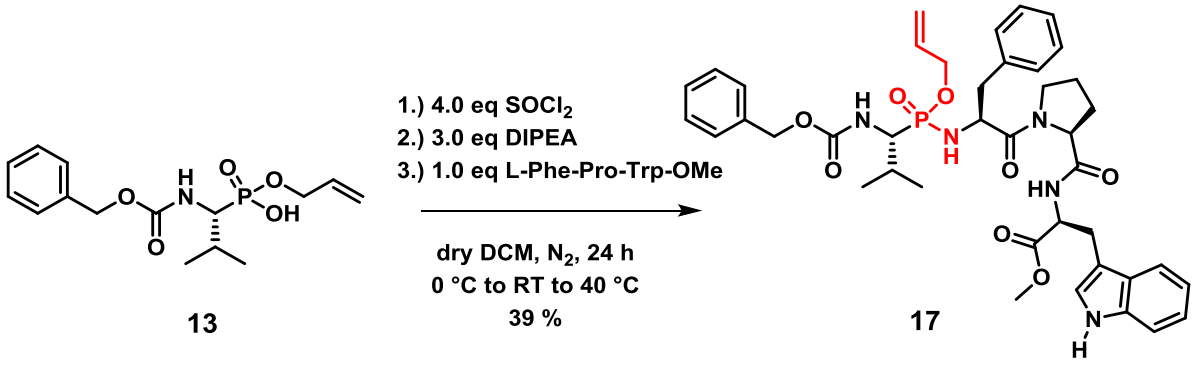

Scheme 19: Synthesis of monoallyl protected phosphonamidate tetrapeptide **17**.[29]

4.2.0 Final deallylation of phosphonamidate dipeptide and tetrapeptide

The removal of the allyl protection group was desired to yield free phosphonamidates, as the last synthetic step towards potential hDPP3 inhibitors. In the publication of Cramer *et al.* a $Pd(PPh_3)_4$-mediated allyl transfer reaction with subsequent nucleophilic attack by diethylamine is the described method for allyl deprotection.[29] The advantage of this procedure is that the generated by-products, with exception to the catalyst, are volatile and are feasible to remove in vacuum. The resulting crude mixture was then subjected to solid phase extraction (SPE) by loading the material onto a conditioned Thermoscientific HyperSep C18 cartridge (500 mg, 3 mL) and eluting the products with H_2O/MeCN mixtures. Previous

attempts by Cramer *et al*. to purify the free phosphonamidates via preparative RP-HPLC resulted in hydrolysis of the molecules.

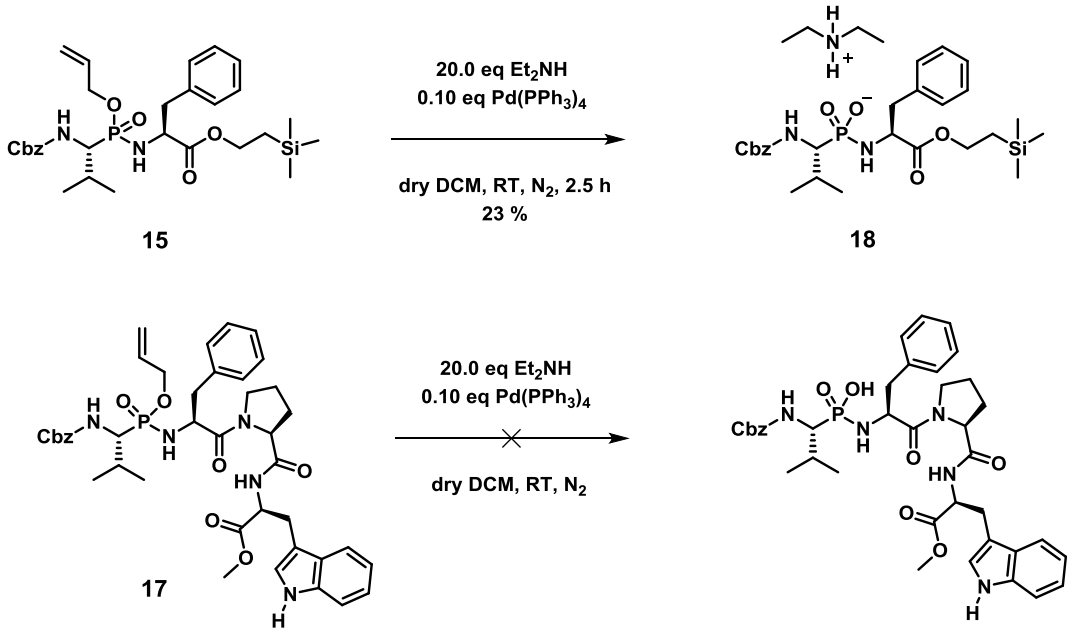

Scheme 20: Deallylation attempts of pseudodipeptide **15** and pseudotetrapeptide **17** using $Pd(PPh_3)_4$.[29]

When pseudodipeptide **15** was investigated in this reaction, full conversion of starting material was indicated after 2.5 h by TLC. The free phosphonamidate compound exhibited tailing on TLC and a 2D-TLC was prepared which revealed no decomposition products along the axis, hence it was reasoned that the compound should be stable on silica gel chromatography. Indeed, after flash chromatography using DCM/MeOH = 10:1 mixture as solvent system a product was isolated in 26 % yield. NMR-experiments (^{1}H, ^{13}C, HSQC, COSY, ^{31}P and ^{29}Si) suggested that the obtained product **18** seemed to be the diethylammonium salt and in HR-MALDI-MS experiments a mass of 631.4 was observed compared to the calculated mass 630.3 (M+Na) of compound **18**. However, the peak integration data is inconsistent with the expected protons of the free phosphonamidate dipeptide **18**. Deallylation reaction with pseudotetrapeptide **17** was employed with the conditions described in Scheme 20 and full conversion of starting material was observed after 3 h by TLC. Unfortunately, the characterized compound isolated after flash chromatography did not match with the desired free phosphonamidate pseudotetrapeptide. ^{1}H-NMR showed a vast number of signals which could not be assigned to a specific product. As a result of these failed experiments, further optimization of deallylation reaction conditions and investigations of the stability of free phosphonamidates are needed to gain further comprehensive insight about the behavior of this substance class.

5 Summary and outlook

Potent and selective inhibitors of the hDPP3 enzyme are desired as molecular tools to acquire a better understanding of the mechanism and physiological roles of the enzyme. In the scope of this thesis (*R*)-hydroxyethylene pseudopeptide ***HER*** (developed by Ivković[12] and Lembacher-Fadum[13]) was taken as a template structure to develop novel phosphonamidate inhibitors as tetrahedral transition state mimetics. A suitable synthetic route towards the first building block (*R*)-α-aminophosphonic acid isoster of valine had been found by Olszewski *et al*. starting from readily available L-dimethyl tartaric acid to furnish (*R,R*)-TADDOL *H*-phosphonate **5** in three steps. Subsequent hydrophosphonylation with (*S*)-*N*-*tert*-butyl-sulfinyl imine **3**, followed by recrystallization gave the major diastereomer of compound **10**. Acidic cleavage of both chiral auxiliaries yielded free (*R*)-α-aminophosphonic acid **11** which was subsequently protected at the *N*-terminus with Cbz. Selective transformation of **12** with $SOCl_2$ and allyl alcohol furnished monoallyl phosphonate **13** as the last step. In conclusion, the core phosphonamidate building block **13** was synthesized in an overall yield of 18 % for the longest linear sequence of 7 steps (Scheme 21).[25-28,30,31]

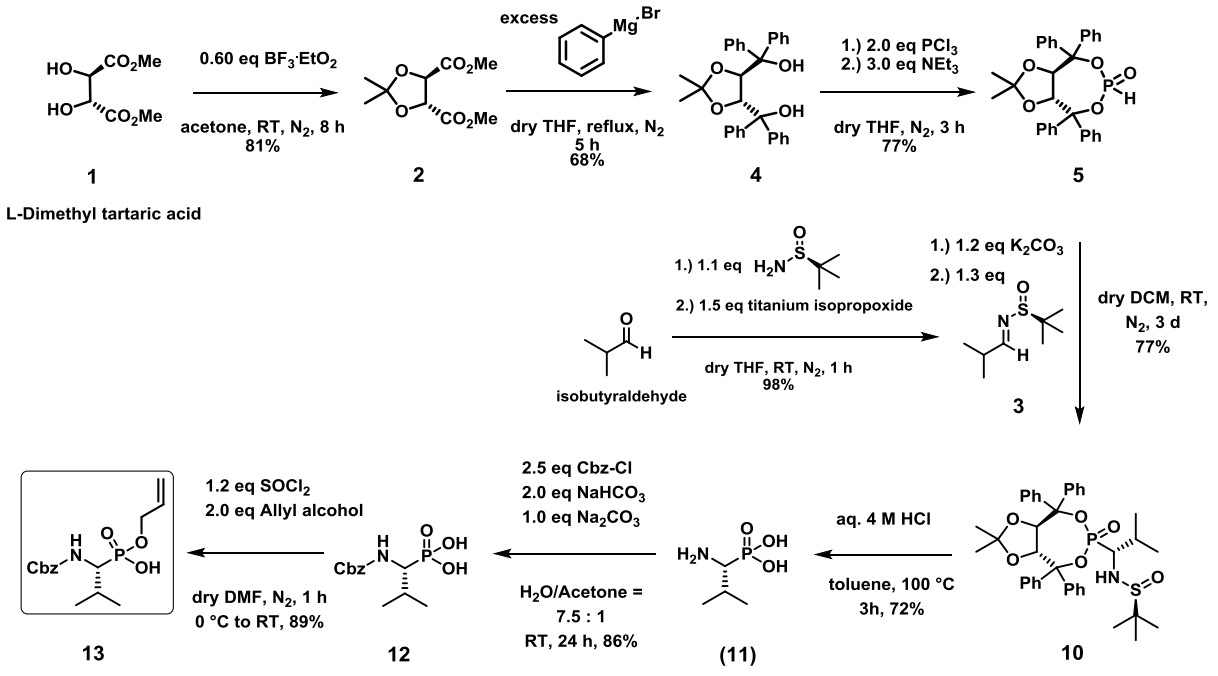

Scheme 21: Summary of the synthesis pathway leading to core phosphonamidate building block **13**.

A phosphonamidate coupling protocol by Cramer *et al.*[29] using $SOCl_2$ and Hünig's base consecutively as activating reagents, was successfully employed. The protected phosphonamidate dipeptides **14** and **15** were produced in moderate yields and even the bulky H-Phe-Pro-Trp-OMe tripeptide furnished pseudotetrapetide **17**, however in low yield of 39 %. Noteworthy the peptide products were obtained as a mixture of diastereomers which were not separated but characterized as a mixture (detailed reaction conditions are depicted in Scheme 22).[29]

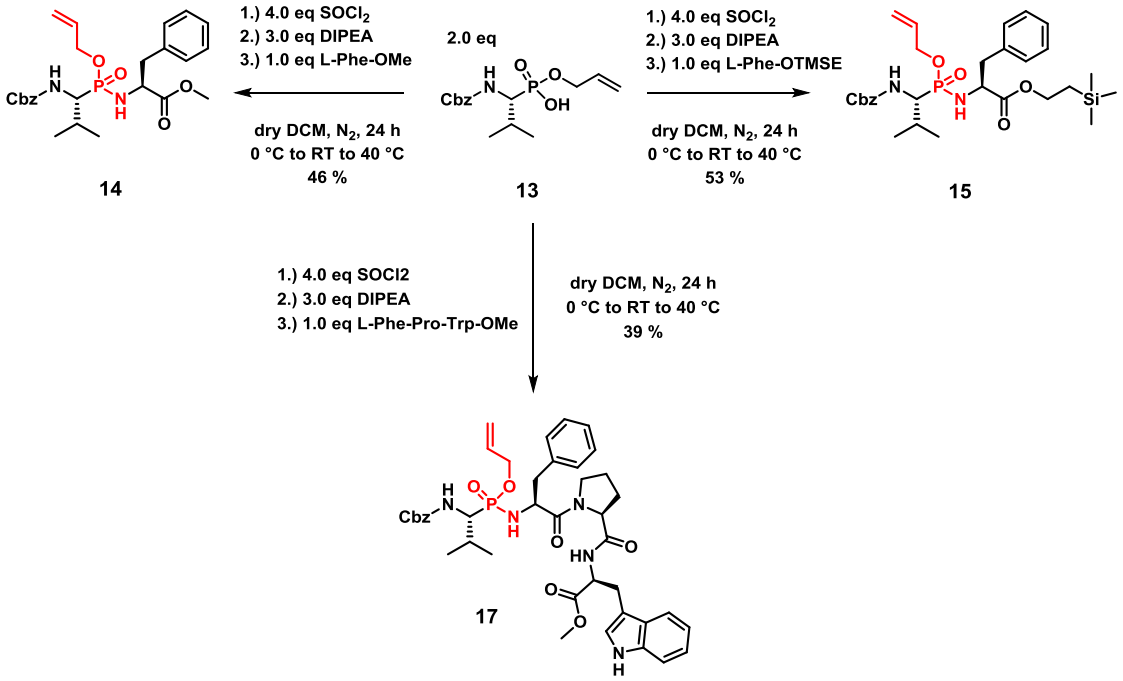

Scheme 22: Succesful phosphonamidate coupling

The final deprotection of the allyl group was carried out via Pd-mediated allyl transfer reaction as described in the work of Cramer *et al*. Deallylation of TMSE-protected dipeptide **15** could be performed with success and free phosphonamidate dipeptide **18** was obtained in 26 % yield suggested as the diethylammonium salt. The deallylation attempt of tetrapeptide **17** gave a very polar product which unfortunately could not be identified.

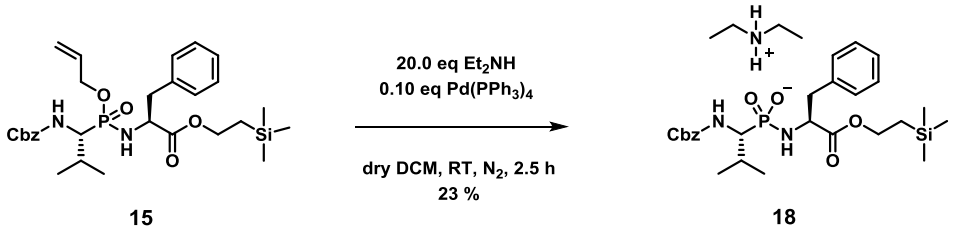

Scheme 23: Removal of the allyl protecting group by activation with $Pd(PPh_3)_4$ and diethylamine.

Fluorescence-based inhibition assays were performed using the synthesized dipeptide **18**, as well as (*R*)-α-aminophosphonic acid **11** and monoallyl ester **13** by Shalinee Jha at the Institute of Biochemistry at Graz University of Technology and results showed no desired inhibition of hDPP3 enzyme.

In conclusion, further investigations of the phosphonamidate substance class are needed after these first results. It was demonstrated that the phosphonamidate coupling protocol of Cramer *et al*. is compatible for the synthesis of selected protected dipeptides and even tetrapeptides, however additional optimization and screening studies for the final deallylation procedure are required to yield the intended free phosphonamidate peptides. Based on decomposition observations of free phosphonamidates the future protection-, coupling- and deprotection-strategy will aim at introducing the phosphonamidate moiety in the last steps followed by a mild deprotection protocol. Finally, since DPP3 shows affinity for the tyrosine fragment in inhibitors such as tynorphin, and exchanging phenylalanine with tyrosine in the peptide sequence may have a beneficial effect on tighter binding of the potential future inhibitors towards DPP3.[5,13,29]

6 Experimental section

6.1 General aspects:

Reactions with moisture and oxygen sensitive reagents were carried out under inert atmosphere with dry solvents and with standard Schlenk techniques. In case a reaction was needed to be carried out in an inert atmosphere the reactants and dry solvents were added to a Schlenk vessel. The vacuum conditions used were typically in the range of 10^{-2}-10^{-3} mbar. The following Schlenk technique was applied: Before addition of chemicals the Schlenk tube containing a magnetic stirring bar was evacuated with oil pump vacuum and heated with a heat-gun. Then the Schlenk apparatus was allowed to cool to room temperature and subsequently purged with nitrogen or argon as inert gas. This process was repeated two times. When cooling was necessary for experiments a cooling bath consisting of water/ice mixture for cooling to 0 °C was prepared. In the case lower temperatures were necessary NaCl and ice were mixed in a 3:1 ratio. The solvents and reagents were added in an inert gas counter-stream (usually N_2) in all cases of dry reactions. All reactions were stirred using Teflon®-coated magnetic stirring bars and sealing Glindemann® PTFE rings were used for glass stoppers. Thermoscientific HyperSep™ C18 500 mg 3 mL cartridges were purchased from Thermo Fisher Scientific. Dry solvents were prepared as is described below and stored under argon.

Molecular sieves (8-12 mesh beads, purchased from Sigma-Aldrich) were activated by heating them in a round-bottom flask equipped with a Schlenk adapter to about 150 °C under vacuum for 24 h until a constant pressure was observed.

Degassing solvents was practiced by bubbling argon from a balloon through the chosen solvent, in an active ultrasonic bath for 20 min.

The chemicals, reagents and solvents, used in this thesis were purchased from the following companies: Alfa Aesar, ABCR, ACROS Organics, Fisher Scientific, Fluka, LOBA-Chemie, Merck, Roth, Sigma-Aldrich, TCI Chemicals and VWR and used without further purification unless stated otherwise.

6.1.1 Solvents:

Dichloromethane (CH_2Cl_2): Dichloromethane with EtOH as stabilizer was dried over P_4O_{10}, distilled, then heated under reflux for 2 d over calcium hydride and once more distilled under argon atmosphere into a brown 1 L Schlenk bottle with activated 4 Å molecular sieves.

Ethanol (EtOH): Ethanol was treated with sodium and diethyl phthalate in an inert distillation apparatus and was slowly heated until formation of hydrogen was observed as intensive evolution of gas. The reaction mixture was heated under reflux for 2 h and was distilled and stored over activated 3 Å molecular sieves in a brown 1 L Schlenk bottle under argon atmosphere.

The ethanol which was used for non-inert purposes was purchased from Merck which was stabilized with 1 % methylethyl ketone and was used without further purification.

Methanol (MeOH): Anhydrous methanol was prepared by heating methanol under reflux over magnesium turnings followed by distillation under argon atmosphere into a brown 1 L Schlenk bottle with activated 3 Å molecular sieves.

Tetrahydrofuran (THF): Anhydrous THF was prepared by heating under reflux over Na for a period of 2 d in argon atmosphere. As an indicator benzophenone was added which is reduced by sodium to a ketylradical, visible as a deep blue color in the absence of water and oxygen. The dry THF was subsequently distilled in a brown 1 L Schlenk bottle and stored under argon atmosphere over 4 Å molecular sieves. Tetrahydrofuran which was used for non-inert reactions and workup procedures was purchased from Roth and the stabilizer was removed by distillation using a rotary evaporator. The solvent was stored over KOH pellets in a brown-glass bottle.

***N*,*N*-Dimethylformamide (DMF):** Anhydrous DMF was purchased from Acros organics, stored over 3 Å molecular sieves. The solvent was transferred to a brown 1 L Schlenk bottle and stored under argon atmosphere and over 3 Å molecular sieves. (The water content was <50 ppm compliant to the specification).

Diethyl ether: Diethyl ether was purchased from Roth and the stabilizer was removed by distillation using a rotary evaporator. The solvent was stored above KOH pellets in a brown-glass bottle.

Water: The water which was used in organic reactions and during workup procedures was deionized by an ion exchanger prior to use.

The solvents **cyclohexane, dichloromethane, ethyl acetate, toluene** and **methanol** were purchased from Fisher Scientific as analytical grade (99.99 %) and were used as obtained.

The solvents **acetone**, **n-heptane**, **Et_2O**, and **$CHCl_3$** were distilled prior to use.

6.1.2 Reagents

$Pd[PPh_3]_4$: Tetrakis(triphenylphosphine)palladium(0) was synthesized by colleague Anna Migglautsch and stored at -18 °C under argon atmosphere in a Schlenk vessel.

6.2 Analytical Methods and Instruments

6.2.1 Thin layer chromatography (TLC)

Thin layer chromatography for analytical purposes was carried out using TLC-plates purchased from Merck (TLC aluminium foil, silica gel 60, F_{254}). In general, the TLC-plates were illuminated using a UV-lamp with λ = 254 nm (fluorescence quenching). Furthermore, a staining reagent was applied and the plates were prepared by heating them with hot air.

$KMnO_4$: 0.3 g $KMnO_4$ and 20 g K_2CO_3 were dissolved in 300 mL H_2O and 5 mL of 5 % aqueous NaOH were added.

CAM-Solution: 2.0 g Cerium(IV)-sulfate, 50.0 g ammonium molybdate and 50 mL conc. H_2SO_4 in 400 mL distilled water.

Ninhydrin: 1.5 g Ninhydrin were dissolved in 100 mL *n*-butanol followed by addition of 3.0 mL AcOH.

6.2.2 Flash chromatography

Preparative column chromatography was carried out with silica gel 60 purchased from ACROS Organics featuring particle size 35-70 µm, 60 Å, N_2-flushed. Depending on the separation problem the 30- to 100- fold (w/w) of the mass of silica gel compared to the amount of weight of dry crude product was used. Crude and sticky reaction mixtures that were hard to transfer from one vessel to another were dissolved in a suitable solvent and were adsorbed on the twofold amount of Celite® (w/w). The substances adsorbed on Celite® were

then carefully dried by rotary evaporation using a connecting piece with a sintered glass frit. The column dimensions were chosen to fit a range between 15-30 cm of column length. The solvent mixtures were selected to adjust the R_f value of the product ranging from 0.10 to 0.40. The solvents used for flash chromatography were purchased from Fisher Scientific as analytical grade solvents.

6.2.3 Gas chromatography with mass selective detection (GC-MS)

Gas chromatography for analytical purposes was carried out with an "Agilent Technologies 7890A GC system" as performing instrument with an integrated polar HP-5MS capillary column ((5 %-phenyl)methylpolysiloxane) displaying the following measurements:
30 m x 250 µm x 0.25 µm. The injection of the analyte was conducted by an "Agilent Technologies 7683 Series Autosampler" in split mode (1/20; inlet temperature 280 °C), using helium 5.0 as carrier gas. The injected compounds were separated by their polarity and boiling point. The gas chromatography was coupled with a mass spectrometry unit containing an electron impact (EI) ionization source with a potential of E = 70 eV and a mass selective detector "Agilent Technologies 5975C inert MSD with Triple Axis Detector.

Temperature programs used:

MT_50_S: 50 °C 1 min, ramp 40 °C/min linear to 300 °C, 300 °C 5 min.

6.2.4 High performance liquid chromatography (HPLC)

HPLC measurements used for analytical purpose were carried out on an "Agilent Technologies 1200 Series" HPLC system with 1260 HiP Degasser G4225A, binary pump SL G1312, autosampler HiP-ALS SL G1367C, thermostated column compartment TCC SL G1316B, multiple wavelength detector G1365C MWD SL with deuterium lamp (λ = 190–400 nm) and subsequent connected mass detector (Agilent Technologies 6120 Quadrupole LC/MS) with an electrospray ionization (ESI) source. Separation of compounds was carried out on a reversed-phase Agilent Poroshell 120 SB-C18 column (3.0 × 100 mm, 2.7 µm) with a Merck LiChroCART® 4-4 pre-column. Detection of signals was achieved at 210 nm or 254 nm wavelength. The mobile phase consisted of acetonitrile (VWR HiPerSolv, HPLC-MS grade) and water (deionized and purified by Barnstead™ Nanopure™ water purification system) with 0.01 % formic acid. The samples were dissolved in HPLC-grade acetonitrile, MeOH or H_2O. The following methods were used:

FAST_POROSHELL120_001HCOOH_8MINGRADIENT.M: oven temperature: 40 °C, flow rate: 0.7 mL/min; 0.0-2.0 min MeCN/H_2O = 10:90 (v/v), 2.0–10.0 min linear increase to MeCN/H_2O = 95:5 (v/v), 10.0-16.0 min hold MeCN/H_2O = 95:5 (v/v).

FAST_POROSHELL120_001HCOOH_10_100.M: oven temperature: 40 °C, flow rate: 0.7 mL/min; 0.0-5.0 min MeCN/H_2O = 10:90 (v/v), 5.0-9.0 min linear increase to MeCN/H_2O = 100:0 (v/v), 9.0-11.5 min hold MeCN/H_2O = 100:0 (v/v).

6.2.4.1 Preparative High performance liquid chromatography (prep. HPLC)

Polar compound isolation attempts were performed on a "Thermo Scientific Dionex UltiMate 3000" system with UltiMate 3000 pump, UltiMate 3000 autosampler, UltiMate 3000 column compartment, UltiMate 3000 diode array detector (deuterium lamp, λ = 190–380 nm) and a UltiMate 3000 automatic fraction collector. Separation of compounds was carried out on a reversed-phase Macherey-Nagel 125/21 Nucleodur® 100-5 C18ec column (21 × 125 mm, 5.0 µm). Detection of signals was achieved at 210 nm or 254 nm wavelength. The mobile phase consisted of acetonitrile (VWR HiPerSolv, HPLC grade) and water (deionized and purified by Barnstead™ Nanopure™ water purification system) with 0.01 % formic acid. The samples were dissolved in HPLC-grade acetonitrile. The following methods were used:

BB_NucleodurC18_001HCOOH_10to90_25minGrad: oven temperature 26 °C, flow rate 15 mL/min; 0.0-2.0 min MeCN/H_2O = 10:90 (v/v), 2.0-27.0 min linear increase to MeCN/H_2O = 90:10 (v/v), 27.0–32.0 min hold MeCN/H_2O = 90:10 (v/v).

BB_NucleodurC18_001HCOOH_10to90: oven temperature 26 °C, flow rate 15 mL/min; 0.0-5.0 min MeCN/H_2O = 10:90 (v/v), 5.0-15.0 min linear increase to MeCN/H_2O = 90:10 (v/v), 15.0–20.0 min hold MeCN/H_2O = 90:10 (v/v).

6.2.5 Nuclear magnetic resonance spectroscopy (NMR)

Analytical ^{1}H- and ^{13}C-NMR spectra were obtained with the following instruments:

Bruker AVANCE III 300 spectrometer with Autosampler: 300.36 MHz (^{1}H-NMR), 75.53 MHz (^{13}C-NMR) or a Varian Unity Inova 500 high resolution spectrometer: 499.88 MHz (^{1}H-NMR) and 125.70 MHz (^{13}C-NMR);

Analytical ^{31}P and ^{29}Si-NMR spectra were recorded on the following instruments:

Varian Unity Inova 500 high resolution spectrometer: 202.35 MHz (^{31}P-NMR), Varian Inova 300 MHz spectrometer: 121.42 MHz (^{31}P-NMR) and Varian Mercury 300 MHz spectrometer: 121.53 MHz (^{31}P-NMR) and 59.64 MHz (^{29}Si-NMR).

The chemical shifts δ are referenced to the residual protonated solvent signals as internal standard. ($CDCl_3$: δ = 7.26 ppm (^{1}H), 77.16 ppm (^{13}C); MeOD-d_4: δ = 3.31 ppm (^{1}H), 49.00 ppm (^{13}C); D_2O: δ = 4.79 (^{1}H)). The abbreviations for signal multiplicities *J* are s (singlet), d (doublet), dd (doublet of doublet), t (triplet), dt (doublet of triplet), td (triplet of doublet), and m (multiplet). The chemical shifts δ are given in ppm (parts per million), the coupling constants *J* in Hz (Hertz). If it deemed necessary for the correct assignment of the signals and structure confirmation, additional 1D spectra APT, and 2D spectra HSQC, HH-COSY and HMBC were recorded. The chemical shifts δ in ppm (parts per million), the deuterated solvent, the coupling constants *J* in Hertz (Hz) and the integral and assignment of the respective signal are presented. Present quaternary atoms are labelled as C_q (from ^{13}C-NMR data) and aromatic protons as C_{arom} (from ^{1}H-NMR data). The deuterated solvents used for nuclear magnetic resonance spectroscopy were purchased from Euriso-top® ($CDCl_3$, MeOH-d_4) and Deutero® (D_2O). Diastereomeric compounds are given as mixtures and no invididual peak list is stated.

6.2.6 Determination of the melting point

The presented melting points are not corrected and were obtained using a Electrothermal "Mel-Temp®" apparatus including an integrated microscope attachment. The temperature was measured using a mercury thermometer and the samples were measured in open capillary tubes.

6.2.7 High-resolution mass spectroscopy (HRMS)

The high-resolution mass spectra displayed were attained using MALDI-TOF on a Waters Micromass® MALDI micro MX™ spectrometer. α-Cyano-4-hydroxycinnamic acid or dithranol (1,8-dihydroxy-9,10-dihydroanthracen-9-one) provided the matrix and PEG (polyethyleneglycol) served as internal standard. Values stated are m/z.

6.2.8 Specific optical rotation

The determination of the specific optical rotation of compounds was performed on a Perkin Elmer Polarimeter 341 with incorporated sodium vapor lamp at a wavelength of $\lambda = 589$ nm (sodium D-line). The samples were measured at 23 or 24 °C and the concentration displayed is given in g/100 mL. The samples were dissolved in $CHCl_3$, H_2O, or MeOH. The measurements were repeated at least 5 times and the mean value is presented.

6.3 Biological assay

Fluorescence-based inhibition assays were performed by Shalinee Jha at the Institute of Biochemistry in the research group Prof. Peter Macheroux at the Graz University of Technology. The subsequent method was used:

6.3.1 Fluorescence-based inhibiton assay

The enzyme activity of hDPPIII was determined by fluorometrically measuring (excitation, 332 nm; emission, 420 nm) the liberation of 2-naphthylamine at 37 °C in a mixture containing 25 µL of 200 µM Arg-Arg-2-naphthylamide as substrate in 50 mM Tris-HCl buffer, pH 8.0, 0.05-0.1 µM enzyme in a total reaction mixture of 235 µL (White, Tissue Culture treated Krystal 2000 96-well plate from Porvair sciences, Norfolk, UK). The activity assay was carried out by continuous measurement of fluorescence of 2-naphthylamide for 30 min (Fluorescent plate reader from Molecular Devices, Sunnyvale CA, USA). For inhibition assay, the inhibitors were added to the mixture without the substrate and incubated for 10 min at RT. The reaction was initiated by the addition of the substrate.

The concentration of an inhibitor that gave 50 % inhibition (IC_{50}) was evaluated through a series of assays with a fixed substrate concentration but with variable inhibitor concentrations. 5 % DMSO were used in the control assay. Calculations of the percent activity in the presence of increasing inhibitor concentrations was calculated in the following manner:

Percent activity = 100 × (Δfluorescence/ Δfluorescence of control)

Percent activity versus concentration of inhibitor (log scale for inhibitor concentration [x-axis] and linear scale for percent activity [y-axis]) was plotted. Percent activity versus log of concentration was fitted to a sigmoidal dose-response curve applying the four parameter logistic equation with the title “log (inhibitor) versus response-Variable slope” in GraphPad Prism.

6.4 Experimental procedures and analytical data

6.4.1 Dimethyl (2*R*,3*R*)-2,3-dihydroxysuccinate (1)

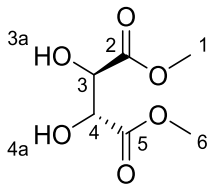

A 250 mL two-neck round-bottom flask with magnetic stirring bar and reflux condenser was dried (evacuated, heated, N_2-purged) and charged with 40 mL dry MeOH and 4.65 g (31 mmol, 1.00 eq) L-(*R,R)*-tartaric acid. The colorless solution was cooled to 0 °C in an ice bath and 11.8 mL (162 mmol, 5.23 eq) thionyl chloride were added at 0 °C (gas evolution). The reaction solution was heated to 70 °C (oil bath) and stirred at 70 °C. After 5 h stirring at this temperature complete conversion was indicated by TLC-control. 20 mL satd. $NaHCO_3$-solution were added to the reaction solution. Vigorous bubbling could be observed and the mixture was stirred for 5 min at RT. All volatile components were removed under reduced pressure with interconnected cooling trap. 40 mL deionized H_2O were added and the reaction mixture was extracted with EtOAc (6 x 40 mL). The combined organic phases were dried over Na_2SO_4, filtrated, and the solvents were removed by rotary evaporation.[42]

$C_6H_{10}O_6$ [178.14 g/mol]

yield: 3.47 g (19.5 mmol, 63 %) light-yellow viscous liquid.

R_f = 0.50 (cyclohexane/EtOAc = 4:1 (v/v), UV 254 nm, staining: CAM = blue).

$[\alpha]_D^{24}$ = 2.143 (c = 3.75, $CHCl_3$).

^{1}H-NMR (300.36 MHz, $CDCl_3$): δ = 4.55 (s, 2H, H-3, H-4), 3.83 (s, 6H, H-1, H-6), 3.45 (s, 2H, H-3a, H-4a).

^{13}C-NMR (75.53 MHz, $CDCl_3$): δ = 172.1 (s, 2C, C_q, C-2, C-5), 72.2 (s, 2C, C-3, C-4), 53.2 (s, 2C, C-1, C-6).

6.4.2 Dimethyl (4*R*,5*R*)-2,2-dimethyl-1,3-dioxolane-4,5-dicarboxylate (2)

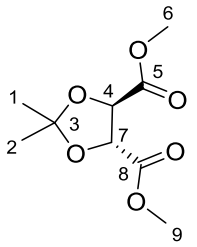

A 500 mL two-neck round-bottom flask with magnetic stirring bar was dried (evacuated, heated, N_2-purged) and charged with 30.0 g (168 mmol, 1.00 eq) (*R*,*R*)-dimethyl tartrate and 301 mL distilled acetone. 26.1 mL (102 mmol, 0.60 eq) $BF_3{\cdot}OEt_2$ (48 % solution) were added to the resulting colorless solution by a dropping funnel over 17 min. Color change from light yellow to dark orange was observed after 3 h stirring at RT. After 5 h reaction time TLC-control of the reaction solution revealed complete conversion. The reaction solution was poured onto 850 mL saturated $NaHCO_3$-solution, vigorous bubbling was observed, and the mixture was stirred for 5 min. The turbid mixture was split into two parts and each was extracted with EtOAc (3 x 500 mL). The combined organic phases were washed with H_2O (2 x 350 mL), dried over Na_2SO_4, filtrated, and the solvents were removed by rotary evaporation. The crude product was purified via flash chromatography (700 g silica gel, 31 x 8.5 cm, eluent: cyclohexane/EtOAc = 4:1 (v/v), fraction size: 300 mL) to yield the desired compound **2** as an orange viscous liquid.[25]

$C_9H_{14}O_6$ [218.21 g/mol]

yield: 29.8 g (137 mmol, 81 %) orange viscous liquid

R_f = 0.30 (cyclohexane/EtOAc = 4:1 (v/v), 254 nm, staining: CAM = blue).

$[\alpha]_D^{24}$ = -22.3 (c = 3.55, $CHCl_3$), lit. $[\alpha]_D^{24}$ = -36.9 (c = 5.1, $CHCl_3$)[25]

^{1}H-NMR (300.36 MHz, $CDCl_3$): δ = 4.79 (s, 2H, H-4, H-7), 3.80 (s, 6H, H-6, H-9), 1.47 (s, 6H, H-1, H-2).

^{13}C-NMR (75.53 MHz, $CDCl_3$): δ = 170.2 (s, 2C, C_q, C-5, C-8), 114.0 (s, 1C, C_q, C-3), 77.1 (s, 2C, C-4, C-7), 52.9 (s, 2C, C-6, C-9), 26.4 (s, 2C, C-1, C-2).

6.4.3 (*S,E*)-2-methyl-*N*-(2-methylpropylidene)propane-2-sulfinamide (3)

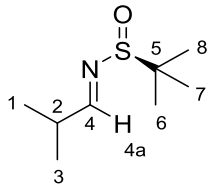

A 250 mL two-neck round-bottom flask with magnetic stirring bar was dried (evacuated, heated, N_2-purged) and charged with 4.51 g (36.1 mmol, 1.1 eq) (*S*)-2-methylpropane-2-sulfinamide and 64 mL dry THF. 3.06 mL (32.9 mmol, 1.0 eq) isobutyraldehyde were added to the colorless slightly turbid solution followed by dropwise addition of 15.04 mL (49.3 mmol, 1.5 eq) titanium isopropoxide via septum over 13 min. Color change to pale yellow was observed and the reaction solution was stirred at RT. After 1 h full conversion was indicated by TLC. 61 mL deionized H_2O were added to the yellow clear reaction solution and formation of significant colorless precipitate was observed. The suspension was extracted with EtOAc (3 x 60 mL) and the combined organic phases were dried over Na_2SO_4, filtrated, and the solvent was removed by rotary evaporation.[27]

$C_8H_{17}NOS$ [175.29 g/mol]

yield: 5.68 g (32.4 mmol, 98 %) light-yellow viscous liquid

R_f = 0.33 (cyclohexane/EtOAc = 5:1 (v/v), 254 nm, staining: $KMnO_4$ = yellow)

$[\alpha]_D^{24}$ = +246.7 (c = 1.12, $CHCl_3$). lit. $[\alpha]_D$ = +320.3 (c = 1.18, $CHCl_3$)[43].

^{1}H-NMR (300.36 MHz, $CDCl_3$): δ = 7.98 (d, $^3J_{HH}$ = 4.3 Hz, 1H, H-4a), 2.71 (d, $^3J_{HH}$ = 4.5 Hz, 1H, H-2), 1.17 (d, $^3J_{HH}$ = 9.2 Hz, 15H, H-1, H-3, H-6, H-7, H-8).

^{13}C-NMR (75.53 MHz, $CDCl_3$): δ = 173.7 (s, 1C, C_q, C-4), 56.6 (s, 1C, C_q, C-5), 35.0 (s, 1C, C-2), 22.4 (s, 3C, C-6, C-7, C-8), 19.0 (s, 2C, C-1, C-3).

6.4.4 ((4*R*,5*R*)-2,2-Dimethyl-1,3-dioxolane-4,5-diyl)bis(diphenylmethanol) (4)

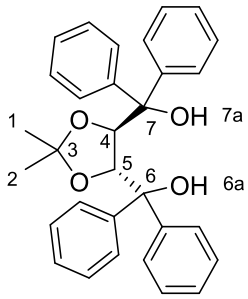

A 1000 mL three-neck round-bottom flask equipped with magnetic stirring bar, reflux condenser and pressure-equalized addition funnel was dried (evacuated, heated, N_2-purged) and charged with 10.4 g (424 mmol, 4.62 eq) magnesium turnings and 0.593 g (2.33 mmol, 0.025 eq) iodine crystals. The addition funnel was charged with 43.5 mL (404.1 mmol, 4.41 eq) bromobenzene and 290 mL dry THF. The magnesium turnings and iodine crystals were dry stirred for 3 min and 40 mL of bromobenzene in dry THF solution were added. Heat evolution and THF evaporation was observed and the reaction mixture was cooled for 3 min in an ice bath followed by addition of the remaining bromobenzene solution over 29 min at a rate in order to maintain reflux of the reaction mixture. Upon complete addition the dark brown reaction mixture was heated to 90 °C (oil bath) to continue reflux and the reaction was stirred for 1 h and subsequently allowed to cool to RT. A solution of 20.01 g (91.7 mmol, 1.0 eq) dimethyl (4*R*,5*R*)-2,2-dimethyl-1,3-dioxolane-4,5-dicarboxylate in 200 mL dry THF was added to the obtained dark brown colored phenylmagnesium bromide Grignard solution via pressure-equalized addition funnel in N_2-counterstream dropwise over 53 min at 0 °C (ice bath cooling). During the addition phase the internal reaction temperature was monitored via thermometer and did not exceed 20 °C. Heat evolution and color change to pale brown was observed during addition. After complete addition, the reaction mixture was heated to 93 °C (oil bath) and stirred for 2 h until TLC-control revealed full conversion. The reaction mixture was slowly cooled to 0 °C (ice bath) followed by subsequent addition of 450 mL saturated NH_4Cl-solution. The formation of colorless precipitate was observed and the reaction mixture was extracted once with 500 mL EtOAc. After the layers were separated the aqueous layer was extracted with EtOAc (3 x 200 mL). The combined organic layers were washed with brine (1 x 250 mL), dried over $MgSO_4$, filtrated, and the solvent was removed by rotary evaporation. The resulting yellow solid was dissolved in 100 mL Et_2O and 300 mL EtOH to form a clear yellow solution. The solvent was removed by rotary evaporation and the obtained yellow foam was dissolved in 20 mL Et_2O followed by addition of 80 mL EtOH. The mixture was cooled in the refrigerator (-18 °C) for 3 d and a colorless precipitate was isolated by

filtration, which was washed first with 200 mL EtOH/Et_2O = 4:1 and then 100 mL EtOH. The colorless solid was dried in oil pump vacuum and heating with oil bath 50 °C for 5 h. The crude colorless product was dissolved in 42 mL toluene and heated to 81 °C (oil bath). The solvent was removed by rotary evaporation. This procedure was repeated once more to remove residual EtOH. The crude yellow product was recrystallized from toluene/n-heptane = 1:1.[25]

$C_{31}H_{30}O_4$ [466.58 g/mol]

yield: 28.9 g (62.0 mmol, 68 %) colorless solid.

R_f = 0.58 (cyclohexane/EtOAc = 3:1 (v/v), UV 254 nm, staining: CAM = blue)

$[\alpha]_D^{24}$ = -67.0 (c = 1.2, $CHCl_3$), lit. $[\alpha]_D^{24}$ = -60.5 (c = 1.0, $CHCl_3$)[44]

mp = 184 °C, lit. 192-194 °C[44].

^{1}H-NMR (300.36 MHz, $CDCl_3$): δ = 7.52 (d, $^3J_{HH}$ = 6.1 Hz, 4H, CH_{arom}), 7.28 (dd, $^2J_{CH}$ = 20.9 Hz, $^3J_{HH}$ = 6.9 Hz, 16H, CH_{arom}), 4.59 (s, 2H, H-4, H-5), 3.99 (bs, 2H, H-6a, H-7a), 1.03 (s, 6H, H-1, H-2).

^{13}C-NMR (75.53 MHz, $CDCl_3$): δ = 146.1 (s, 2C, C_q, C_{arom}), 142.8 (s, 2C, C_q, C_{arom}), 128.7 (s, 4C, C_{arom}), 128.6 (s, 4C, C_{arom}), 127.7 (d, 5C, C_{arom}), 127.4 (d, 5C, C_{arom}), 109.7 (s, 1C, C_q C-3), 81.1 (s, 2C, C-4, C-5), 78.3 (s, 2C, C_q, C-6, C-7), 27.3 (s, 2C, C-1, C-2).

6.4.5 (3a*R*,8a*R*)-2,2-Dimethyl-4,4,8,8-tetraphenyltetrahydro-[1,3]dioxolo[4,5-e][1,3,2]dioxaphosphepine 6-oxide (5)

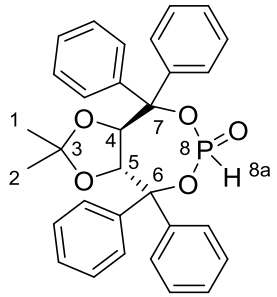

A 250 mL two-neck round-bottom flask with magnetic stirring bar was dried (evacuated, heated, N_2-purged) and charged with 74 mL dry THF, 2.64 mL (30.0 mmol, 2.0 eq) PCl_3 and 6.33 mL (45.0 mmol, 3.0 eq) triethylamine at 0 °C (ice bath cooling). After 10 min stirring at 0 °C a solution of 7.00 g (15.0 mmol 1.0 eq) (*R*,*R*)-TADDOL in 74 mL dry THF was added dropwise over 19 min via syringe to the pale green colored reaction mixture. The reaction mixture was stirred for 80 min at 0 °C followed by addition of 2.11 mL (15.0 mmol, 1.0 eq) triethylamine and 270 µL (15.0 mmol, 1.0 eq) deionized H_2O to the turbid colorless reaction mixture at 0 °C. The reaction mixture was allowed to warm to RT and was stirred for 1.5 h. The reaction mixture was filtrated through a pad of $MgSO_4$, which was rinsed with THF (2 x 50 mL). The combined filtrates were concentrated in vacuo. The crude colorless foamy solid was dissolved in 30 mL DCM and the solvent was removed by rotary evaporation. The crude product was purified via flash chromatography (425 g silica gel, 29 x 6.3 cm, eluent: cyclohexane/EtOAc = 5:1 to 3:1 (v/v), fraction size: 100 mL) to yield the desired compound **5** as orange viscous liquid.[26]

$C_{31}H_{29}O_5P$ [512.54 g/mol]

yield: 5.90 g (11.5 mmol, 77 %) colorless solid.

R_f = 0.13 (cyclohexane/EtOAc = 5:1 (v/v), 254 nm, staining: CAM = blue)

$[\alpha]_D^{24}$ = -173.8 (c = 1.31, $CHCl_3$), lit.: $[\alpha]_D^{21}$ = -268.4 (c = 0.275, $CHCl_3$)[45]

mp = 215-220 °C, lit.: 224-226 °C.[45]

^{1}H-NMR (300.36 MHz, $CDCl_3$): δ = 7.52 (t, $^3J_{HH}$ = 6.5 Hz, 4H, CH_{arom}), 7.26 (ddd, $^2J_{CH}$ = 22.3 Hz, $^3J_{HH}$ = 13.0 Hz, $^3J_{HH}$ = 6.5 Hz 15H, CH_{arom}), 7.01 (d, $^1J_{HP}$ = 726.6 Hz, 1H, H-8a), 5.29 (d, $^3J_{HH}$ = 8.0 Hz, 1H, H-4), 5.14 (d, $^3J_{HH}$ = 8.0 Hz, 1H, H-5), 0.68 (s, 3H, H-1), 0.49 (s, 3H, H-2).

^{13}C-NMR (75.53 MHz, $CDCl_3$): δ = 143.8 (d, $^3J_{CP}$ = 2.6 Hz, 1C, C_q, C_{arom}), 143.3 (d, $^3J_{CP}$ = 1.8 Hz, 1C, C_q, C_{arom}), 139.3 (d, $^3J_{CP}$ = 8.6 Hz, 1C, C_q, C_{arom}), 139.1 (d, $^3J_{CP}$ = 6.3 Hz, 1C, C_q, C_{arom}), 128.9 (s, 4C, C_{arom}), 128.8 (s, 4C, C_{arom}), 128.6 (s, 4C, C_{arom}) 128.4 (s, 1C, C_{arom}), 128.3 (s, 1C, C_{arom}), 128.1 (s, 1C, C_{arom}), 128.0 (s, 1C, C_{arom}), 127.6 (s, 1C, C_{arom}) 127.5 (s, 1C, C_{arom}), 127.0 (s, 1C, C_{arom}) 126.9 (s, 1C,C_{arom}), 114.5 (s, 1C, C_q, C-3), 88.8 (d, $^2J_{CP}$ = 9.1 Hz, $^2J_{CP}$ = 2.6 Hz, 2C, C_q, C-6, C-7), 80.2 (d, $^3J_{CP}$ = 2.8 Hz, 1C, C-4), 79.9 (d, $^3J_{CP}$ = 1.6 Hz, 1C, C-5), 26.8 (s, 1C, C-1), 26.4 (s, 1C, C-2).

6.4.6 (*S*)-1-Methoxy-1-oxo-3-phenylpropan-2-aminium hydrochloride (6)

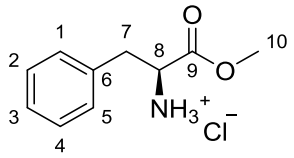

A 100 mL three-neck round-bottom flask with magnetic stirring bar was dried (evacuated, heated, N_2-purged) and charged with 3.62 g (21.8 mmol, 1.0 eq) L-phenylalanine and 22 mL dry MeOH. L-Phenylalanine was not fully dissolved and the stirred suspension was cooled to -20 °C in an ice/NaCl bath in a Dewar vessel. After 10 min 6.55 mL (90.12 mmol, 4.1 eq) $SOCl_2$ were added dropwise via dropping funnel over 18 min at -20 °C. The reaction mixture turned into an unstirrable suspension and additional 15 mL dry MeOH were added. After 30 min the reaction mixture was allowed to warm to RT. The reaction mixture turned into a clear pale yellow colored solution and was stirred overnight at RT. After 15 h the reaction solidified due to MeOH evaporation by N_2-stream. Additional 30 mL MeOH were added to give a pale yellow clear solution. Since no full conversion was observed additional 3.16 mL (43.58 mmol, 2.0 eq) $SOCl_2$ were added dropwise over 3 min. TLC-control after 2 d indicated full conversion. Residual $SOCl_2$ and the solvent MeOH was removed under reduced pressure (oil pump vacuum) with an cooling trap. The crude colorless solid was redissolved in 30 mL MeOH and the solvent was removed under reduced pressure.[32]

$C_{10}H_{14}ClNO_2$ [215.68 g/mol]

yield: 2.63 g (12.2 mmol, 56 %) colorless solid.

R_f = 0.65 (n-butanol/AcOH/H_2O = 3:1:1 (v/v/v), 254 nm, staining: Ninhydrin = orange/red)

$[\alpha]_D^{24}$ = 7.99 (c = 1.33, MeOH). lit. $[\alpha]_D^{20}$ = +15.6 (c = 1.00, MeOH).[46]

mp = 150-155 °C. lit.: 150-151 °C.[46]

^{1}H-NMR (300.36 MHz, MeOD-d_4): δ = 7.33 (dt, $^3J_{CH}$ = 20.3 Hz, $^3J_{HH}$ = 6.6 Hz, 5H, H-1, H-2, H-3, H-4, H-5), 4.36 (t, $^3J_{HH}$ = 6.7 Hz, 1H, H-8), 3.81 (s, 3H, H-10), 3.22 (dd, $^2J_{HH}$ = 14.5 Hz, $^3J_{HH}$ = 6.7 Hz, 2H, H-7).

^{13}C-NMR (75.53 MHz, MeOD-d_4): δ = 170.4 (s, 1C, C_q, C-9), 135.3 (s, 1C, C_q, C-6), 130.4 (s,2C, C-1, C-5), 130.2 (s, 2C, C-2, C-4), 129.0 (s, 1C, C-3), 55.2 (s, 1C, C-8), 53.6 (s, 1C, C-10),37.4 (s, 1C, C-7).

6.4.7 (*S*)-2-(Trimethylsilyl)ethyl (tert-butoxycarbonyl)-L-phenylalaninate (7)

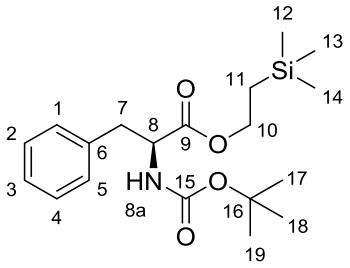

A 100 mL Schlenk vessel with magnetic stirring bar was dried (evacuated, heated, N_2-purged) and charged with 2.01 g (7.54 mmol, 1.0 eq) Boc-Phe-OH, 1.55 g (7.92 mmol, 1.05 eq) EDC·HCl and 17 mL dry DCM. 1.15 mL (7.92 mmol, 1.05 eq) trimethylsilylethanol were added to the colorless reaction solution and the reaction was cooled to 0 °C in an ice bath. 0.1 g (0.8 mmol, 0.106 eq) 4-DMAP were added to the reaction solution at 0 °C, the ice bath was removed to allow the light yellow colored reaction to warm to RT. After 2 h TLC-control revealed full conversion of starting material and the reaction solution was diluted with 30 mL DCM and consecutively washed with deionized water (20 mL), aqueous 3M HCl-solution (20 mL), satd. $NaHCO_3$ solution (20 mL), and brine (20 mL). The combined aqueous layers were extracted with DCM (3 x 20 mL) and the combined organic layers were dried over $MgSO_4$, filtrated and the solvent was removed under reduced pressure. The crude product was purified via flash chromatography (83 g silica gel, 31 x 3.7 cm, eluent: cyclohexane/EtOAc = 15:1 (v/v) , fraction size: 55 mL) to yield the desired compound **7** as a colorless viscous liquid.[36]

$C_{19}H_{31}NO_4Si$ [365.55 g/mol]

yield: 2.18 g (5.96 mmol, 79 %) colorless viscous liquid.

R_f = 0.24 (cyclohexane/EtOAc = 15:1 (v/v), UV 254 nm, staining: CAM = blue)

^{1}H-NMR (300.36 MHz, $CDCl_3$): δ = 7.34-7.20 (m, 3H, H-2, H-3, H-4), 7.14 (d, $^3J_{HH}$ = 6.6 Hz, 2H, H-1, H-5), 4.97 (d, $^3J_{HH}$ = 7.2 Hz, 1H, H-8a), 4.54 (d, $^3J_{HH}$ = 6.6 Hz, 1H, H-8), 4.18 (td, $^2J_{HH}$ = 7.6 Hz, $^3J_{HH}$ = 5.0 Hz, 2H, H-10), 3.19-2.95 (m, 2H, H-7), 1.41 (s, 9H, H-17, H-18, H-19), 0.95 (dd, $^2J_{HH}$ = 10.3 Hz, $^3J_{HH}$ = 6.7 Hz, 2H, H-11), 0.03 (s, 9H, H-12, H-13, H-13).

^{13}C-NMR (75.53 MHz, $CDCl_3$): δ = 172.1 (s, 1C, C_q, C-9), 155.2 (s, 1C, C_q, C-15), 136.3 (s, 1C, C_q, C-6), 192.5 (s, 2C, C-1, C-5), 128.6 (s, 2C, C-2, C-4), 127.1 (s, 1C, C-3), 79.9 (s, 1C, C-16), 63.8 (s, 1C, C-10), 54.7 (s, 1C, C-8), 38.6 (s, 1C, C-7), 28.4 (s, 3C, C-17, C-18, C-19), 17.5 (s, 1C, C-11), -1.4 (s, 3C, C-12, C-13, C-14).

6.4.8 (*S*)-1-Oxo-3-phenyl-1-(2-(trimethylsilyl)ethoxy)propan-2-aminium hydrochloride (8)

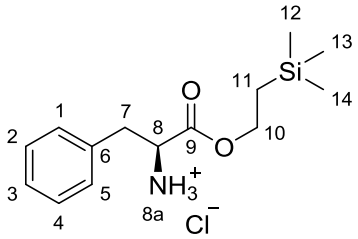

A 50 mL round-bottom flask equipped with a Schlenk adapter with magnetic stirring bar was dried (evacuated, heated, N_2-purged) and charged with 2.17 g (5.94 mmol, 1.0 eq) (*S*)-2-(trimethylsilyl)ethyl (tert-butoxycarbonyl)-L-phenylalaninate. The glass stopper was replaced by a rubber septum and 24 mL (96 mmol, 16.2 eq) 4 M HCl in 1,4-dioxane were added via syringe to give a colorless solution which was stirred at RT. After 1 h TLC-control revealed full conversion and all volatile components were removed in oil pump vacuum with interconnected cooling trap. The crude colorless solid was dissolved in EtOH (2 x 20 mL) and MeOH (1 x 20 mL) and the solvent was removed in vacuum after each addition. The crude product was used in the following steps without further purification. [36]

$C_{14}H_{28}ClNO_2Si$ [301.89 g/mol]

yield: 1.72 g (5.70 mmol, 96 %) colorless sticky solid.

R_f = 0.04 (cyclohexane/EtOAc/AcOH = 2:1:1 % (v/v/v), UV 254 nm, staining: CAM = blue)

mp = 135-140 °C.

$[\alpha]_D^{24}$ = +0.15 (c = 1.16, $CHCl_3$).

^{1}H-NMR (300.36 MHz, $CDCl_3$): δ = 8.78 (s, 3H, H-8a), 7.29 (t, $^3J_{HH}$ = 7.2 Hz, 5H, H-1, H-2, H-3, H-4, H-5), 4.33 (s, 1H, H-8), 4.25-4.07 (m, 2H, H-10), 3.40 (dd, $^2J_{HH}$ = 17.3 Hz, $^3J_{HH}$ = 5.7 Hz, 2H, H-7), 0.89 (dd, $^2J_{HH}$ = 10.3 Hz, $^3J_{HH}$ = 6.4 Hz, 2H, H-11),-0.01 (s, 9H, H-12, H-13, H-14).

^{13}C-NMR (75.53 MHz, $CDCl_3$): δ = 168.8 (s, 1C, C_q, C-9), 134.1 (s, 1C, C_q, C-6), 129.9 (s, 2C, C-1, C-5), 129.1 (s, 2C, C-2, C-4), 127.8 (s, 1C, C-3), 65.2 (s, 1C, C-10), 54.4 (s, 1C, C-8), 36.5 (s, 1C, C-7), 17.4 (s, 1C, C-11), 1.47 (s, 3C, C-12, C-13, C-14).

6.4.9 (9*H*-Fluoren-9-yl)methyl (tert-butoxycarbonyl)-L-phenylalaninate (9)

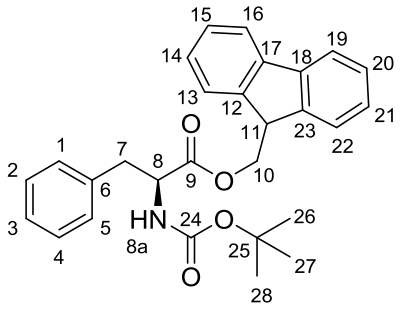

A dry 100 mL Schlenk vessel with magnetic stirring bar was dried (evacuated, heated, N_2-purged) and charged with 1.61 g (6.06 mmol, 1.0 eq) Boc-Phe-OH and 23 mL dry DCM. 1.05 mL (6.03 mmol, 1.0 eq) DIPEA were added and the colorless reaction solution was cooled to 0°C in an ice bath. A solution of 1.75 g (6.76 mmol, 1.12 eq) 9-fluorenylmethyl chloroformate in 8 mL DCM was added dropwise over 10 min at 0 °C (gas evolution). After 7 min 89.3 mg (740 µmol, 0.12 eq) 4-DMAP were added and the reaction solution was stirred at 0 °C. After 1.5 h TLC-control revealed full conversion. The reaction was diluted with 20 mL DCM and consecutively washed with 5 % citric acid (1 x 25 mL) and brine (1 x 25 mL). The organic phase was dried over Na_2SO_4, filtrated, and the solvent was removed in vacuum. The crude product was purified via flash chromatography (279 g silica gel, 24 x 6.5 cm, eluent: cyclohexane/EtOAc = 12:1 (v/v), fraction size: 186 mL) to yield the desired compound **9** as colorless viscous liquid.[37]

$C_{28}H_{29}NO_4$ [443.54 g/mol]

yield: 1.41 g (3.18 mmol, 53 %) colorless solid.

R_f = 0.04 (cyclohexane/EtOAc = 12:1 (v/v), UV 254 nm, staining: CAM = blue)

$[\alpha]_D^{24}$ = -7.5 (c = 1.26, $CHCl_3$).

mp = 110-115 °C.

^{1}H-NMR (300.36 MHz, $CDCl_3$): δ = 7.91-6.95 (m, 13H, H-1, H-2, H-3, H-4, H-5, H-13, H-14 , H-15, H-16, H-19, H-20, H-21, H-22), 4.96 (d, $^3J_{HH}$ = 7.2 Hz, 1H, H-8a), 4.65 (d, $^3J_{HH}$ = 6.1 Hz, 1H, H-8), 4.43 (t, $^3J_{HH}$ = 8.4 Hz, 2H, H-10), 4.13 (t, $^3J_{HH}$ = 7.2 Hz, 1H, H-11), 3.02 (dd, $^2J_{HH}$ = 9.9 Hz, $^3J_{HH}$ = 6.3 Hz, 2H, H-7), 1.42 (s, 9H, H-26, H-27, H-28).

^{13}C-NMR (75.53 MHz, $CDCl_3$): δ = 172.1 (s, 1C, C_q, C-9), 155.2 (s, 1C, C_q, C-24), 143.6 (s, 2C, C_q, C-12, C-23), 141.5 (s, 2C, C_q, C-17, C-18), 136.1 (s, 1C, C_q, C-6), 129.4 (s, 2C, C-2, C-4), 128.7 (s, 2C, C-1, C-5), 128.0 (s, 2C, C-15, C-20), 127.3 (s, 2C, C-16, C-19), 127.2

(s, 1C, C-3), 125.2 (s, 2C, C-14, C-21), 120.2 (s, 2C, C-13, C-22), 80.1 (s, 1C, C_q, C-25), 67.3 (s, 1C, C-10), 54.7 (s, 1C, C-8), 46.9 (s, 1C, C-11), 38.5 (s, 1C, C-7), 28.4 (s, 3C, C-26, C-27, C-28).

6.4.10 (*S*)-*N*-((1*R*)-1-((3a*R*,8a*S*)-2,2-Dimethyl-6-oxido-4,4,8,8-tetraphenylpentahydro-[1,3]dioxolo[4,5-e][1,2]oxaphosphepin-6-yl)-2-methylpropyl)-2-methylpropane-2-sulfinamide (10)

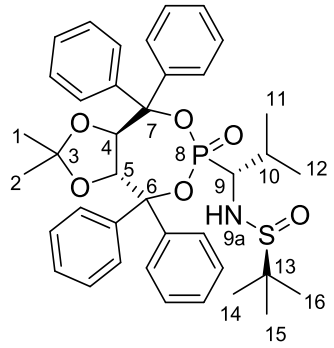

A 500 mL three-neck round-bottom flask equipped with magnetic stirring bar and reflux condenser was dried (evacuated, heated, N_2-purged) and charged with 4.87 g (9.50 mmol, 1.0 eq) (3a*R*,8a*R*)-2,2-dimethyl-4,4,8,8-tetraphenyltetrahydro-[1,3]dioxolo[4,5 e][1,3,2] dioxaphosphepine 6-oxide and dissolved in 90 mL dry DCM. 1.62 g (11.4 mmol, 1.2 eq) K_2CO_3 were added to the colorless solution. After 10 min stirring a solution of 2.19 g (12.3 mmol, 1.3 eq) (*S*,*E*)-2-methyl-*N*-(2-methylpropylidene)propane-2-sulfinamide in 40 mL DCM was added dropwise over 10 min via syringe through a septum. The turbid colorless reaction mixture was stirred at RT (K_2CO_3 did not dissolve completely). After 17 h stirring at RT TLC-control revealed incomplete conversion and subsequently 397 mg (2.85 mmol, 0.3 eq) K_2CO_3 and 512 mg (2.85 mmol, 0.3 eq) (*S*,*E*)-2-methyl-*N*-(2-methylpropylidene)-propane-2-sulfinamide were added to the reaction mixture, which was stirred at RT for 3 d until full conversion of the starting materials was detected by TLC. 80 mL H_2O were added to the colorless turbid reaction mixture followed by extraction with DCM (3 x 60 mL), drying over Na_2SO_4, filtration and removing the solvents in vacuum. The crude product was purified by recrystallization from 320 mL Et_2O.[29]

$C_{39}H_{46}NO_6PS$ [687.83 g/mol]

yield: 5.02 g (7.30 mmol, 77 %) colorless solid.

R_f = 0.24 (cyclohexane/EtOAc = 3:1 (v/v), UV 254 nm, staining: CAM = blue)

$[\alpha]_D^{24}$ = -173.4 (c = 1.0, $CHCl_3$), lit. $[\alpha]_D^{20}$ = -163.0 (c = 1.0, $CHCl_3$)[29].

mp = 220 °C lit.: 86-88 °C.[29]

^{1}H-NMR (300.36 MHz, $CDCl_3$): δ = 7.55 (dd, $^{2}J_{CH}$ = 16.8 Hz, $^{3}J_{HH}$ = 7.8 Hz, 8H, CH_{arom}), 7.47-7.15 (m, 12H, CH_{arom}), 5.55 (d, $^{3}J_{HH}$ = 7.8 Hz, 1H, H-4), 5.34 (d, $^{3}J_{HH}$ = 7.8 Hz, 1H, H-5), 3.70 (dd, $^{2}J_{HH}$ = 20.0, $^{3}J_{HH}$ = 7.4 Hz, 1H, H-9), 3.43 (dd, $^{2}J_{HH}$ = 12.4 Hz, $^{3}J_{HH}$ = 8.2 Hz, 1H, H-9a), 2.42 (d, $^{3}J_{HH}$ = 6.8 Hz, 1H, H-10), 0.96 (d, $^{3}J_{HH}$ = 12.2 Hz, 15H, H-11, H-12, H-13, H-14, H-15, H-16), 0.77 (s, 3H, H-1), 0.55 (s, 3H, H-2).

^{13}C-NMR (75.53 MHz, $CDCl_3$): δ = 144.9 (d, $^{2}J_{CP}$ = 7.4 Hz, 1C, C_q, C_{arom}), 144.3 (s, 1C, C_q, C_{arom}), 139.9 (s, 1C, C_{arom}), 139.7 (d, $^{2}J_{CP}$ = 9.9 Hz, 1C, C_{arom}), 130.2 (s, 2C, C_{arom}), 129.5 (s, 2C, C_{arom}), 128.7 (s, 2C, C_{arom}), 128.4 (s, 2C, C_{arom}), 128.2 (s, 2C, C_{arom}), 128.1 (s, 2C, C_{arom}), 127.7 (s, 2C, C_{arom}), 127.6 (s, 2C, C_{arom}), 127.3 (s, 2C, C_{arom}), 127.0 (s, 2C, C_{arom}), 114.1 (s, 1C, C_q, C-3), 92.4 (d, $^{2}J_{CP}$ = 14.1 Hz, 1C, C_q C-6), 87.3 (d, $^{2}J_{CP}$ = 8.4 Hz, 1C, C_q, C-7), 79.2 (d, $^{2}J_{CP}$ = 2.8 Hz, 1C, C-4), 78.9 (d, $^{2}J_{CP}$ = 8.4 Hz, 1C, C-5), 58.6 (d, $^{1}J_{CP}$ = 149.4 Hz, 1C, C-9), 57.0 (s, 1C, C_q, C-13), 30.4 (d, $^{2}J_{CP}$ = 5.3 Hz, 1C, C-10), 27.2 (s, 1C, C-1), 26.7 (s, 1C, C-2), 22.7 (s, 3C, C-14, C-15, C-16), 20.6 (d, $^{3}J_{CP}$ = 16.6 Hz, 1C, C-11), 17.2 (s, 1C, C-12).

^{31}P-NMR (121.4 MHz, $CDCl_3$): δ = 20.6 (s, 1P, P-8).

6.4.11 (*R*)-1-Amino-2-methylpropyl)phosphonic acid (11)

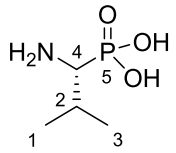

A 500 mL three-neck round-bottom flask equipped with magnetic stirring bar and reflux condenser was charged with 3.49 g (5.08 mmol, 1.0 eq) (*S*)-*N*-((*R*)-1-((3a*R*,8a*R*)-2,2-dimethyl-6-oxido-4,4,8,8-tetraphenyltetrahydro-[1,3]dioxolo[4,5-e][1,3,2] dioxaphosphepin-6-yl)-2-methylpropyl)-2-methylpropane-2-sulfinamide, 117 mL toluene, and 117 mL aqueous 4M HCL-solution. The turbid colorless biphasic mixture was heated and stirred vigorously at 105 °C in an oil bath. After 2.5 h HPLC-control revealed full conversion of the starting material and the colorless reaction mixture was allowed to cool to RT. The layers were separated in a separation funnel. The aqueous layer was concentrated by rotary evaporation and dried in oil pump vacuum. The crude viscous liquid was dissolved in 4 mL dry EtOH and 300 µL propylene oxide were added. [Safety note: Propylene oxide is carcinogenic and volatile, consequently special care needs to be taken during handling to avoid health hazards]. Upon addition formation of a colorless precipitate was observed and the mixture was placed in the freezer (-18 °C) for crystallization. After 3 d the colorless crystals were collected by filtration, which were washed with cold Et_2O (2 x 5 mL) and the product was dried in oil pump vacuum.[29]

$C_4H_{12}NO_3P$ [153.12 g/mol]

yield: 563 mg (3.67 mmol, 72 %) colorless solid.

R_f = 0.24 (n-butanol/AcOH/H_2O = 3:1:1 (v/v/v), staining: Ninhydrin = red)

$[\alpha]_D^{24}$ = +0.8 (c = 1.11, 2M NaOH), lit.: $[\alpha]_D^{20}$ = +1.0 (c = 1.0, 2M NaOH)[29].

mp = 265-270 °C, lit.: 260-263 °C.[29]

^{1}H-NMR (300.36 MHz, D_2O-d_2): δ = 3.09 (dd, $^2J_{HH}$ = 14.0 Hz, $^3J_{HH}$ = 6.3 Hz, 1H, H-4), 2.22 (m, 1H, H-2), 1.09 (dd, $^2J_{HH}$ = 12.1 Hz, $^3J_{HH}$ = 6.9 Hz, 6H, H-1, H-3).

^{13}C-NMR (75.53 MHz, D_2O-d_2): δ = 54.9 (d, $^1J_{CP}$ = 141.6 Hz, 1C, C-4), 27.6 (s, 1C, C-2), 18.8 (dd, $^3J_{CP}$ = 145.0 Hz, $^3J_{CP}$ = 6.8 Hz, 2C, C-1, C-3).

^{31}P-NMR (121.42 MHz, D_2O-d_2): δ = 12.8 (s, 1P, P-5).

6.4.12 (*R*)-(1-(((Benzyloxy)carbonyl)amino)-2-methylpropyl)phosphonic acid (12)

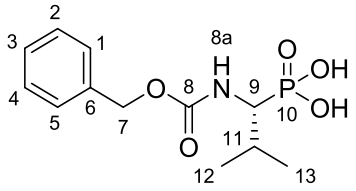

A 25 mL round-bottom flask equipped with magnetic stirring bar was charged with 357 mg (2.33 mmol, 1.0 eq) (*R*)-(1-amino-2-methylpropyl)phosphonic acid, 10.1 mL deionized H_2O, 512 mg (4.66 mmol, 2.0 eq) Na_2CO_3, and 235 mg (2.33 mmol, 1.0 eq) $NaHCO_3$. 1.3 mL acetone were added to the colorless reaction solution and the reaction was cooled to 0 °C in an ice bath. After 10 min 509 µL (3.50 mmol, 1.5 eq) benzyl chloroformate were added dropwise over 1 min to the reaction solution at 0 °C. The ice bath was removed and the reaction was allowed to warm to RT and stirred. The pH of the reaction was monitored every hour and in case pH = 9 was observed additional 285 mg (2.70 mmol, 1.15 eq) Na_2CO_3 were added to the reaction to maintain a pH > 8. TLC-control of the reaction after 19 h revealed incomplete conversion. The reaction was cooled to 0 °C in an ice bath and additional 331 µL (2.33 mmol, 1.0 eq) benzyl chloroformate were added to the turbid colorless reaction mixture and the cooling bath was removed after addition. After stirring for 4.5 h full conversion was detected by TLC. The solvent was evaporated under reduced pressure and the colorless residue was dissolved in 20 mL deionized H_2O and extracted with Et_2O (3 x 18 mL). The organic layer was discarded. The aqueous phase was acidified with 8 mL aqueous 4 M HCl-solution to pH = 1, (colorless precipitate formation). Upon addition of 10 mL EtOAc the precipitate dissolved again. The layers were separated and the aqueous phase was extracted with EtOAc (3 x 19 mL) and the combined organic phases were dried over Na_2SO_4, filtrated, and the solvent was removed in vacuum. The colorless crude product was dried in oil pump vacuum and was used in the subsequent step without further purification.[30]

$C_{12}H_{18}NO_5P$ [287.25 g/mol]

yield: 577 mg (2.01 mmol, 86 %) colorless solid.

R_f = 0.24 (n-butanol/AcOH/H_2O = 3:1:1 (v/v/v), UV 254 nm)

$[\alpha]_D^{24}$ = -12.4 (c = 1.02, MeOH).

mp = 75-80 °C

^{1}H-NMR (300.36 MHz, MeOD-d_4): δ = 7.32 (dd, $^{2}J_{CH}$ = 15.4 Hz, $^{3}J_{HH}$ = 7.5 Hz, 5H, H-1, H-2, H-3, H-4, H-5), 5.12 (s, 2H, H-7), 3.84 (dd, $^{2}J_{HH}$ = 18.7 Hz, $^{3}J_{HH}$ = 4.7 Hz, 1H, H-9), 2.29-2.09 (m, 1H, H-11), 1.17-1.08 (m, 6H, H-12, H-13).

^{13}C-NMR (75.53 MHz, MeOD-d_4): δ = 159.0 (d, $^{3}J_{CP}$ = 6.9 Hz, 1C, C_q, C-8), 138.3 (s, 1C, C_q, C-6), 129.4 (s, 2C, C-2, C-4), 129.0 (s, 1C, C-3), 128.8 (s, 2C, C-1, C-5), 67.8 (s, 1C, C-7), 55.5 (d, $^{1}J_{CP}$ = 153.1 Hz, 1C, C-4), 30.4 (d, $^{2}J_{CP}$ = 4.4 Hz, 1C, C-11), 21.2 (d, $^{3}J_{CP}$ = 11.2 Hz, 1C, C-1), 18.5 (d, $^{3}J_{CP}$ = 5.4 Hz, 1C, C-3).

^{31}P-NMR (121.42 MHz, MeOD-d_4): δ = 22.2 (d, $^{1}J_{CP}$ = 58.1 Hz, 1P, P-10).

6.4.13 Benzyl ((1*R*)-1-((allyloxy)(hydroxy)phosphoryl)-2-methylpropyl)carbamate (13)

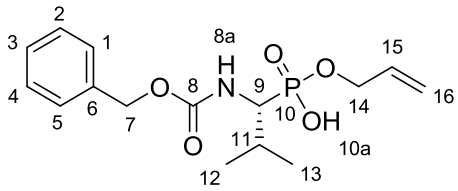

A 10 mL Schlenk vessel equipped with magnetic stirring bar was dried (evacuated, heated, N_2-purged) and charged with 241.3 mg (0.839 mmol, 1.0 eq) (*R*)-(1-(((benzyloxy)carbonyl) amino)-2-methylpropyl)phosphonic acid and 2.80 mL dry DMF. The reaction solution was cooled to -14 °C in a NaCl/ice bath and after 4 min 73 µL (1.01 mmol, 1.2 eq) $SOCl_2$ were added to the reaction solution (gas evolution). After 45 min stirring 115 µL (1.68 mmol, 2.0 eq) allyl alcohol were added to the light yellow colored reaction solution at -5 °C. After addition the cooling bath was removed and the reaction was allowed to warm to RT. Full conversion of the starting material was detected after 1 h and all volatile components were removed under reduced pressure. The light yellow residue was dissolved in 9 mL saturated $NaHCO_3$ and the solution was extracted with EtOAc (3 x 10 mL). The organic layer was discarded. The aqueous layer was acidified from pH = 8 to pH = 1 by addition of 7 mL aqueous 4 M HCl (colorless precipitate formation). Upon addition of 10 mL EtOAc the precipitate dissolved again. The layers were separated and the aqueous layer was extracted with EtOAc (3 x 10 mL). The combined organic layers were dried over Na_2SO_4, filtrated, and the solvent was removed under reduced pressure. The crude product was dried in oil pump vacuum and was used without further purification.[31]

$C_{15}H_{22}NO_5P$ [327.32 g/mol]

yield: 245 mg (0.748 mmol, 89 %) colorless solid.

R_f = 0.66 (DCM/MeOH = 2:1 (v/v), UV 254 nm, staining: CAM = blue).

$[\alpha]_D^{24}$ = -17.6 (c = 1.22, $CHCl_3$).

mp = 90-95 °C.

^{1}H-NMR (300.36 MHz, $CDCl_3$): δ = 9.97 (s, 1H, 10a), 7.33 (s, 5H, H-1, H-2, H-3, H-4, H-5), 5.85 (dd, $^2J_{HH}$ = 10.5 Hz,$^3J_{HH}$ = 5.2 Hz, 1H, H-15), 5.53-4.84 (m, 5H, H-7, H-16, H-8a), 4.49 (s, 2H, H-14), 4.05 (m, 1H, H-9), 2.19 (s, 1H, H-11), 1.24-0.69 (m, 6H, H-12, H-13).

^{13}C-NMR (75.53 MHz, $CDCl_3$): δ = 156.6 (d, $^3J_{CP}$ = 6.6 Hz, 1C, C_q, C-8), 136.4 (s, 1C, C_q, C-6), 132.7 (d, $^3J_{CP}$ = 6.4 Hz, 1C, C-15), 128.7 (s, 2C, C-2, C-4), 128.3 (s, 1C, C-3), 128.2 (s,

2C, C-1, C-5), 118.2 (s, 1C, C-16), 67.4 (s, 1C, C-7), 66.6 (d, $^{2}J_{CP}$ = 6.8 Hz, 1C, C-14), 53.0 (d, $^{1}J_{CP}$ = 155.3 Hz, 1C, C-9), 29.1 (d, $^{2}J_{CP}$ = 4.3 Hz, 1C, C-11), 20.6 (d, $^{3}J_{CP}$ = 12.5 Hz, 1C, C-12), 17.8 (d, $^{3}J_{CP}$ = 4.3 Hz, 1C, C-13).

^{31}P-NMR (121.42 MHz $CDCl_3$): δ = 26.7 (s), 26.0 (s).

HR-MS (MALDI-TOF): *m/z* $[M+Na]^+$ calcd. for $C_{15}H_{22}NO_5PNa$: 350.1133; found: 350.1116.

6.4.14 Methyl ((allyloxy)((*R*)-1-(((benzyloxy)carbonyl)amino)-2-methylpropyl)phosphoryl)-L-phenylalaninate (14)

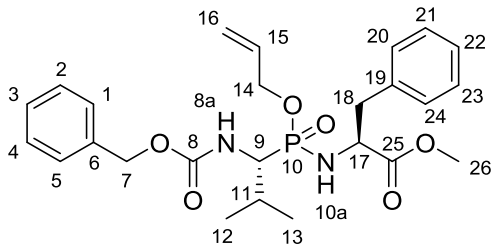

A 20 mL Schlenk vessel with magnetic stirring bar was dried (evacuated, heated, N_2-purged) and charged with 1 mL dry DCM and cooled to 0 °C (ice bath). 42 µL (575 µmol, 4.0 eq) $SOCl_2$ were added followed by dropwise addition of a solution of 95 mg (290 µmol, 2.0 eq) benzyl ((1*R*)-1-((allyloxy)(hydroxy)phosphoryl)-2-methylpropyl)carbamate in 1.5 mL DCM over 28 min at 0 °C. After addition the cooling bath was removed and the reaction was stirred at RT for 3 h. Subsequently all volatile components were removed in vacuum with interconnected cooling trap. The colorless viscous residue was dissolved in 2.0 mL dry DCM and 75.1 µL (431 µmol, 3.0 eq) DIPEA were added (gas evolution, color change to yellow). After 3 min 32.2 mg (144 µmol, 1.0 eq) (*S*)-1-methoxy-1-oxo-3-phenylpropan-2-aminium hydrochloride were added to the yellow colored solution and the reaction was heated to 40 °C in an oil bath and stirred overnight. Full conversion was observed after 12 h by TLC-control. The light yellow reaction solution was diluted with 6 mL EtOAc and consecutively washed with 5 % citric acid (3 x 10 mL), 1M HCl (1 x 10 mL), 1M NaOH (1 x 10 mL) and brine (1 x 10 mL). The separated organic layer was dried over Na_2SO_4, filtrated, and the solvent was removed in vacuum. The crude product was purified via flash chromatography (6 g silica gel, 30 x 1.4 cm, eluent: cyclohexane/EtOAc = 1:1 (v/v), fraction size: 1.5 mL). The product was obtained as a mixture of diastereomers.[29]

$C_{25}H_{33}N_2O_6P$ [488.52 g/mol]

yield: 32.6 mg (66.7 µmol, 46 %) colorless solid.

R_f = 0.23 (cyclohexane/EtOAc = 1:1 (v/v), UV 254 nm, staining: CAM = blue).

$[\alpha]_D^{24}$ = -0.54 (c = 1.03, $CHCl_3$).

mp = 105-110 °C.

^{1}H-NMR (300.36 MHz, $CDCl_3$, mixture of 2 diastereomers assigned on the basis of COSY & HSQC): δ = 7.66-6.90 (m, 10H, H-1, H-2, H-3, H-4, H-5, H-20, H-21, H-22, H-23, H-24), 5.93-5.64 (m, 1H, H-15), 5.34-4.91 (m, 5H, H-7, H-16, H-8a), 4.65-4.12 (m, 3H, H-14, H-17), 4.12-3.82 (m, 1H, H-9), 3.74-3.57 (m, 3H, H-26), 3.22-2.70 (m, 3H, H-18, H-10a), 2.27-2.05 (m, 1H, H-11), 0.95 (dd, $^{2}J_{HH}$ = 15.8 Hz, $^{3}J_{HH}$ = 6.7 Hz, 6H, H-12, H-13).

^{13}C-NMR (75.53 MHz, $CDCl_3$, mixture of 2 diastereomers assigned on the basis of COSY & HSQC): δ = 173.5 (s, 1C, C_q, C-25), 156.6 (d, $^{3}J_{CP}$ = 13.8 Hz, 1C, C_q, C-8), 136.3 (s, 1C,C_q, C-6), 136.0 (s, 1C, C_q, C-19), 133.2 (d, $^{3}J_{CP}$ = 3.1 Hz, 1C, C-15), 129.7-129.5 (m, 4C, C-2, C-4, C-21, C-23) 128.9-128.6 (m, 2C, C-20, C-24),128.4-128.2 (m, 3C, C-3, C-1, C-5), 127.3-127.1 (m, 1C, C-22), 117.7 (s, 1C, C-16), 67.3 (s, 1C, C-7), 64.9 (d, $^{2}J_{CP}$ = 7.3 Hz, 1C, C-14), 64.5 (d, $^{2}J_{CP}$ = 6.8 Hz, 1C, C-14), 55.6 (s, 1C, C-17) 55.2-53.6 (m, 1C, C-9), 52.4 (d, *J* = 15.3 Hz, 1C, C-26), 40.9 (s, 1C, C-18), 29.1 (d, $^{2}J_{CP}$ = 15.5 Hz, 1C, C-11), 21.1-17.6 (m, 2C, C-12, C-13).

^{31}P-NMR (121.42 MHz, $CDCl_3$): δ = 27.9 (s), 27.8 (s).

HR-MS (MALDI-TOF): *m/z* $[M+Na]^+$ calcd. for $C_{25}H_{33}N_2O_6PNa$: 511.1974;
found: 511.1973.

6.4.15 2-(Trimethylsilyl)ethyl ((allyloxy)((*R*)-1-(((benzyloxy)carbonyl)amino)-2-methylpropyl)phosphoryl)-L-phenylalaninate (15)

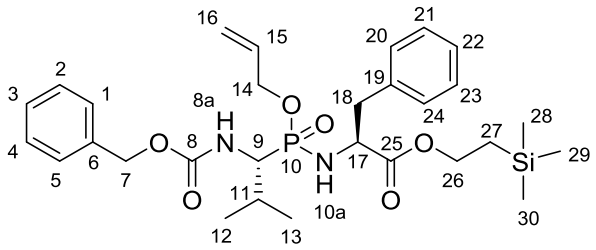

A 20 mL Schlenk vessel with magnetic stirring bar was dried (evacuated, heated, N_2-purged) and charged with 1.6 mL dry DCM and cooled to 0 °C (ice bath). 100 µL (1.33 mmol, 4.0 eq) $SOCl_2$ were added followed by dropwise addition of a solution of 214 mg (662 µmol, 2.0 eq) benzyl ((1*R*)-1-((allyloxy)(hydroxy)phosphoryl)-2-methylpropyl)carbamate in 1.9 mL DCM over 37 min at 0°C. After addition, the cooling bath was removed and the yellow colored reaction was stirred at RT for 3 h. Subsequently all volatile components were removed in vacuum with interconnected cooling trap. The colorless viscous residue was dissolved in 3.2 mL dry DCM and 175 µL (994 µmol, 3.0 eq) DIPEA were added (gas evolution). After 3 min, 101 mg (331 µmol, 1.0 eq) (*S*)-1-oxo-3-phenyl-1-(2-(trimethylsilyl)ethoxy)propan-2-aminium hydrochloride were added to the yellow colored solution and the reaction was heated to 40 °C in an oil bath and stirred overnight. Full conversion was observed after 12 h by TLC-control. The solvent was removed in vacuum and the yellow-colored residue was dissolved in 9 mL EtOAc and consecutively washed with 5 % citric acid (3 x 10 mL), 1M HCl (1 x 10 mL), 1M NaOH (1 x 10 mL), and brine (1 x 10 mL). The separated organic layer was dried over Na_2SO_4, filtrated, and the solvent was removed in vacuum. The crude product was purified via flash chromatography (15 g silica gel, 19 x 2.5 cm, eluent: cyclohexane/EtOAc = 3:1 (v/v), fraction size: 9 mL). The product was obtained as a mixture of diastereomers.[29]

$C_{29}H_{43}N_2O_6PSi$ [574.73 g/mol]

yield: 94 mg (164 µmol, 49 %) colorless viscous liquid.

R_f = 0.10 (cyclohexane/EtOAc = 3:1 (v/v), UV 254 nm, staining: CAM = blue).

$[\alpha]_D^{24}$ = -3.68 (c = 4.7, $CHCl_3$).

^{1}H-NMR (300.36 MHz, $CDCl_3$, mixture of 2 diastereomers assigned on the basis of COSY & HSQC): δ = 7.54-7.02 (m, 10H, H-1, H-2, H-3, H-4, H-5, H-20, H-21, H-22, H-23, H-24),

5.35 (d, $^{3}J_{HH}$ = 10.5 Hz, 1H, H-8a), 5.30-4.99 (m, 4H, H-7, H-16), 4.54-3.81 (m, 6H, H-9, H-14, H-17, H-26), 3.24-3.05 (m, 1H, H-18a), 3.04-2.73 (m, 1H, H-18b), 2.34-1.98 (m, 1H, H-11), 1.09-0.68 (m, 8H, H-12, H-13, H-27), 0.02 (d, *J* = 5.9 Hz, 9H, H-28, H-29 H-30).

^{13}C-NMR (75.53 MHz, $CDCl_3$, mixture of 2 diastereomers assigned on the basis of COSY & HSQC): δ = 173.2 (s, 1C, C_q, C-25), 156.7 (d, $^{3}J_{CP}$ = 13.8 Hz, 1C, C_q, C-8), 136.4 (s, 1C, C_q, C-6), 136.1 (s, 1C, C_q, C-19), 133.2 (m, 1C, C-15), 129.8-129.4 (m, 4C, C-2, C-4, C-21, C-23), 128.7-128.4 (m, 2C, C-20, C-24), 128.3-128.0 (m, 3C, C-3, C-1, C-5), 127.2-126.9 (m, 1C, C-22), 117.5 (s, 1C, C-16), 67.2 (s, 1C, C-7), 64.9 d, $^{2}J_{CP}$ = 6.9 Hz, 1C, C-14), 64.4 (d, $^{2}J_{CP}$ = 7.0 Hz, 1C, C-14), 63.8 (d, *J* = 18.7 Hz, 1C, C-26), 55.6-53.1 (m, 1C, C-9), 55.1 (s,1C, C-17), 40.9 (s, 1C, C-18), 29.0 (d, $^{2}J_{CP}$ = 22.7 Hz, 1C, C-11), 21.1-20.5 (m, 2C, C-12, C-13), 18.1-17.2 (m, 1C, C-27), -1.47 (s, 3C, C-28, C-29, C-30).

^{31}P-NMR (121.42 MHz, $CDCl_3$): δ = 28.0 (s), 26.9 (s).

HR-MS (MALDI-TOF): *m/z* $[M+Na]^+$ calcd. for $C_{29}H_{43}N_2O_6PSiNa$: 597.2526;
found: 597.2532.

6.4.16 Methyl (tert-butoxycarbonyl)-L-phenylalanyl-L-prolyl-L-tryptophanate (16)

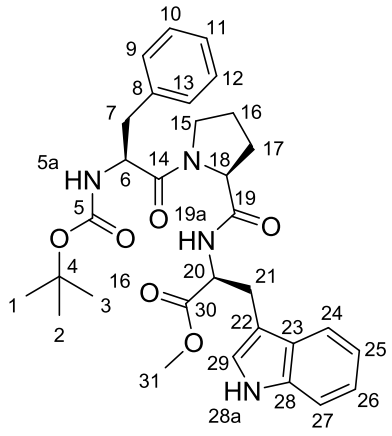

Boc-deprotection of Boc-Pro-Trp-OMe: A 10 mL round-bottom flask equipped with magnetic stirring bar was charged with 201 mg (484 µmol, 1.2 eq) Boc-Pro-Trp-OMe and 300 µL ethanethiol. 930 µL (12.2 mmol, 30 eq) trifluoroacetic acid were added to the heterogenous mixture to give a gold-yellow colored solution, which was stirred at RT. Full conversion was observed after 1 h by TLC-control and subsequently all volatile components were removed in vacuum. The residue was dissolved in 3.8 mL EtOAc and 933 µL 25 % aqueous NH_3-solution were added. The layers were separated and the aqueous layer was extracted with EtOAc (3 x 4 mL). The combined organic layers were washed with brine (1 x 5 mL), dried over Na_2SO_4, filtrated, and the solvent was removed in vacuum. The crude H-Pro-Trp-OMe was dried in oil pump vacuum and was used in the subsequent step without further purification.

Peptide coupling: A dry 10 mL Schlenk vessel with magnetic stirring bar was dried (evacuated, heated, N_2-purged) and charged with 108 mg (407 µmol, 1.0 eq) Boc-Phe-OH and 2.7 mL dry DMF followed by the addition of 75 µL (429 µmol, 1.05 eq) DIPEA and cooling the reaction solution to 0 °C in an ice bath. 184 mg (485 µmol, 1.2 eq) HBTU were added to the reaction at 0 °C and after 7 min of activation time a solution of the crude H-Pro-Trp-OMe (484 µmol, 1.2 eq) and 140 µL (802 µmol, 2.0 eq) DIPEA in 2 mL dry DMF were added at 0 °C. The ice bath was removed and the yellow colored reaction solution was stirred at RT for 1 h until TLC-control indicated full conversion. 7 mL brine were added to the reaction solution, the layers were separated, and the aqueous layer was extracted with EtOAc (3 x 7 mL). The combined organic layers were washed with brine (3 x 6 mL), dried over Na_2SO_4, filtrated, and the solvent was removed in vacuum. The crude product was purified via flash chromatography (40 g silica gel, 14 x 4.0 cm, eluent: cyclohexane/EtOAc = 1:1 (v/v), fraction size: 27 mL) followed by washing with

H_2O (4 x 4 mL; product was dissolved in EtOAc) and brine (1 x 5 mL) in order to remove remaining tetramethylurea to yield the desired compound **16** as colorless solid.[12]

$C_{31}H_{38}N_4O_6$ [562.67 g/mol]

yield: 162.2 mg (288 µmol, 71 %) colorless solid.

R_f = 0.19 (cyclohexane/EtOAc = 1:1 (v/v), UV 254 nm, staining: cold CAM = red, after heating: blue).

$[\alpha]_D^{24}$ = +6.2 (c = 1.09, $CHCl_3$).

mp = 70-75 °C.

^{1}H-NMR (300.36 MHz, $CDCl_3$, mixture of 2 rotamers assigned on the basis of COSY & HSQC): δ = 8.30 (s, 1H, H-28a), 7.70 (d, $^3J_{HH}$ = 7.9 Hz, 1H, H-19a), 7.65-7.48 (m, 1H, H-24), 7.40-6.86 (m, 10H, H-9, H-10, H-11, H-12, H-13, H-25, H-26, H-27, H-28a, H-29), 5.35-5.14 (m, 1H, H-5a), 4.84 (d, $^3J_{HH}$ = 6.4 Hz, 1H, H-20), 4.63-4.43 (m, 2H, H-6, H-18), 3.68 (s, 3H, H-31), 3.57-3.38 (m, 2H, H-15), 3.32 (bs, 2H, H-21), 2.67 (bs, 2H, H-7), 2.19 (bs, 1H, H-17), 1.83 (bs, 3H, H-16, H-17), 1.41 (d, *J* = 20.2 Hz, 9H, H-1, H-2, H-3).

^{13}C-NMR (75.53 MHz, $CDCl_3$, mixture of 2 rotamers assigned on the basis of COSY & HSQC): δ = 172.4 (s, 1C, C_q, C-30), 171.7 (s, 1C, C_q, C-19), 170.9 (s, 1C, C_q, C-14), 155.3 (s, 1C, C_q, C-5), 136.2 (s, 2C, C-8, C-28), 129.6 (s, 2C, C-12, C-10), 128.5 (s, 2C, C-13, C-9), 127.7 (s, 1C, C-23), 126.9 (s, 1C, C-11), 123.6 (s, 1C, C-29), 122.2 (s, 1C, C-26), 119.6 (s, 1C, C-25), 118.6 (s, 1C, C-24), 111.4 (s, 1C, C-27), 109.9 (s, 1C, C_q, C-22), 79.9 (s, 1C, C_q, C-4), 60.5 (s, 1C, C-18), 53.4 (s, 1C, C-20), 53.2 (s, 1C, C-6), 52.5 (s, 1C, C-31), 47.4 (s, 1C, C-15), 39.0 (s, 1C, C-7), 28.5 (s, 3C, C-1, C-2, C-3), 27.7 (s, 1C, C-21), 27.5 (s, 1C, C-17), 25.0 (s, 1C, C-16).

HR-MS (MALDI-TOF): *m/z* $[M+Na]^+$ calcd. for $C_{31}H_{38}N_4O_6Na$: 585.2689; found: 585.2695.

6.4.17 Methyl ((allyloxy)((*R*)-1-(((benzyloxy)carbonyl)amino)-2-methylpropyl)phosphoryl)-L-phenylalanyl-L-prolyl-L-tryptophanate (17)

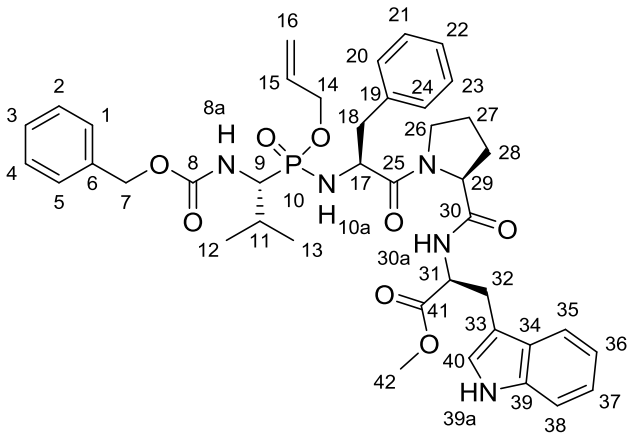

Boc-deprotection of Boc-Phe-Pro-Trp-OMe: A 25 mL round-bottom flask equipped with magnetic stirring bar was charged with 90 mg (160 µmol, 1.0 eq) Boc-Phe-Pro-Trp-OMe and 2.0 mL 4 M HCl in 1,4-dioxane to give a dark orange solution, which was stirred at RT. Full conversion was observed after 60 min by TLC-control and subsequently all volatile components were removed in vacuum.

Phosphonamide coupling: A 10 mL Schlenk vessel with magnetic stirring bar was dried (evacuated, heated, N_2-purged) and charged with 1.7 mL dry DCM and cooled to 0 °C (ice bath). 47 µL (640 µmol, 4.0 eq) $SOCl_2$ were added followed by dropwise addition of a solution of 106 mg (320 µmol, 2.0 eq) benzyl ((1*R*)-1-((allyloxy)(hydroxy)phosphoryl)-2-methylpropyl)carbamate in 1.2 mL dry DCM over 25 min at 0 °C. After addition, the cooling bath was removed and the yellow colored reaction was stirred at RT for 3 h. Subsequently all volatile components were removed in vacuum with interconnected cooling trap. The colorless viscous residue was dissolved in 2.45 mL dry DCM and 87 µL (480 µmol, 3.0 eq) DIPEA were added (gas evolution). After 13 min the crude H-Phe-Pro-Trp-OMe (160 µmol, 1.0 eq) were added to the yellow colored solution and the reaction was heated to 40 °C in an oil bath and stirred overnight. Full conversion was observed after 12 h by TLC-control. The solvent was removed in vacuum and the yellow-colored residue was dissolved in 8 mL EtOAc and consecutively washed with 5 % citric acid (3 x 10 mL), 1M HCl (1 x 10 mL), 1M NaOH (1 x 10 mL) and brine (1 x 10 mL). The combined aqueous layers were extracted with EtOAc (3 x 10 mL). The combined organic layers were dried over Na_2SO_4, filtrated, and the solvent was removed in vacuum. The crude product was purified via flash chromatography (13 g silica gel, 19 x 2.5 cm, eluent: DCM/MeOH = 20:1 (v/v), fraction size: 8 mL). The product was obtained as a mixture of diastereomers.[29]

$C_{41}H_{50}N_5O_8P$ [771.85 g/mol]

yield: 42.4 mg (54.9 µmol, 34 %) colorless viscous liquid.

R_f = 0.13 (DCM/MeOH = 20:1 (v/v), UV 254 nm, staining: cold CAM = orange, after heating: blue).

$[\alpha]_D^{20}$ = -0.011 (c = 0.09, $CHCl_3$).

^{1}H-NMR (499.89 MHz, $CDCl_3$, mixture of 2 diastereomers and rotamers assigned on the basis of COSY & HSQC): δ = 8.44 (s, 1H, H-39a), 7.73-7.50 (m, 1H, H-35), 7.37-7.02 (m, 15 H, H-1, H-2, H-3, H-4, H-5, H-20, H-21, H-22, H-23, H-24, H-34, H-35, H-36, H-37, H-38, H-40), 6.04-5.65 (m, 1H, H-15), 5.26-5.04 (m, 5H, H-8a, H-7, H-16), 4.87-4.76 (m, 1H, H-31), 4.48-4.33 (m, 1H, H-29), 4.31-4.22 (m, 1H, H-17), 4.21-3.93 (m, 2H, H-14), 4.10-3.82 (m, 1H, H-9), 3.70 (s, 3H, H-42), 3.55-3.40 (m, 2H, H-26), 3.39-3.26 (m, 2H, H-32), 2.51 (dd, $^2J_{HH}$ = 14.0 Hz, $^3J_{HH}$ = 7.8 Hz, 2H, H-18), 2.16-2.05 (m, 2H, H-11, H-28a), 1.88-1.70 (m, 3H, H-27, H-28b), 0.94 (dd, $^2J_{HH}$ = 19.5 Hz, $^3J_{HH}$ = 6.9 Hz, 6H, H-12, H-13).

^{13}C-NMR (125.70 MHz, $CDCl_3$, mixture of 2 diastereomers and rotamers assigned on the basis of COSY & HSQC): δ = 172.3 (s, 1C, C_q, C-41), 171.2 (s, 1C, C_q, C-30), 170.9 (s, 1C, C_q, C-25), 156.7 (d, $^3J_{CP}$ = 6.7 Hz, 1C, C_q, C-8), 136.9 (s, 1C, C_q, C-6), 136.6 (s, 1C, C_q, C-19), 136.3 (s, 1C, C_q, C-39), 133.3 (d, $^3J_{CP}$ = 6.8 Hz, 1C, C-15), 129.8 (s, 2C, C-23, C-21), 128.7 (s, 2C, C-24, C-20), 128.6 (s, 2C, C-5, C-1), 128.5 (s, 1C, C-3), 128.2 (s, 2C, C-4,C-2), 127.8 (s, 1C, C_q, C-34), 126.9 (s, 1C, C-22), 124.0 (s, 1C, C-40), 122.1 (s, 1C, C-37), 119.6 (s, 1C, C-36), 118.6 (s, 1C, C-35), 117.4 (s, 1C, C-16), 111.4 (s, 1C, C-38), 109.7 (s, 1C, C_q, C-33), 67.4 (s, 1C, C-7), 64.8 (d, $^2J_{CP}$ = 7.0 Hz, 1C, C-14), 64.3 (d, $^2J_{CP}$ = 7.1 Hz, 1C, C-14), 60.3 (s, 1C, C-29), 54.8 (d, $^1J_{CP}$ = 139.2 Hz, 1C, C-9), 53.8 (s, 1C, C-17), 53.3 (s, 1C, C-31), 52.4 (s, 1C, C-42), 47.3 (s, 1C, C-26), 40.6 (s, 1C, C-18), 29.1 (d, $^2J_{CP}$ = 31.2 Hz, 1C, C-11), 27.7 (s, 1C, C-28), 27.5 (s, 1C, C-32), 25.1 (s, 1C, C-27), 20.9 (d, $^3J_{CP}$ = 12.0 Hz, 1C, C-12), 18.0 (d, $^3J_{CP}$ = 4.3 Hz, 1C, C-13).

^{31}P-NMR (202.35 MHz, $CDCl_3$): δ = 29.0 (s), 28.4 (s), 28.2 (s), 28.0 (s).

HR-MS (MALDI-TOF): *m/z* $[M+Na]^+$ calcd. for $C_{41}H_{50}N_5O_8PNa$: 794.3295;
found: 794.3286.

6.4.18 *P*-((*R*)-1-(((Benzyloxy)carbonyl)amino)-2-methylpropyl)-*N*-((*S*)-1-oxo-3-phenyl-1-(2-(trimethylsilyl)ethoxy)propan-2-yl)phosphonamidate diethylammonium (18)

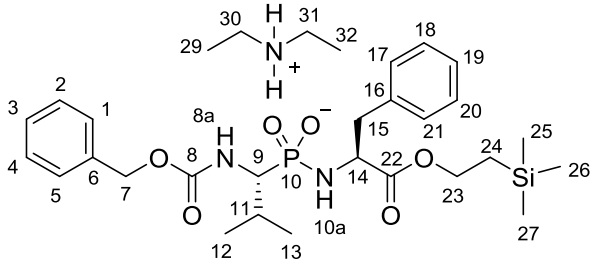

A 10 mL round-bottom flask equipped with Schlenk adapter and magnetic stirring bar was dried (evacuated, heated, N_2-purged) and charged with 34.8 mg (60.5 µmol, 1.0 eq) 2-(trimethylsilyl)ethyl((allyloxy)((*R*)-1-(((benzyloxy)carbonyl)amino)-2-methyl propyl)phosphoryl)-L-phenylalaninate, 1.0 mL dry DCM, 125 µL (1.21 mmol, 20.0 eq) diethylamine. The colorless solution was degassed (5 min N_2 bubbling in ultrasonic bath). After addition of 7.4 mg (6.40 µmol, 0.1 eq) $Pd(PPh_3)_4$ a yellow solution was obtained, which was stirred at RT. After 2.5 h full conversion was detected by TLC and subsequently all volatile components were removed in vacuum. The crude product was purified via flash chromatography (4 g silica gel, 10 x 1.5 cm, eluent: DCM/MeOH = 10:1 (v/v), fraction size: 2 mL).[29]

$C_{30}H_{50}N_3O_6PSi$ [607.80 g/mol]

yield: 8.5 mg (14.0 µmol, 23 %) colorless viscous liquid.

R_f = 0.10 (DCM/MeOH = 10:1 (v/v), UV 254 nm, staining: CAM = blue).

^{1}H-NMR (300.36 MHz, MeOD-d_4): δ = 7.42-7.12 (m, 10H, H-1, H-2, H-3, H-4, H-5, H-17, H-18, H-19, H-20, H-21), 5.13-5.05 (m, 2H, H-7), 4.22-4.00 (m, 2H, H-23), 3.80-3.50 (m, 6H, H-9, H-14, H-30, H-31), 3.08-3.00 (m, 1H, H-15a), 2.97-2.80 (m,-2.80 (m, 1H, H-15b), 2. 32-2.10 (m, 1H, H-11), 1.02-0.81 (m, 14H, H-12, H-13, H-24, H-29, H-32), 0.18 to -0.14 (m, 9H, H-25, H-26, H-27).

^{13}C-NMR (75.53 MHz, MeOD-d_4): δ = (1C, C_q, C-22, missing, low intensity), (1C, C_q, C-8, missing, low intensity), (s, 1C, C_q, 138.3 (s, 1C, C_q, C-6), 138.2 (s, 1C, C_q , C-16) 130.5-130.3 (m, 4C, C-2, C-4, C-18, C-20), 129.7-129.4 (m, 2C, C-17, C-21), 129.3 (s, 1C, C-3), 129.0-128.8 (m, 2C, C-1, C-5), 127.9 (s, 1C, C-19), 67.7 (s, 1C, C-7),64.3 (s, 1C, C-23), 60.0 (s, 2C, C-30, C-31) 56.6 (s, 1C, C-14), 54.9 (d, $^1J_{CP}$ = 151.1 Hz, 1C, C-9), 41.5 (s, 1C,

C-15), 30.4 (s, 1C, C-11), 22.5-21.4 (m, 2C, C-12, C-13), 18.7-18.1 (m, 3C, C-24, C-29, C-32), -1.42 (s, 3C, C-25, C-26, C-27).

^{31}P-NMR (121.53 MHz, MeOD-d_4): δ = 18.0 (s, 1P, P-5).

^{29}Si-NMR (121.53 MHz, MeOD-d_4): δ = -0.34 (s, 1Si, Si-25).

7 References:

[1] J. M. Berg, J. L. Tymoczko, L. Stryer, *Biochemie*, Springer-Verlag Berlin Heidelberg, 2013, pp. 219-220. DOI: 10.1007/978–3-8274–2989-6_8.

[2] A. K. Gosh, S. Gemma, *Structure-based Design of Drugs and other Bioactive Molecules: Tools and Strategies*, Wiley-VCH Verlag Weinheim Germany, 2014, pp. 355-369. DOI: 10.1002/9783527665211.

[3] A. R. Leach, J. Harren, *Structure-based Drug Discovery*, Springer, Berlin Germany, 2007. DOI: 10.1007/1-4020-4407-0.

[4] G. Schneider, U. Fechner, *Nature Rev. Drug Discov.* **2005**, *4*, 649–63.

[5] S. C. Prajapati, S. S. Chauhan, *FEBS Journal* **2011**, 278, 3256–3276. DOI:10.1111/j.1742-4658.2011.08275.x.

[6] Y. Yamamoto, J. Hashimoto, M. Shimamura, T. Yamaguchic, T. Hazato, *Peptides*, **2000**, *21*, 503–508.

[7] G. A. Bezerra, E. Dobrovetsky, R. Viertlmayr, A. Dong, A. Binter, M. Abramic, P. Macheroux, S. Dhe-Paganon, K. Gruber, *Proc. Natl. Acad. Sci. U.S.A.* **2012**,109, 6525–6530. DOI: 10.1073/pnas.1118005109.

[8] R. Khokha, A. Murthy, A. Weiss, *Nat. Rev. Immunol.* **2013**, *13*, 649–665. DOI: 10.1038/nri3499.

[9] W. N. Lipscomb, N. Sträter, *Chem. Rev.* **1996**, *96*, 2375-2433. DOI: 10.1021/cr950042j.

[10] P. Kumar, V. Reithofer, M. Reisinger, S. Wallner, T. Pavkov-Keller, P. Macheroux, K. Gruber, *Sci. Rep.* **2016**, *6*, 23787. DOI: 10.1038/srep23787.

[11] M. Baršun, N. Jajčanin, B. Vukelić, J. Špoljarić, M. Abramić, *Biol. Chem.* **2007**, *388*, 343-348. DOI: 10.1515/BC.2007.039.

[12] J. Ivković, Studies Towards the Structure-based Design of Inhibitors of Dipeptidyl Peptidase-3 and Rhodesain. PhD Thesis, Graz University of Technology, 2016.

[13] C. Lembacher-Fadum, Structure-Base Design and Synthesis of Potential Inhibitors of DPP III, MSc Thesis, Graz University of Technology, 2016.

[14] K. Gluza, P. Kafarski, *Drug Discov.* **2013**, 325–372. DOI: 10.5772/52504.

[15] V. L. Schramm, *Annu. Rev. Biochem.* **2011**, *80*, 703–732. DOI: 10.1146/annurev-biochem-061809-100742.

[16] D. W. Cushman, H. S. Cheung, E. F. Sabo, M. A. Ondetti, *Biochemistry*, **1977**, *16*, 5484-5491. DOI: 10.1021/bi00644a014.

[17] M. A. Ondetti, B. Rubin, D. W. Cushman, *Science*, **1977**, *196*, 441-444. DOI: 10.1126/science.191908.

[18] M. Ordóñez, H. Rojas-Cabrera, C. Cativiela, C. *Tetrahedron* **2009**, *65*, 17–49. DOI: 10.1016/j.tet.2008.09.083.

[19] S. Cherenok, A. Vovk, I. Muravyova, A. Shivanyuk, V. Kukhar, J. Lipkowski, V. Kalchenko, *Org. Lett.* **2006**, 8, 549–552. DOI: 10.1021/ol052469a.

[20] Y. Q. Yu, D. Z. Xu, *Synthesis* **2015**, *47*, 1869–1876. DOI: 10.1055/s-0034-1380523.

[21] T. Komiyama, H. Suda, T. Aoyagi, T. Takeuchi, H. Umezawa, K. Fujimoto, S. Umezawa, *Arch. Biochem. Biophys*. **1975**, *171*, 727–731. DOI: 10.1016/0003-9861(75)90085-5.

[22] E. D. Thorsett, E. E. Harris, E. R. Peterson, W. J. Greenlee, A. A. Patchett, E. H. Ulm, T. C. Vassil, *Proc. Natl. Acad. Sci. USA* **1982**, *79*, 2176–2180.

[23] E. W. Petrillo, Jr. and M. A. Ondetti, *Med. Res. Rev.* **1982**, *2*, 1–41.

[24] T. K. Olszewski,.; M Majewski. *Tetrahedron Asymmetry* **2015**, *26*, 846–852. DOI: 10.1016/j.tetasy.2015.06.008.

[25] A. K. Beck, P. Gysi, L La Vecchia, D. Seebach, *Org. Synth.* **1999**, *76*, 12. DOI 10.15227/orgsyn.076.0012.

[26] X. Linghu, J. P. Potnick, J. S. Johnson, *J. Am. Chem. Soc.* **2004**, *126*, 3070–3071. DOI: 10.1021/ja0496468.

[27] P. Chen, X. Su, W. Zhou, Y. Xiao, J. Zhang, *Tetrahedron* **2016**, *72*, 2700–2706. DOI: 10.1016/j.tet.2015.12.002.

[28] A. Isidro-Llobet, M. Alvarez, F. Albericio, *Chem. Rev*. **2009**, *109*, 2455–2504. DOI: 10.1021/cr800323s.

[29] J. Cramer, G. Klebe, *Synthesis* **2017**, *49*, 1857–1866. DOI: 10.1055/s-0036-1588393.

[30] A. D Pehere, A. D. Abell, *Tetrahedron Lett.* **2011**, *52*, 1493–1494. DOI: 10.1016/j.tetlet.2011.01.102.

[31] M. Hoffmann, *Synthesis* **1986**, *7*, 557-559. DOI: 10.1055/s-1986-31701.

[32] J. Liu, W. Chen, Y. Xu, S. Ren, W. Zhang, Y. Li, *Bioorg. Med. Chem.* **2015**, *23*, 1963–1974. DOI: 10.1016/j.bmc.2015.03.034.

[33] M. Leypold, P. W. Wallace, M. Kljajic, M. Schnittmayer, J. Pletz, C. Illaszewicz-Trattner, G. M. Guebitz, R. Birner-Gruenberger, R. Breinbauer, *Tetrahedron Lett.* **2015**, *56*, 5619-5622. DOI: 10.1016/j.tetlet.2015.08.061.

[34] J. Grembecka, A. Mucha, T. Cierpicki, P. Kafarski, *J. Med. Chem.* **2003**, *46*, 2641–2655. DOI: 10.1021/jm030795v.

[35] M. H. Serrano-Wu, A. Regueiro-ren, D. R. St. Laurent, T. M. Carroll, B. N. Balasubramanian, *Tetrahedron Lett.* **2001**, *42*, 8593–8595. DOI: 10.1016/S0040-4039(01)01859-7.

[36] Z. E. Wilson, S. Fenner, S. V. Ley, *Angew. Chem. Int. Ed*. **2015**, *54*, 1284–1288.

[37] S. A. M. Mérette, A. P. Burd, J. J. Deadman *Tetrahedron Lett.* **1999**, *40*, 753-754. DOI: 10.1016/S0040-4039(98)02364-8.

[38] R. Hirschmann, K. M. Yager, C. M. Taylor, J. Witherington, P. A. Sprengeler, B. W. Phillips, W. Moore, A. B. Smith, *J. Am. Chem. Soc.* **1997**, *119*, 8177–8190. DOI: 10.1021/ja962465o

[39] P. G. M. Wuts, T. W. Greene, *Greene's Protective Groups in Organic Synthesis*, John Wiley & Sons, **2007**, pp. 575-576. DOI: 10.1002/0470053488.

[40] R. Bartholomäus, F. Dommershausen, M. Thiele, N. S. Karanjule, K. Harms, U. Koert, *Chem. - Eur. J.* **2013**, *19*, 7423–7436. DOI: 10.1002/chem.201204545.

[41] S. Banala, P. Ensle, R. D. Süssmuth, *Angew. Chem. Int. Ed.* **2013**, *52*, 9518–9523. DOI: 10.1002/anie.201302266.

[42] X. Gao, J. Han, L. Wang, *Org. Lett.* **2015**, *17*, 4596–4599. DOI: 10.1021/acs.orglett.5b02323.

[43] S. T. Ruan, J. M. Luo, Y. Du, P. Q. Huang, *Org. Lett.*, **2011**, 13, 4938-4941. DOI: 10.1021/ol2020384.

[44] X. Hu, Z. Shan, W. Li, *J. Fluor. Chem.* **2010**, *131*, 505-509.

[45] X. Jiang, A. J . Minnaard, B. Hessen, B. L. Feringa, A. L. L. Duchateau, J. G. O. Andrien, J. A. F. Boogers, J. G. De Vries, *Org. Lett.* **2003**, *5*, 1503–1506. DOI: 10.1021/ol034282u.

[46] T. Shiraiwa, Y. Kawashima, A. Ikaritani, Y. Suganuma, R. Saijoh, *Chem. Pharm. Bull.* **2006**, *54*, 1170-1174. DOI: 10.1248/cpb.54.1170.

8 Abbreviations

Analytical methods:

$[\alpha]_D^{24}$	specific optical rotation at 24 °C
^{13}C-NMR	carbon nuclear magnetic resonance spectroscopy
^{1}H-NMR	proton nuclear magnetic resonance spectroscopy
amu	atomic mass unit
APT	attached proton test
BP	base peak
bs	broad singlet
C_{arom}	aromatic carbon
CH_{arom}	aromatic proton
C_q	quarternary carbon
d	doublet
dd	double of doublet
ESI	electrospray ionization
eV	electron volt
GC	gas chromatography
GC-MS	gas chromatography coupled with mass spectroscopy
HH-COSY	proton-proton correlation spectroscopy
HPLC	high performance liquid chromatography
HPLC-MS	high performance liquid chromatography coupled with mass-spectroscopy
HR-MALDI-MS	high resolution matrix assisted laser desorption ionization mass spectrometry
HRMS	high resolution mass spectrometry

HSQC	heteronuclear single quantum coherence
Hz	Hertz
Intens.	intensity
J	signal multiplicity
m	multiplet
m/z	mass/charge-ratio
M^+	molecule peak
mp	melting point
NMR	nuclear magnetic resonance spectroscopy
q	quadruplet
RP-HPLC	reversed phase-HPLC
R_f	retention factor
s	singlet
t	triplet
TLC	thin layer chromatography
TOF	time of flight
t_R	retention time
UV	ultraviolet
δ	chemical shift

Chemical abbreviations:

1,2-DCE	1,2-dichloroethane
4-DMAP	4-(dimethylamino)-pyridine
AcOH	acetic acid
Boc	*tert*-butoxycarbonyl
CAM	cerium ammonium molybdate

Cbz	benzyloxycarbonyl
Cbz-Cl	benzyl chloroformate
$CDCl_3$	deuterated chloroform
D_2O	deuterium oxide
DIPEA	*N*,*N*-diisopropyldiethylamine (Hünig's base)
DMSO-d_6	deuterated dimethylsulfoxide
EDC·HCl	1-ethyl-3-(3-dimethylaminopropyl)carbodiimid hydrochloride
Et_2O	diethyl ether
Et_3N	triethylamine
Et_2NH	diethylamine
EtOAc	ethyl acetate
EtOH	ethanol
EtSH	ethanethiol
Fmoc-Cl	9-fluorenylmethylchloroformate
HBTU	2-(1*H*-Benzotriazol-1-yl)-1,1,3,3-tetramethyluronium hexafluorophosphate
MeCN	acetonitrile
MeOH	methanol
MeOD-d_4	deuterated methanol
Ph	phenyl
Phe	phenylalanine

Pro	proline
$TBAF{\cdot}3H_2O$	tetrabutylammonium fluoride trihydrate
TFA	trifluoroacetic acid
THF	tetrahydrofuran
Trp	tryptophan
Val	valine

Biological abbreviations:

AIDS	acquired immune deficiency syndrome
B. craniifer	*Blaberus craniifer*
DNA	deoxyribonucleic acid
HIV	human immunodeficiency virus
IC_{50}	half maximal inhibitory concentration
K_d	dissociation constant
K_i	inhibitory constant
RNA	ribonucleic acid

Others:

(v/v)	volume/volume
(v/v/v)	volume/volume/volume
(w/w)	weight/weight
°C	degree Celsius

Å	Ångström unit
cm	centimeter
conc.	concentrated
d	day/-s
EI	electron impact
eq	equivalent
et al.	*et alii* (lat.: and co-workers)
g	gram
h	hour/-s
L	liter
m	meter
M	molar (mol/l)
min	minute/-s
mL	milliliter
mm	millimeter
nm	nanometer
nM	nanomolar
pH	negative logarithm of the hydronium ion concentration
pK_a	negative logarithmic acid dissociation constant
ppm	parts per million
rac	racemic

RT	room temperature
λ	wavelength
λ_{max}	absorption maximum
µL	microliter
µm	micrometer
µM	micromolar
µmol	micromol

9 Danksagung

Ich möchte mich an erster Stelle sehr bei Prof. Rolf Breinbauer für die Aufnahme in seiner Arbeitsgruppe bedanken. Danke Rolf, dass du mir dein Vertrauen für dieses anspruchsvolle aber auch spannende Thema an der Schnittstelle zwischen Organischer Chemie und Biochemie gegeben hast. Vielen Dank für dein Engagement und deine Geduld beim Betreuen meiner Arbeit und dass man dich jederzeit bei Ungewissheiten fragen konnte.

Vielen Dank auch an Herrn Prof. Christian Slugovc für die Rolle als Zweitprüfer bei meiner Verteidigung der Arbeit. Einen weiteren herzlichen Dank möchte ich gerne an Christan Lembacher-Fadum richten, welcher mich in dieses Thema eingeführt hat und mir eine große Hilfestellung im Labor und beim Kennenlernen der HPLC und prep. HPLC war. Dankeschön an meine Laborkolleginnen Julia Blesl, Kathrin Heckenbichler und Anna Migglautsch ! Danke, dass ich euch um unterstüztende Ratschläge fragen durfte und für die angenehme und lustige Zeit im Labor! An dieser Stelle möchte ich mich bei der gesamten Arbeitsgruppe bedanken, Patrick Dobrounig, Carina Doler, Thomas Schlatzer, Martin Vareka und Marko Kljajic. Dankeschön an das NMR-Team Prof. Hansjörg Weber und Ing. Carina Illaszewicz-Trattner für die Hilfestellung bei der NMR-Analytik. Dankeschön an Dr. Gernot Strohmeier für sein Fachwissen und die Unterstützung bei HPLC-relevanten Fragen. Ing. Frau Karin Bartl, möchte ich großen Dank aussprechen für die Messungen der HRMS-Proben und ihre Unterstützung beim Auswerten der Spektren. Vielen Dank auch an Peter Urdl und Peter Plachota, die mir bei technischen Problemen weitergeholfen haben. Großer Dank gilt auch Astrid Nauta, die mir bei organisatorischen Aspekten sehr geholfen hat. Dankeschön auch an Elisabeth Seitler, Gerhard Thomann und Alexander Fragner für die Unterstüzung und Wartung im Labor.

Besonders möchte ich mich bei meinen Eltern, Jörg und Martina sowie meiner Schwester Felicitas bedanken. Danke dass ihr mir die Möglichkeit gegeben habt, ein Studium an der Universität zu beginnen und mich finanziell sowieso moralisch bei meinen Entscheidungen unterstützt habt. Vielen Dank für eure Ratschläge und Aufmunterung bei schwierigen Lebenssituationen. Zuletzt möchte ich mich bei allen Freunden bedanken, die ich während des Studiums kennengelernt habe und mich währendessen begleitet haben.

10 Appendix: NMR Spectra

^{1}H and ^{13}C-NMR spectra of dimethyl (2*R*,3*R*)-2,3-dihydroxysuccinate (1)

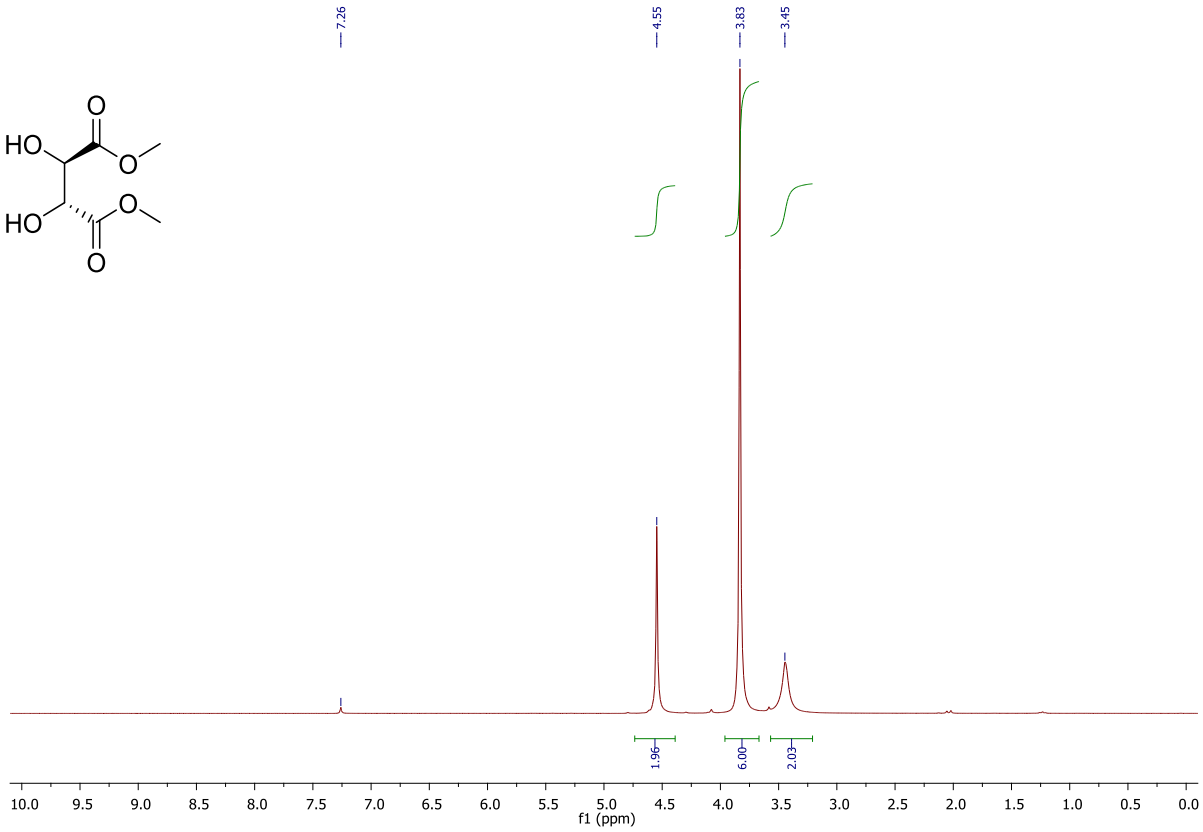

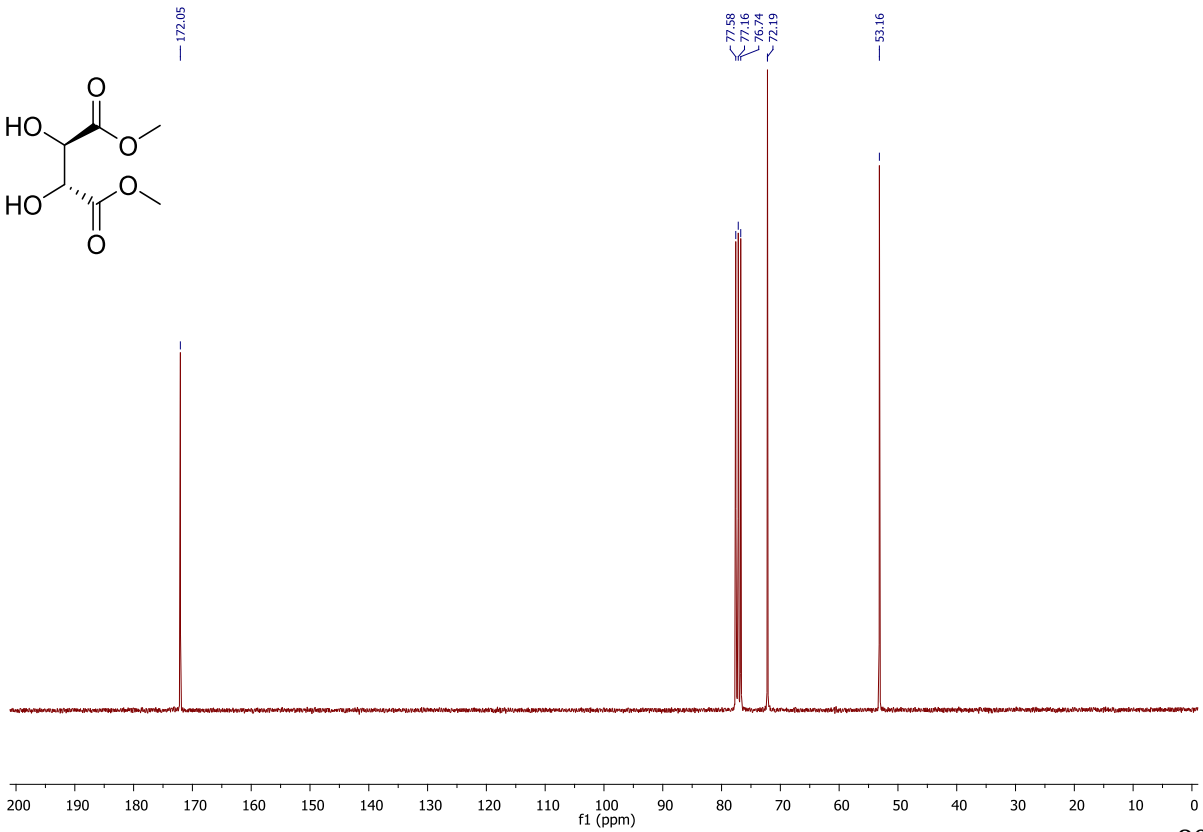

^{1}H and ^{13}C-NMR spectra of dimethyl (4*R*,5*R*)-2,2-dimethyl-1,3-dioxolane-4,5-dicarboxylate (2)

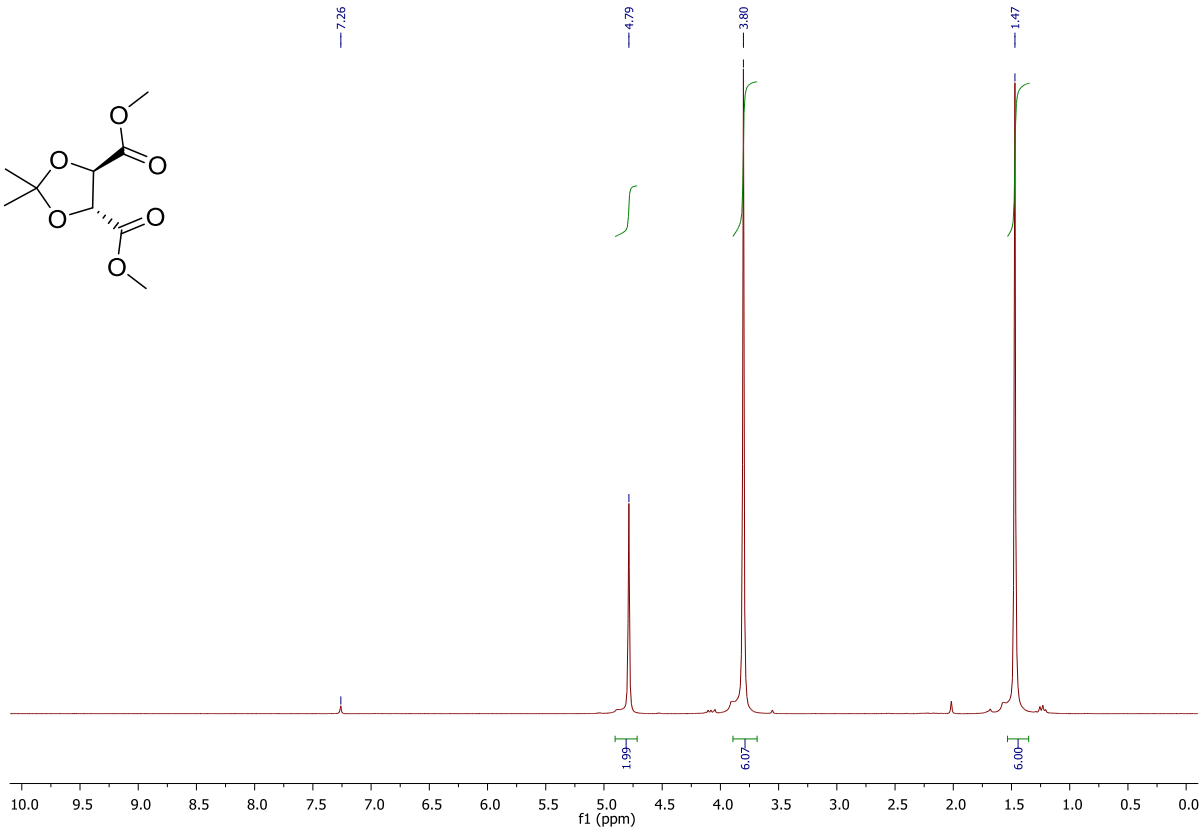

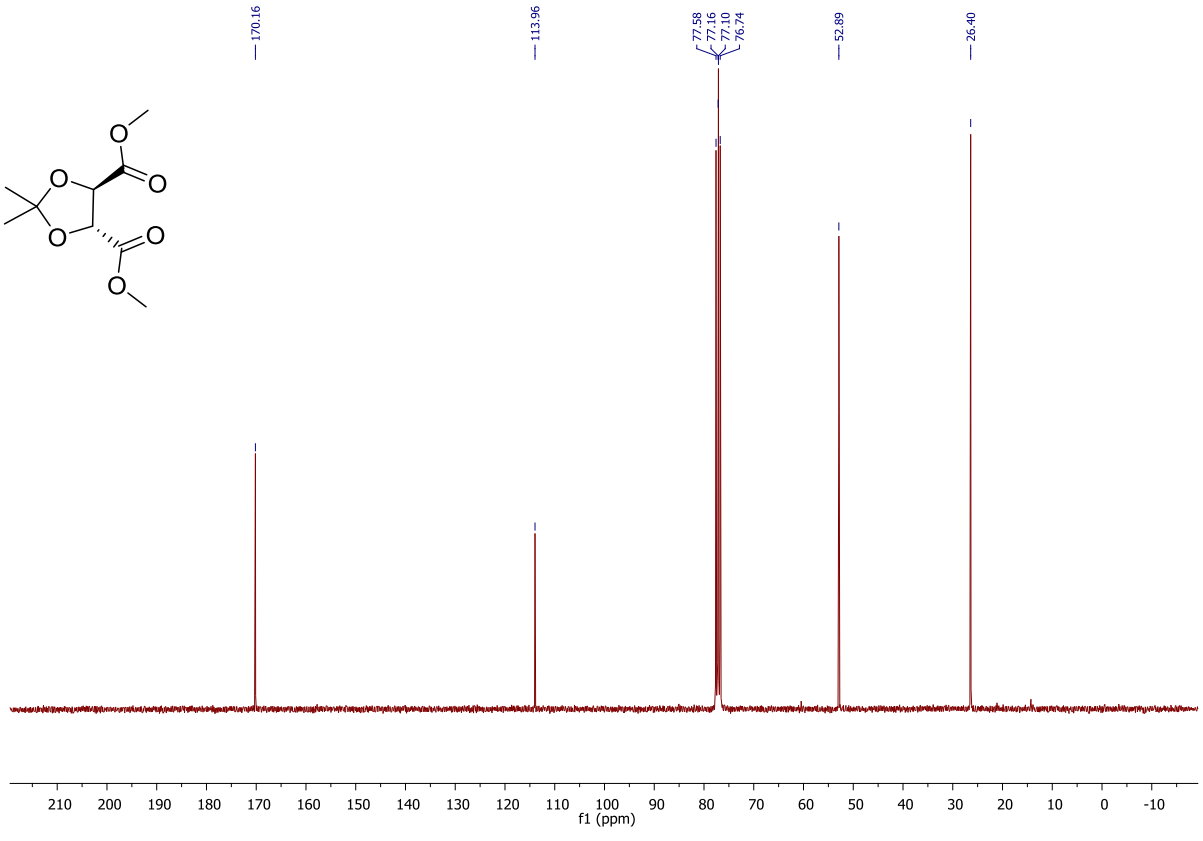

^{1}H and ^{13}C-NMR spectra of (*S*,*E*)-2-methyl-*N*-(2-methylpropylidene)propane-2-sulfinamide (3)

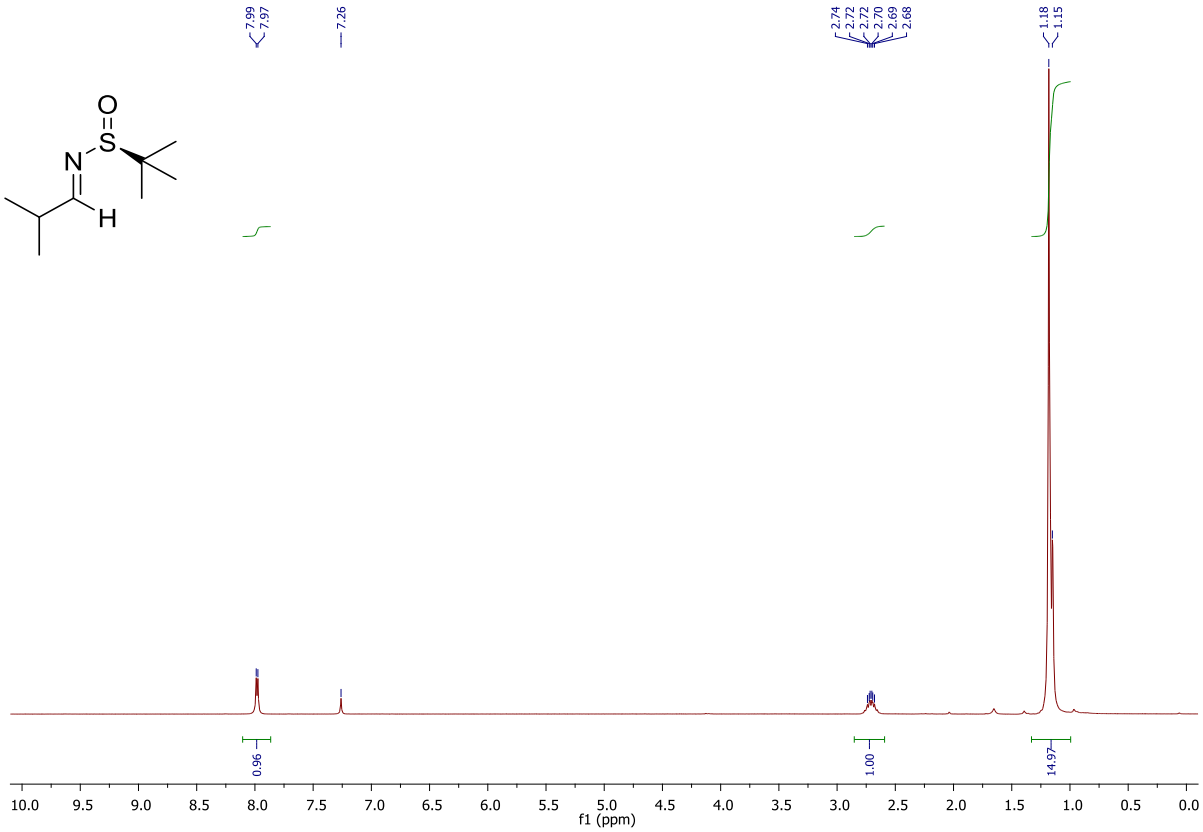

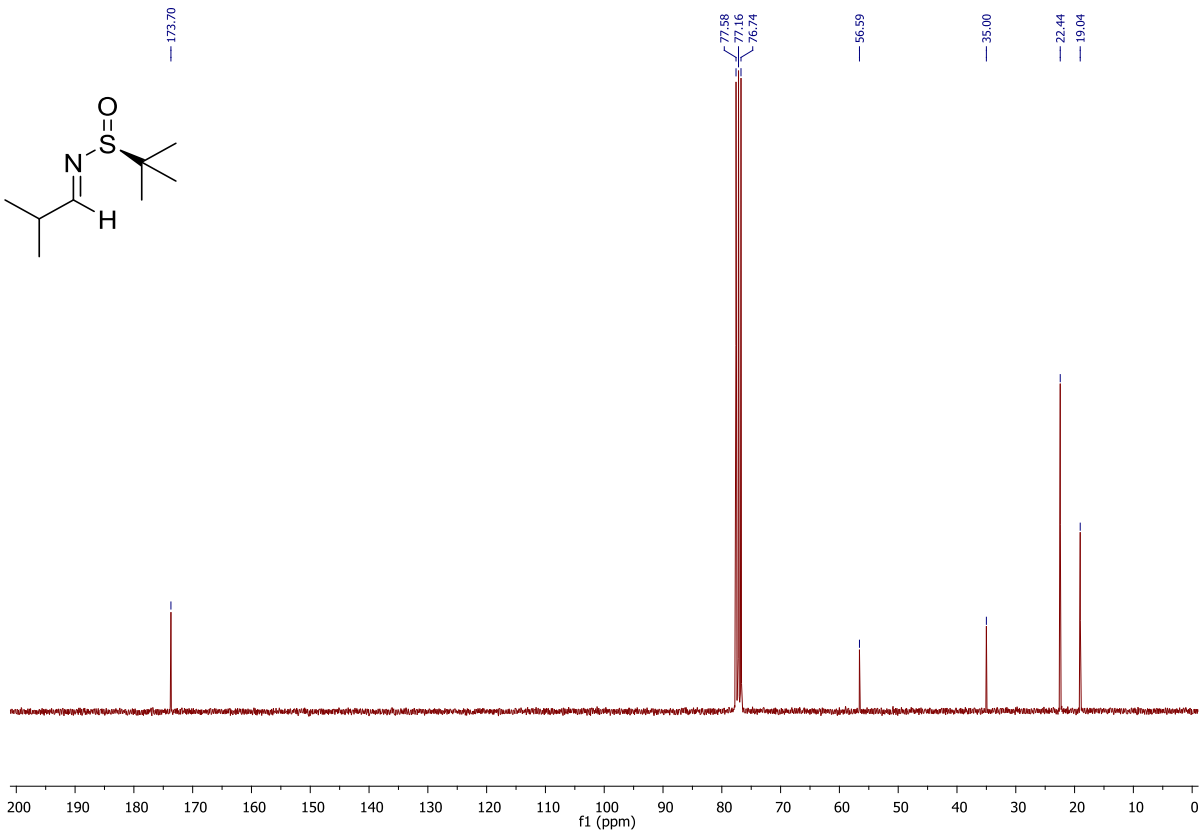

^{1}H and ^{13}C-NMR spectra of ((4*R*,5*R*)-2,2-dimethyl-1,3-dioxolane-4,5-diyl)bis(diphenylmethanol) (4)

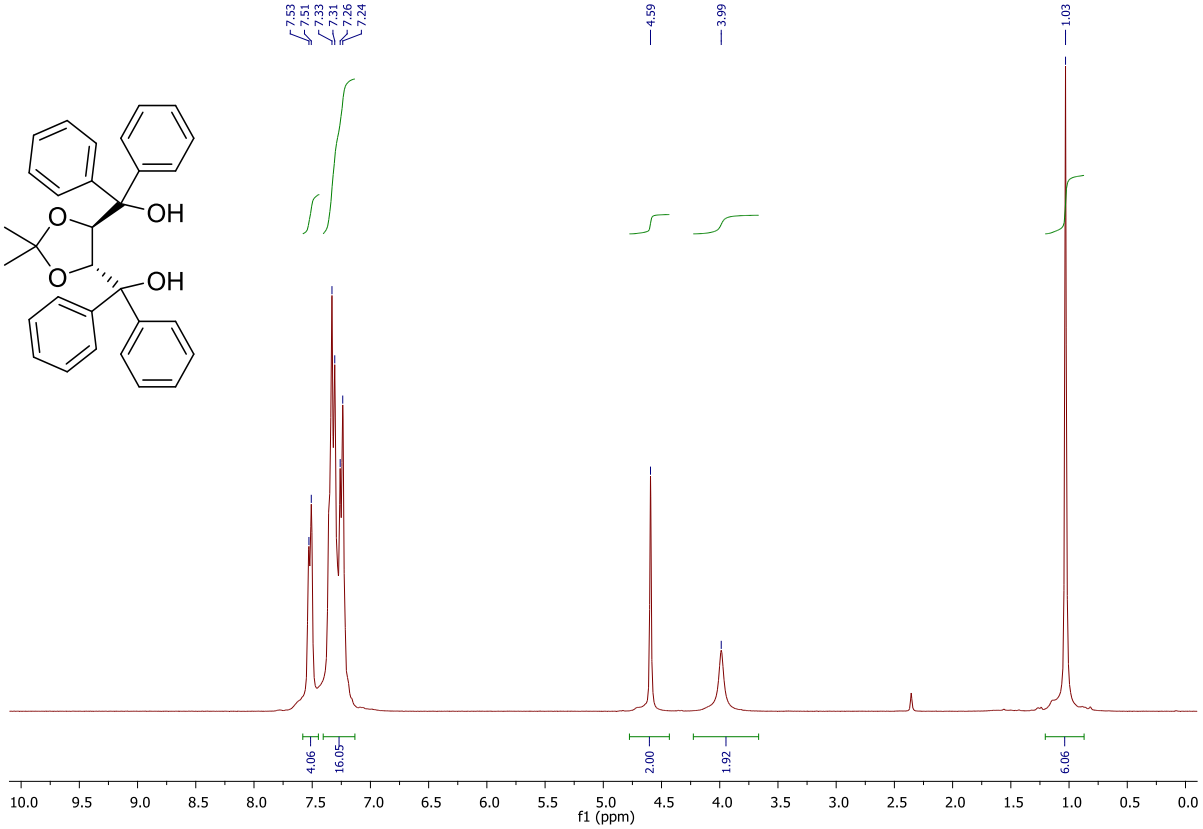

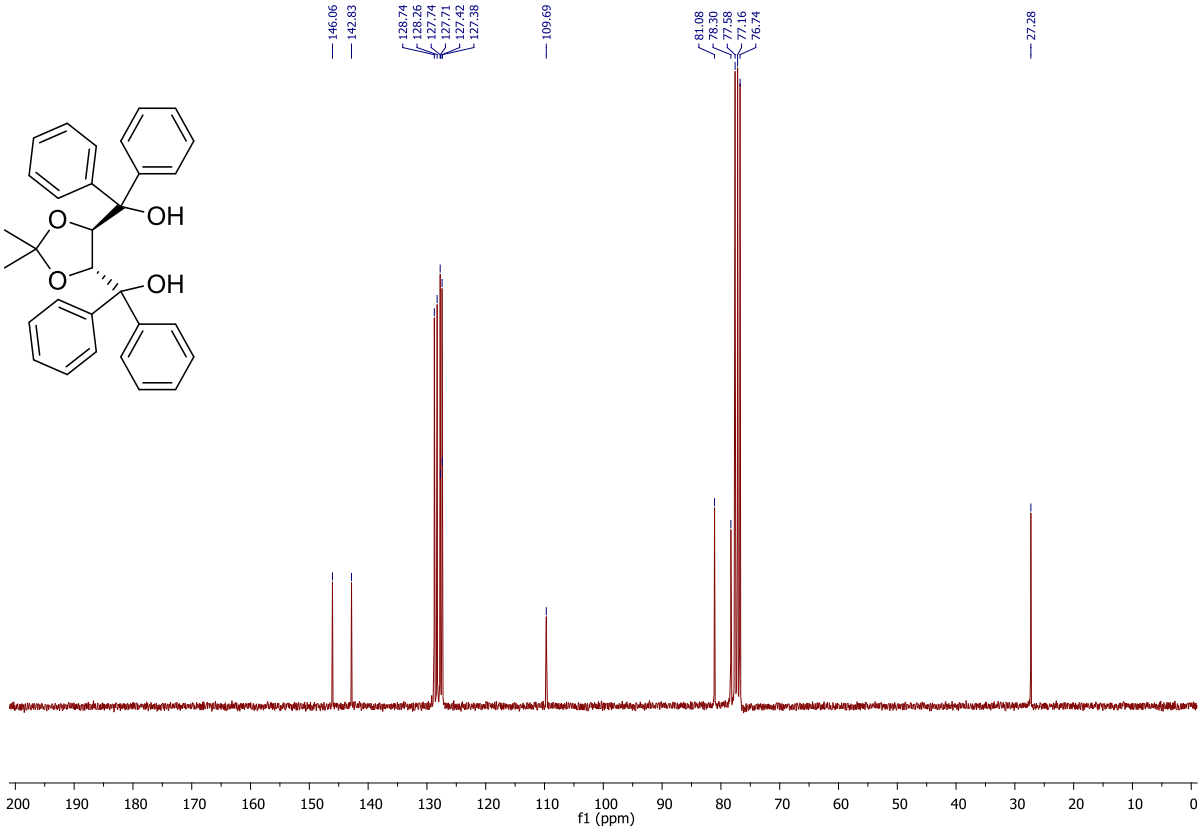

^{1}H, ^{13}C-NMR spectra of (3a*R*,8a*R*)-2,2-dimethyl-4,4,8,8-tetraphenyltetrahydro [1,3]dioxolo[4,5-e][1,3,2]dioxaphosphepine 6-oxide (5)

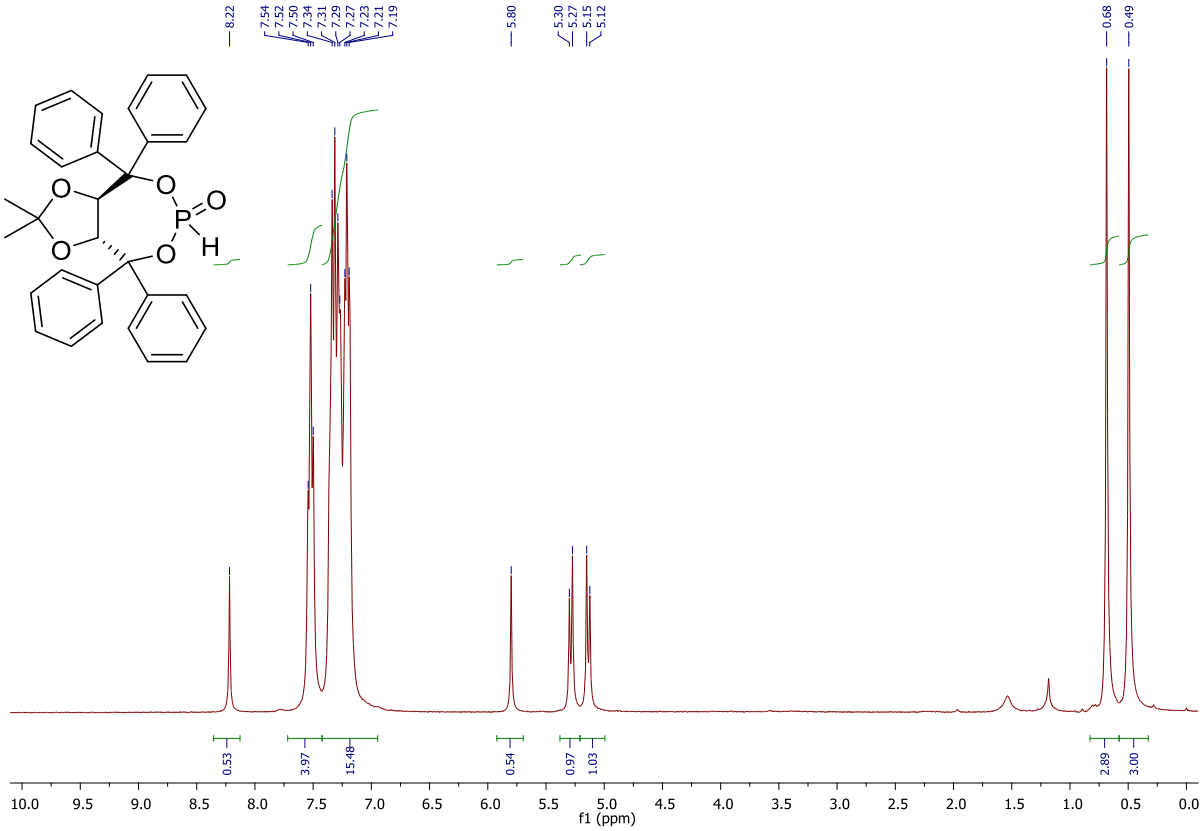

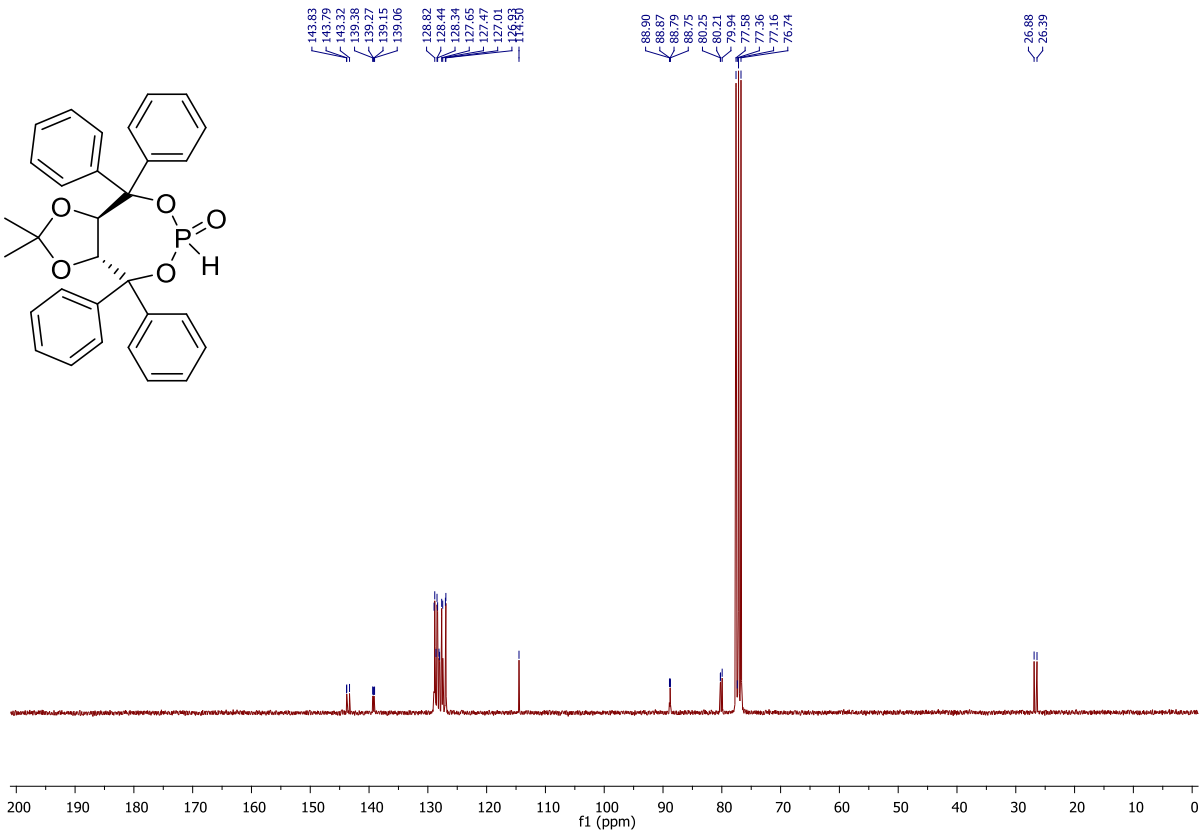

^{1}H and ^{13}C-NMR spectra of (*S*)-1-methoxy-1-oxo-3-phenylpropan-2-aminium hydrochloride (6)

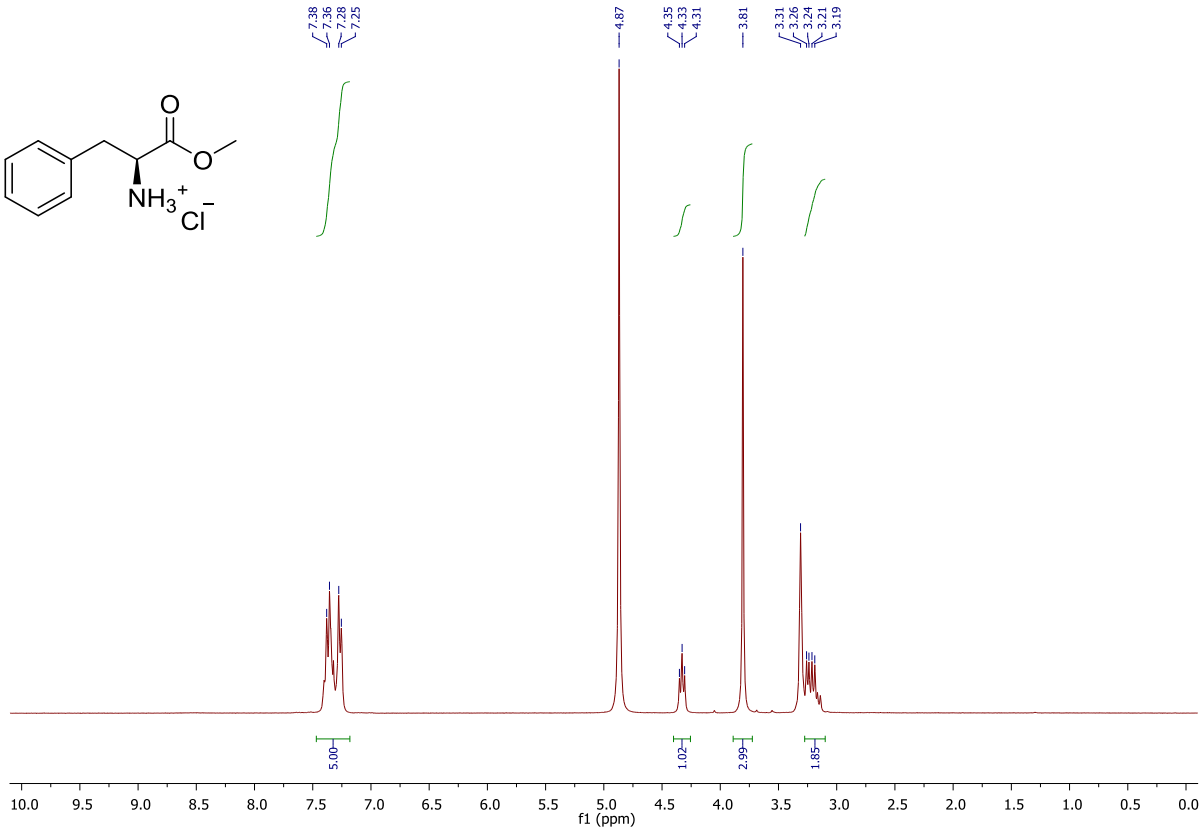

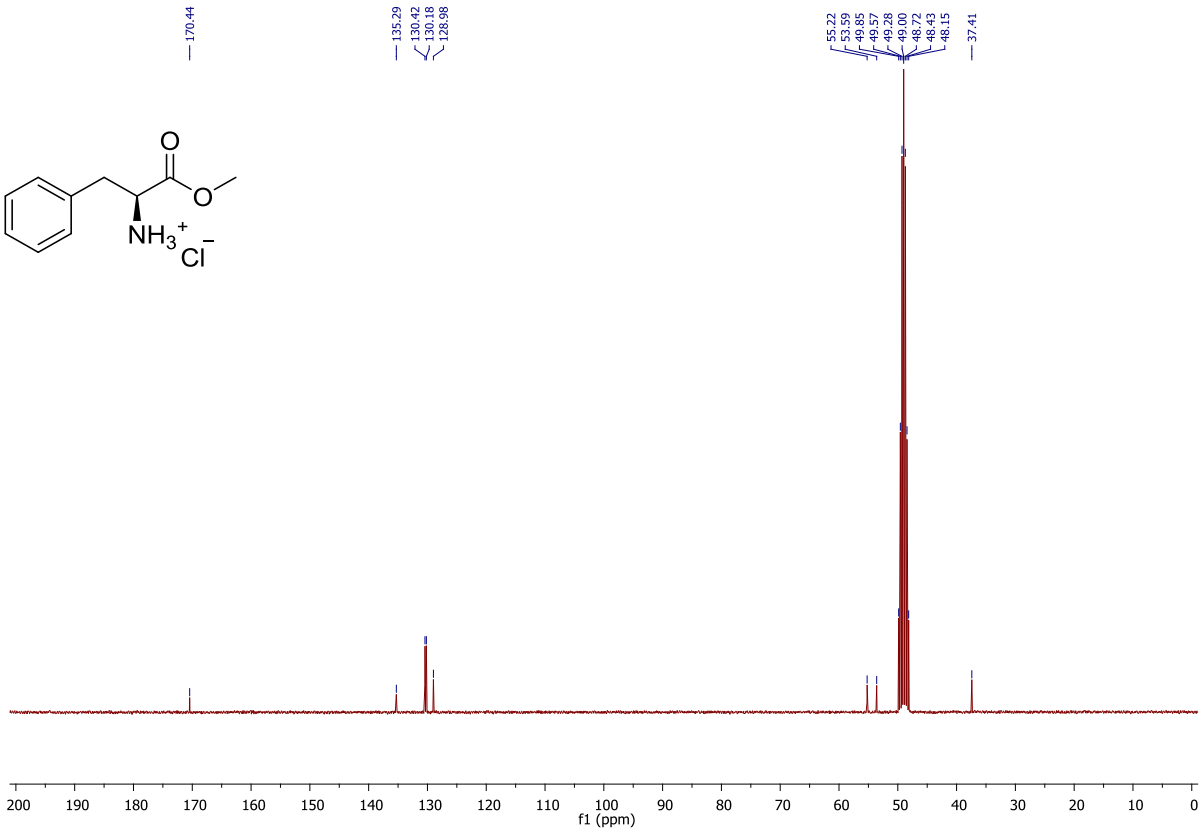

^{1}H and ^{13}C-NMR spectra of (*S*)-2-(trimethylsilyl)ethyl (tert-butoxycarbonyl)-L-phenylalaninate (7)

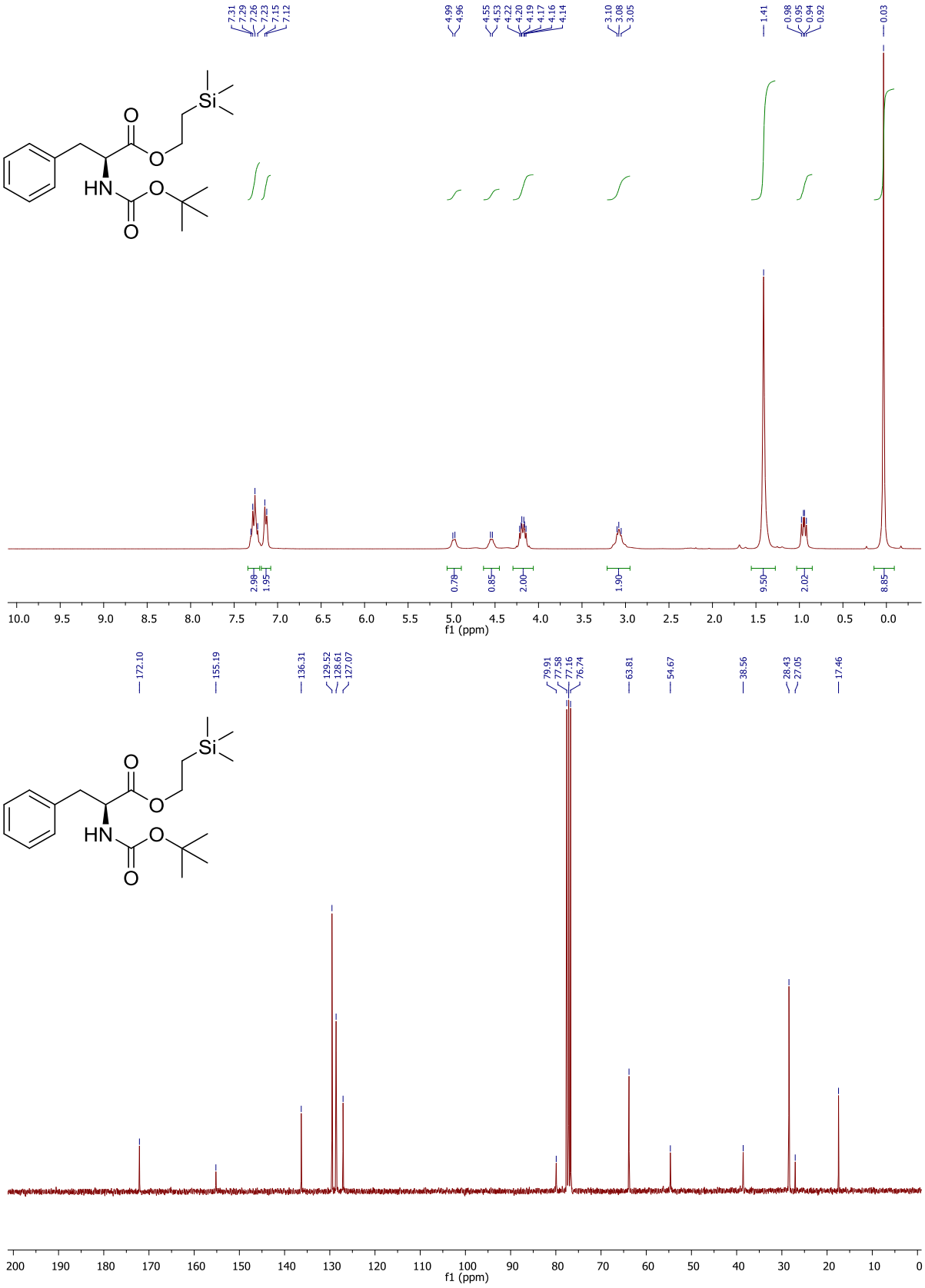

^{1}H and ^{13}C-NMR spectra of (*S*)-1-oxo-3-phenyl-1-(2-(trimethylsilyl)ethoxy)propan-2-aminium hydrochloride (8)

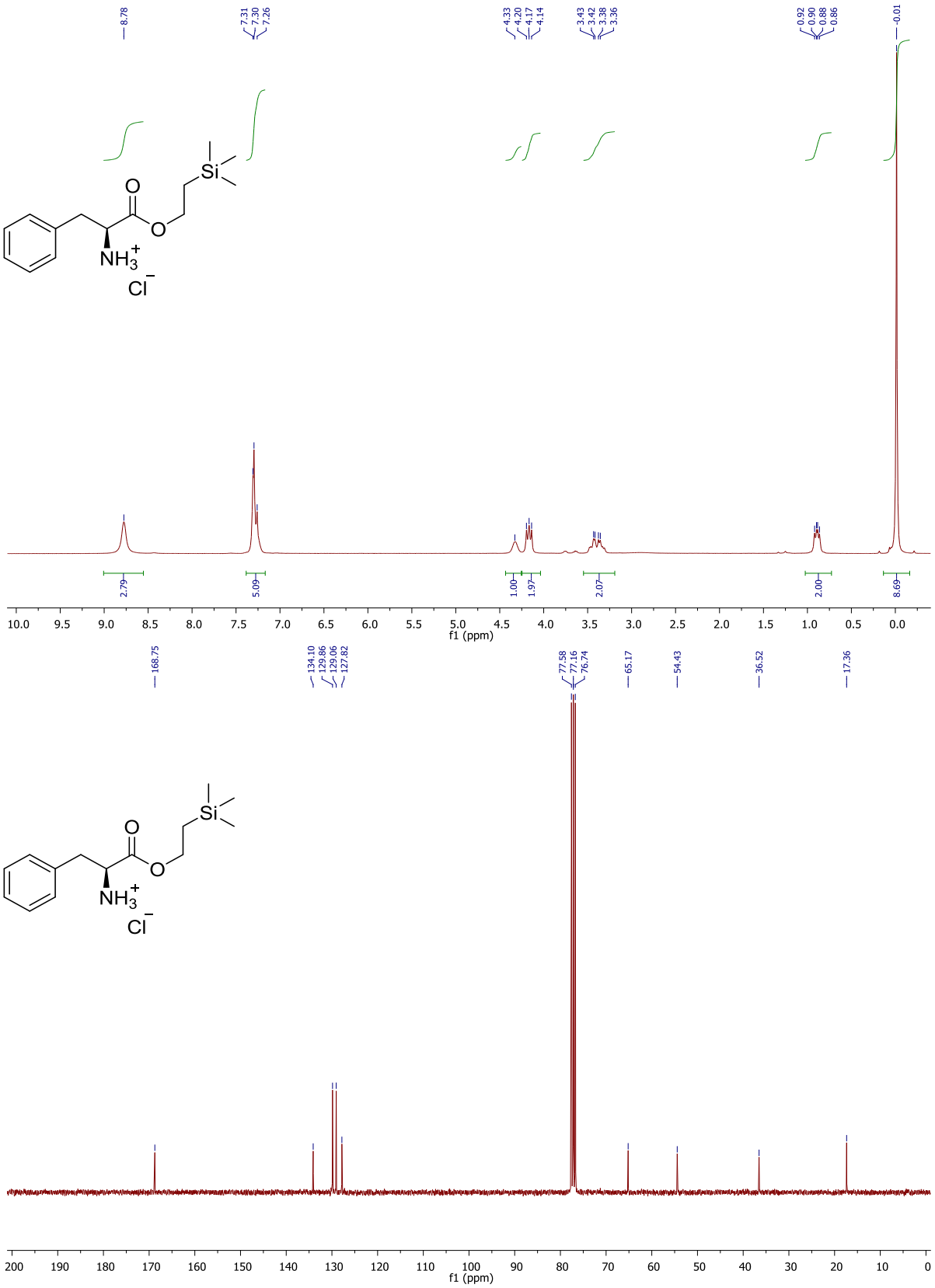

^{1}H and ^{13}C-NMR spectra of (9H-Fluoren-9-yl)methyl (tert-butoxycarbonyl)-L-phenylalaninate (9)

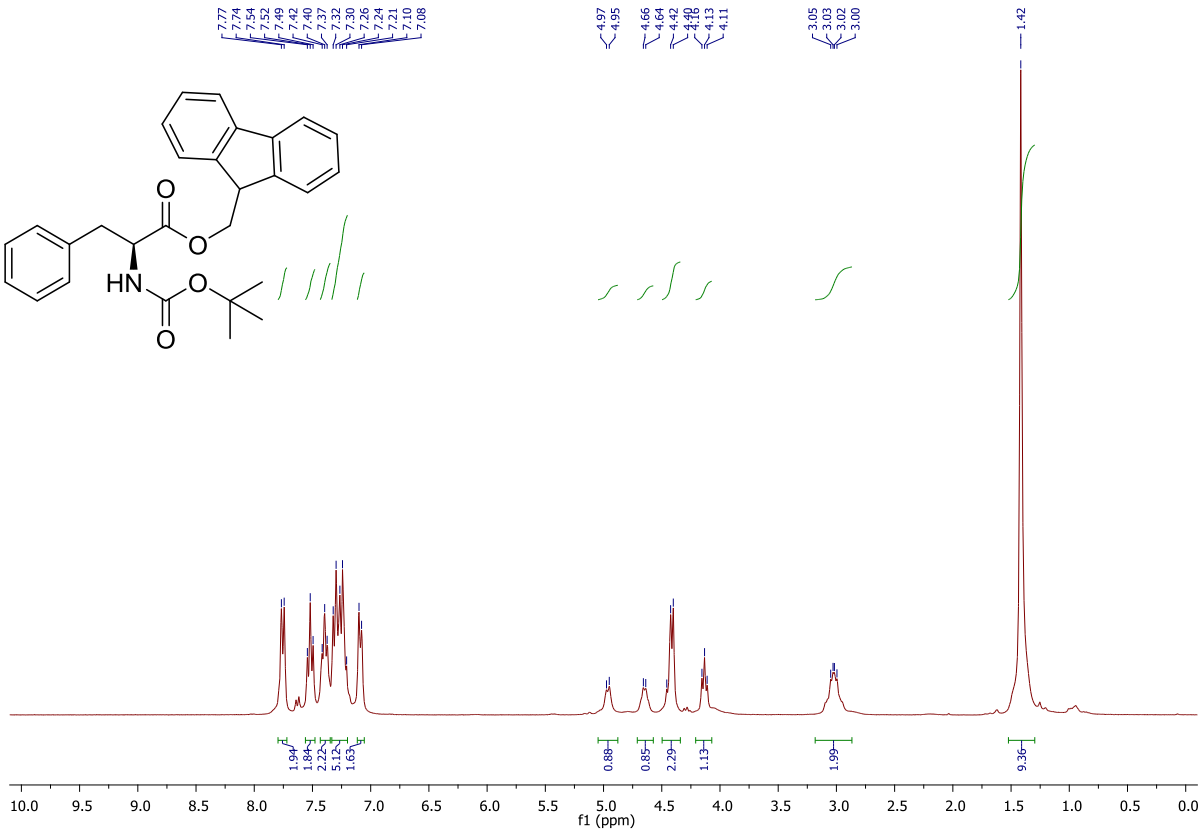

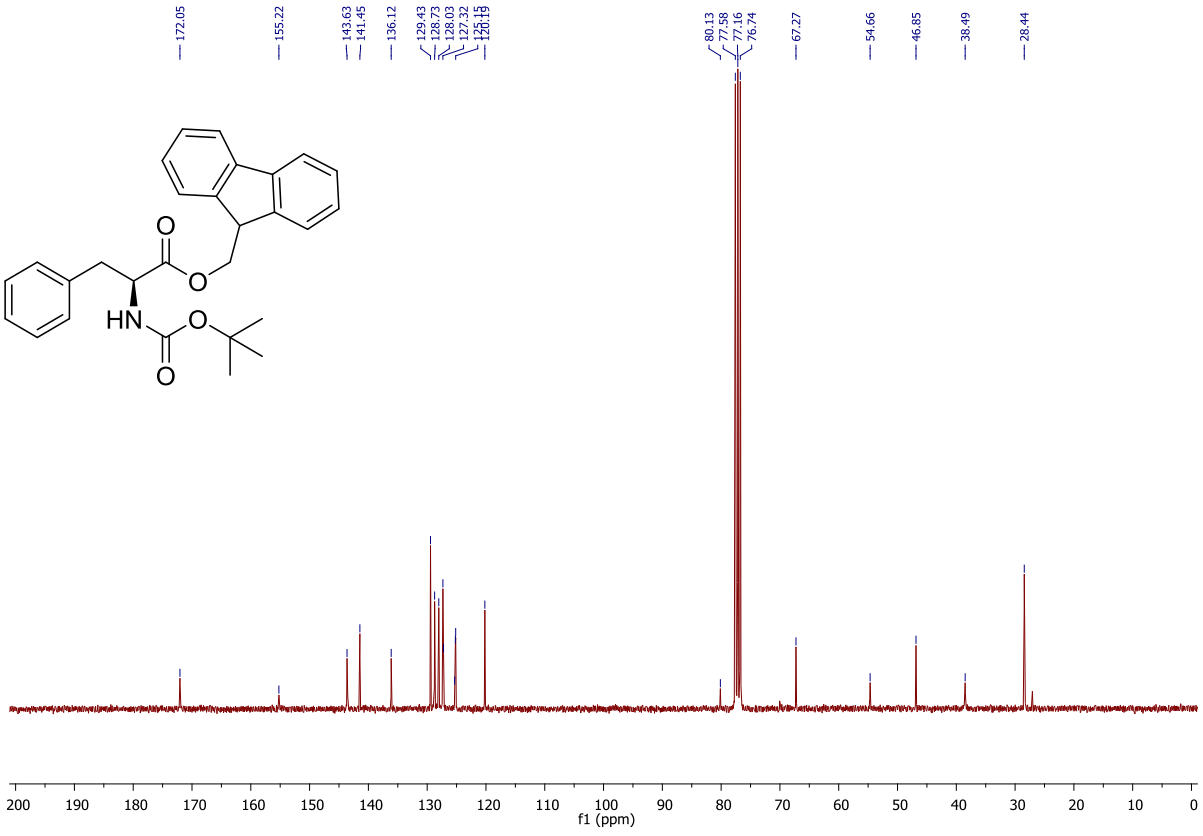

^{1}H, ^{13}C and ^{31}P-NMR spectra of (*S*)-*N*-((1*R*)-1-((3a*R*,8a*S*)-2,2-dimethyl-6-oxido-4,4,8,8-tetraphenylpentahydro-[1,3]dioxolo[4,5-e][1,2]oxaphosphepin-6-yl)-2-methylpropyl)-2-methylpropane-2-sulfinamide (10)

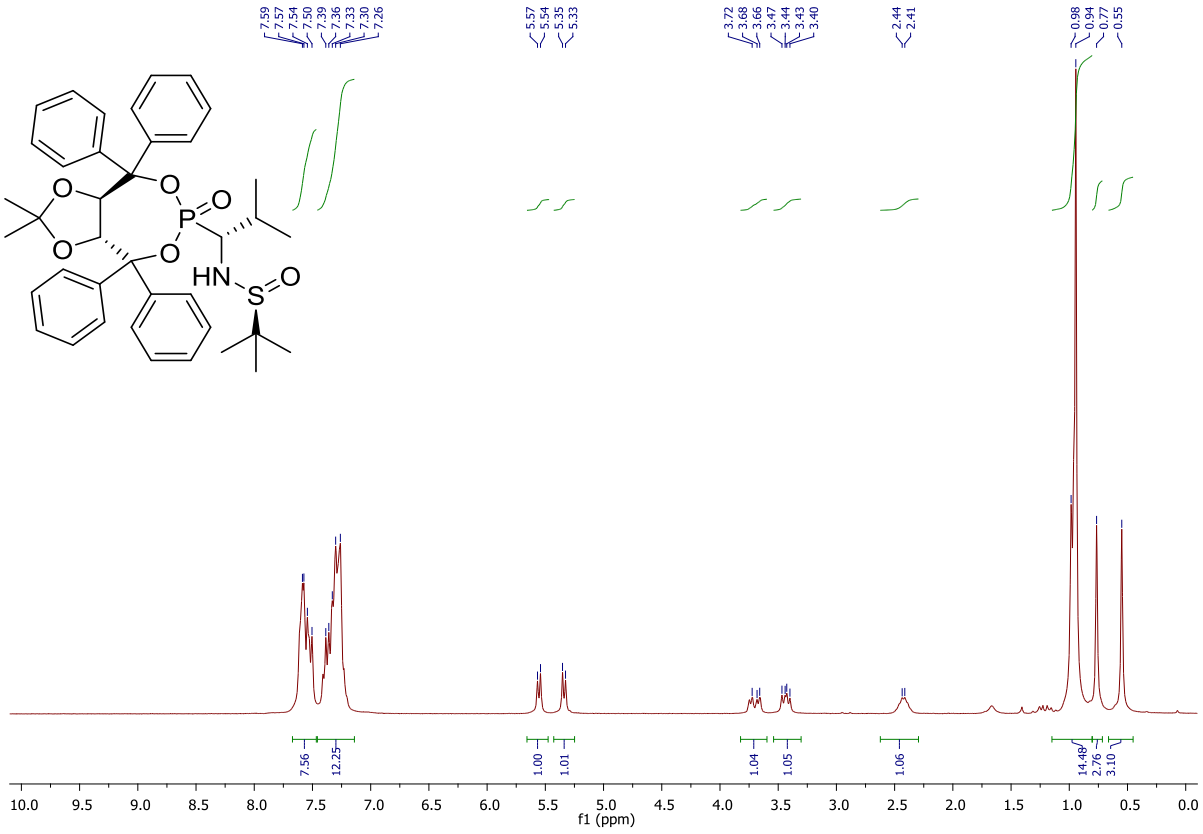

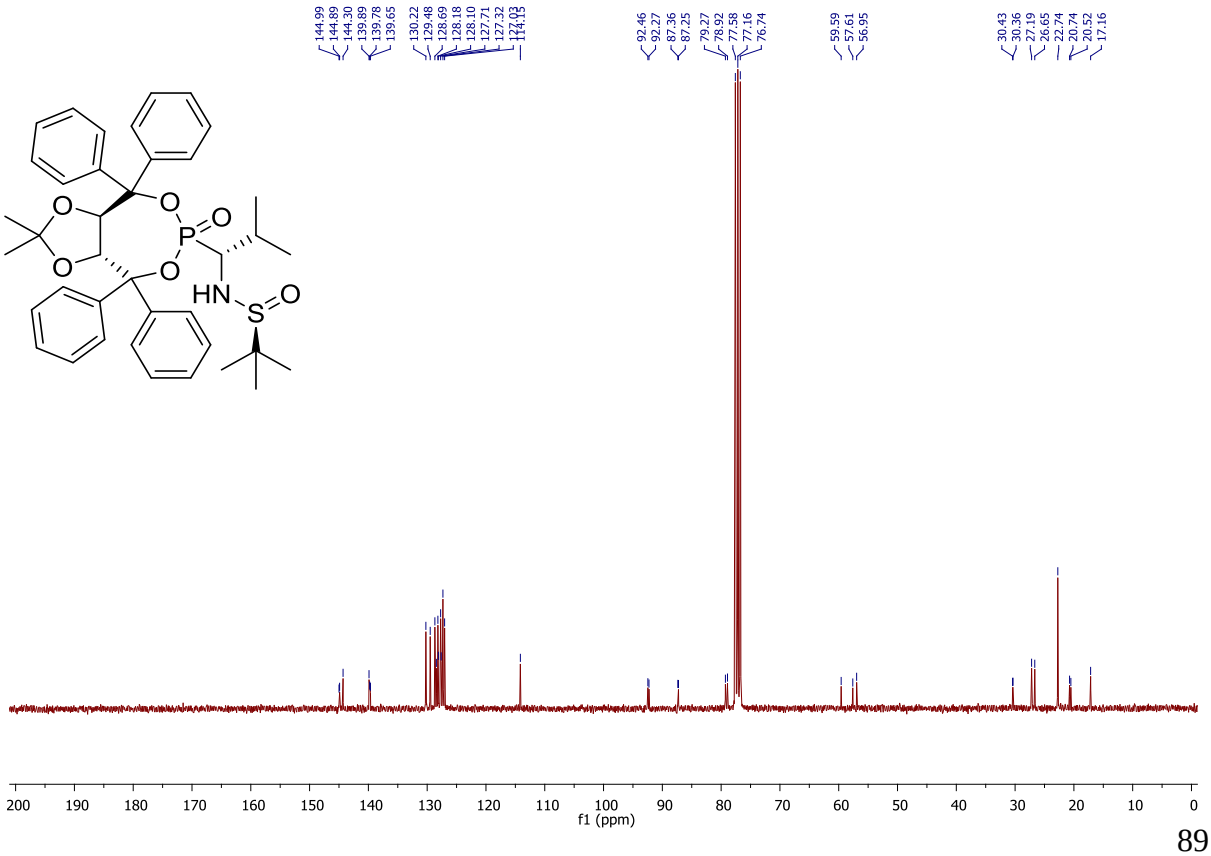

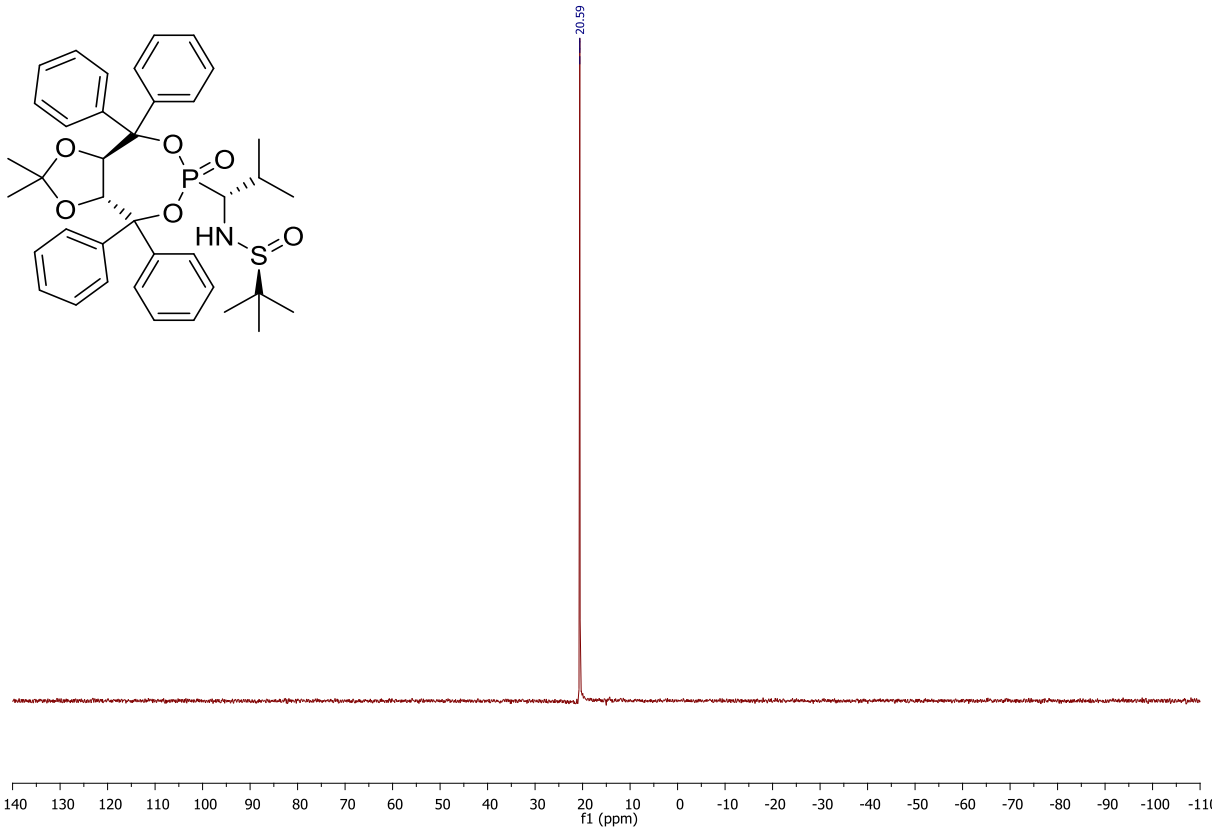
20.59
O
O
P
O
O
O
HN
S
O
140 130 120 110 100 90 80 70 60 50 40 30 20 10 0 -10 -20 -30 -40 -50 -60 -70 -80 -90 -100
f1 (ppm)

^{1}H, ^{13}C and ^{31}P-NMR spectra of (*R*)-1-amino-2-methylpropyl)phosphonic acid (11)

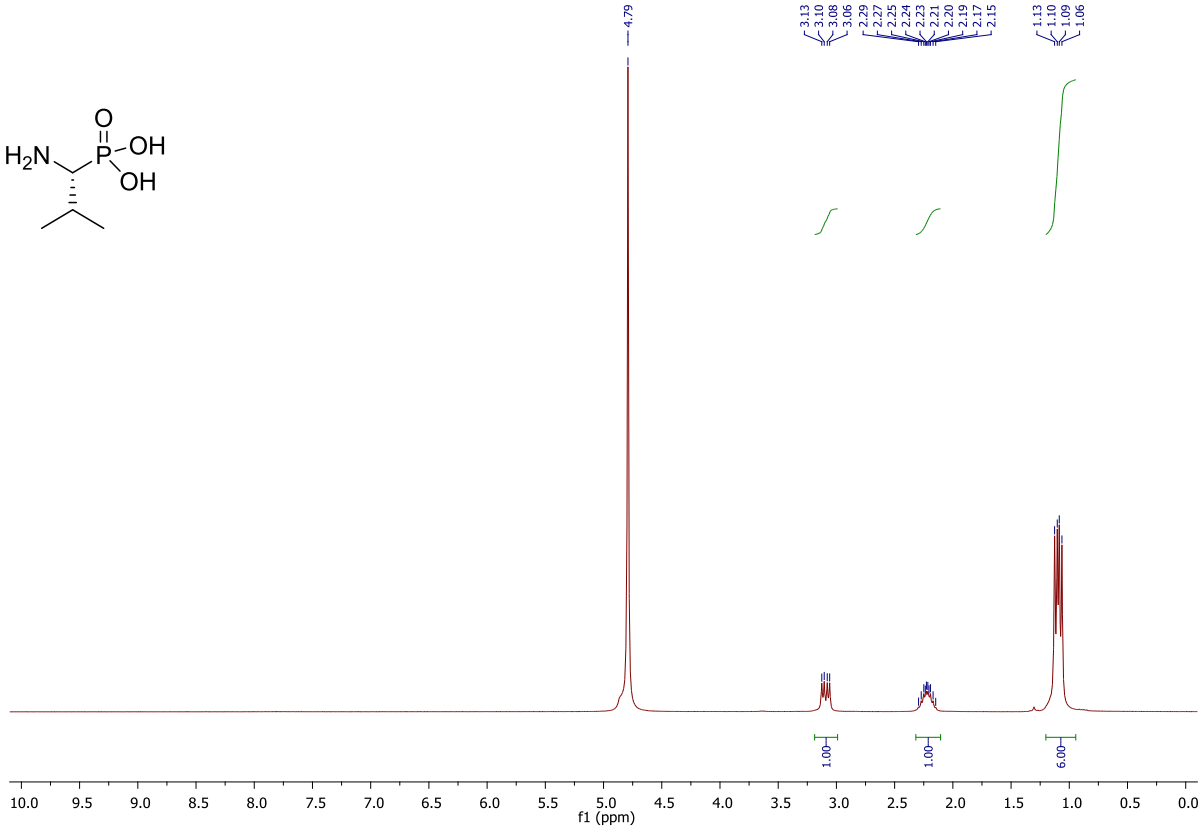

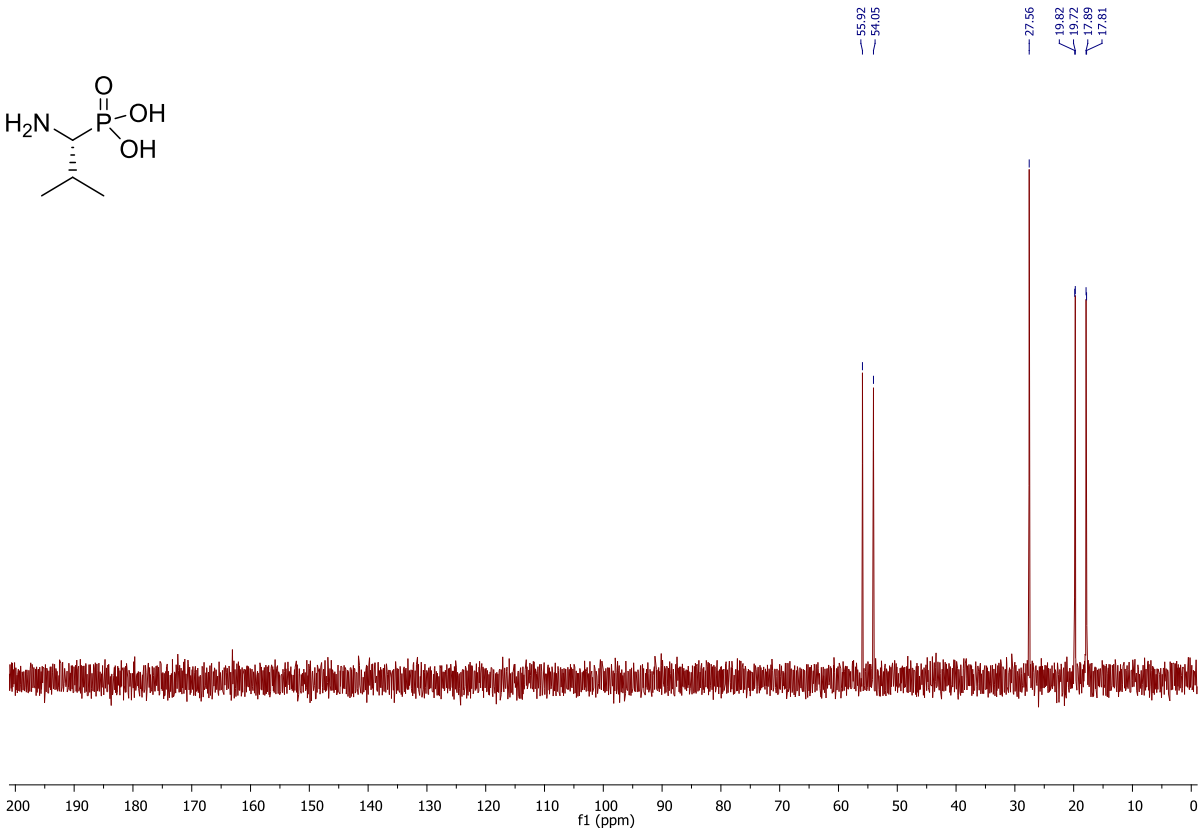

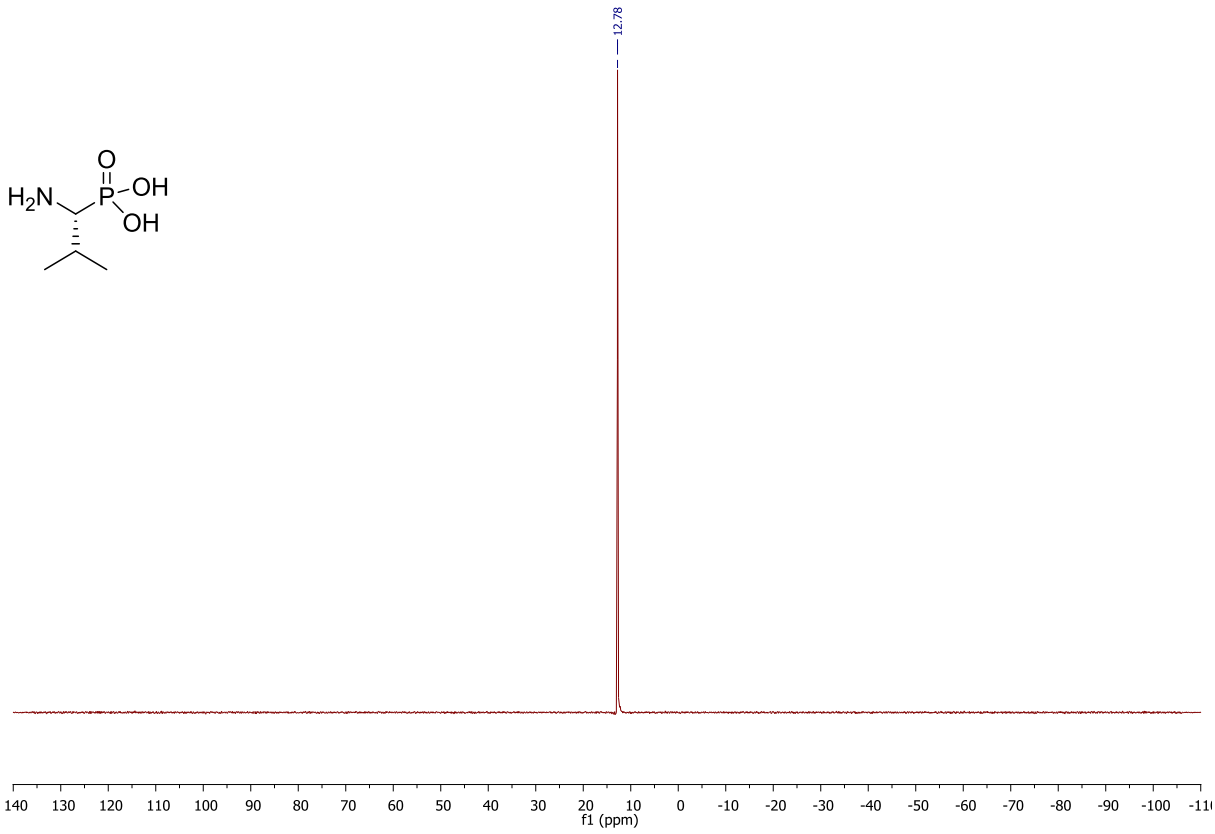
12.78
O
H2N
P
OH
OH
140 130 120 110 100 90 80 70 60 50 40 30 20 10 0 -10 -20 -30 -40 -50 -60 -70 -80 -90 -100
f1 (ppm)

^{1}H, ^{13}C and ^{31}P-NMR spectra of (*R*)-(1-(((benzyloxy)carbonyl)amino)-2-methylpropyl)phosphonic acid (12)

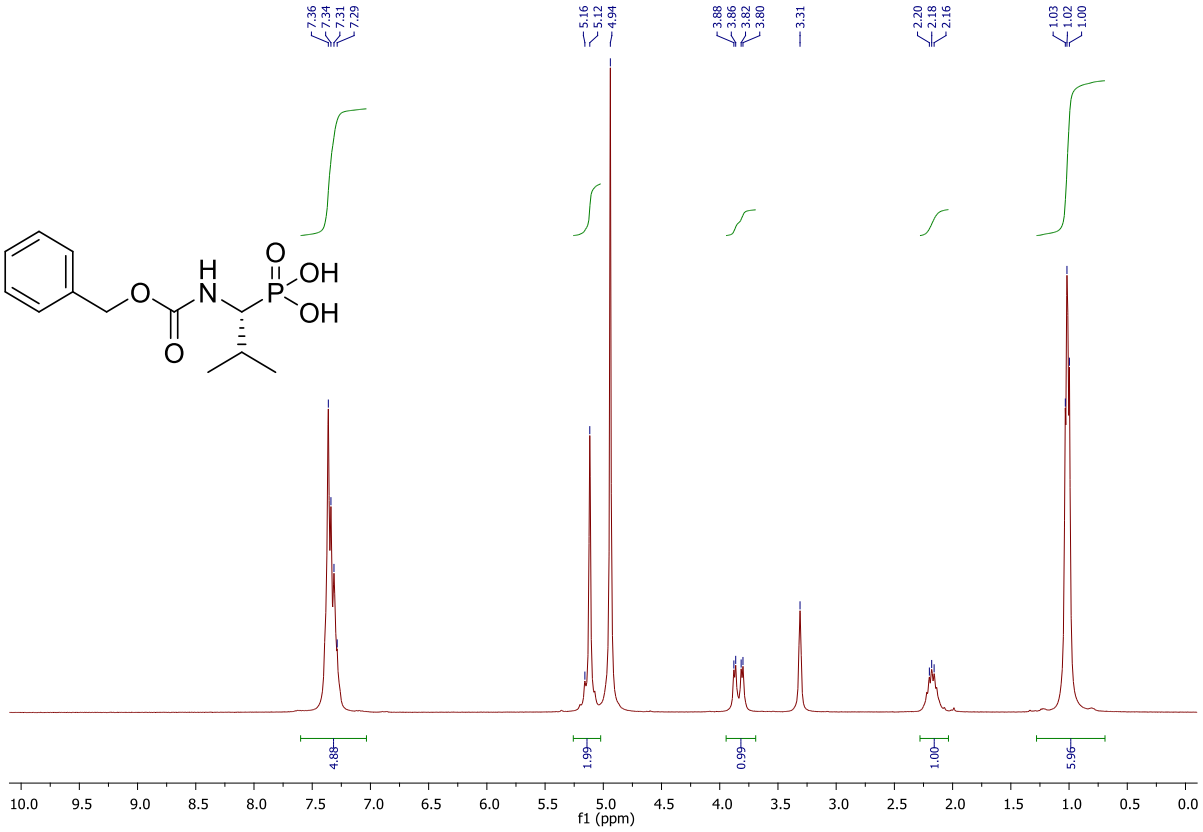

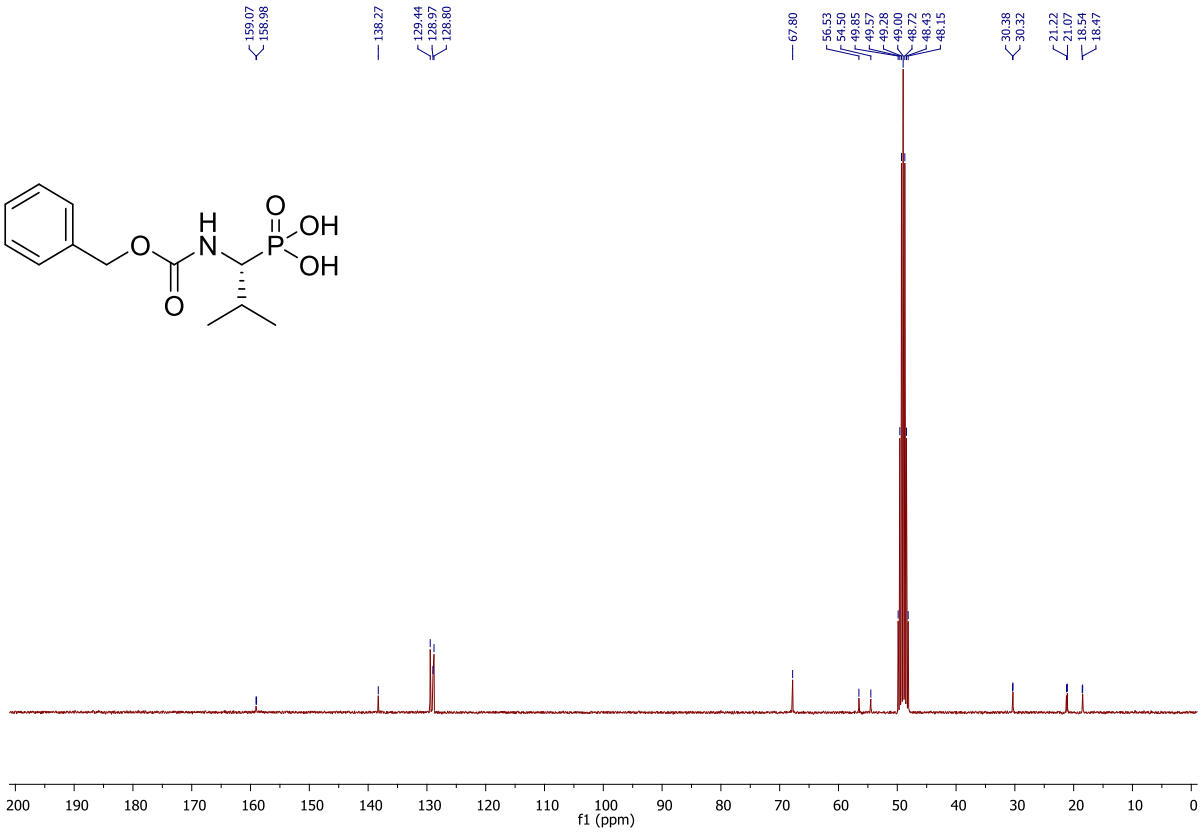

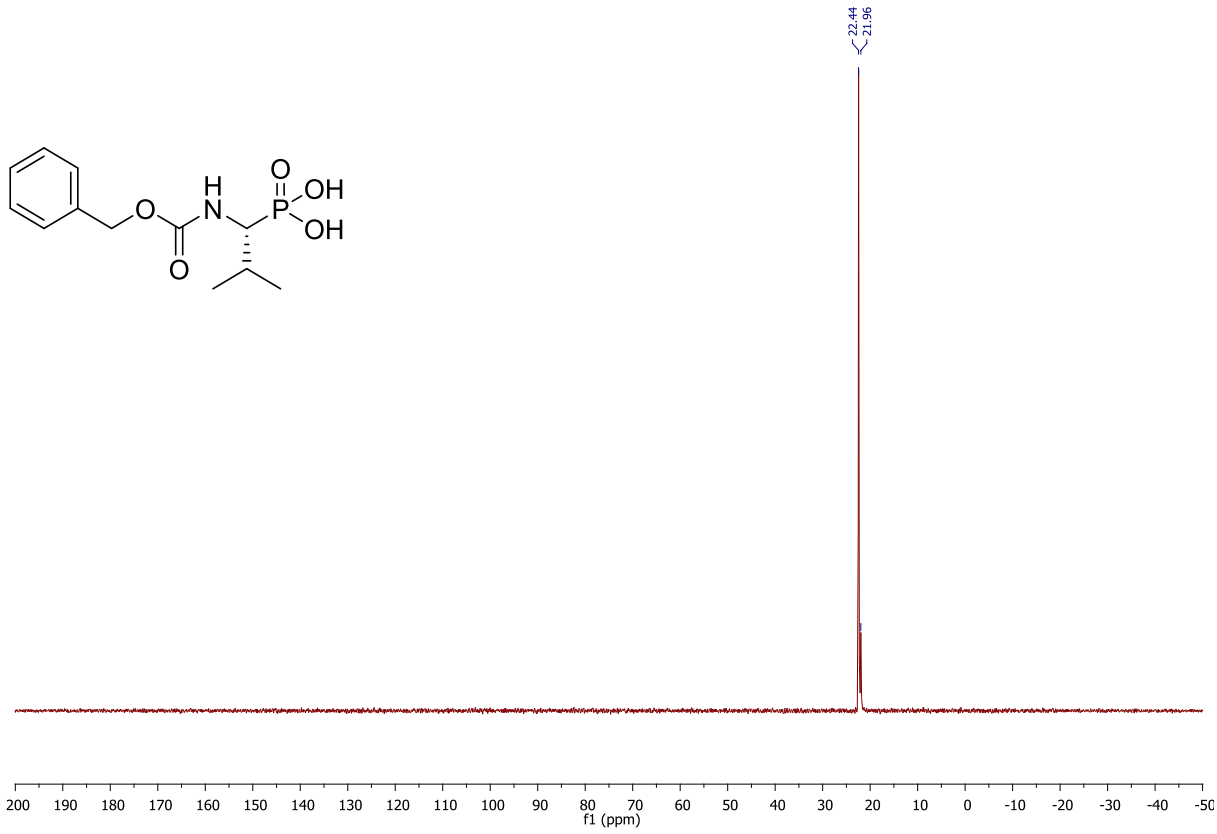
22.44
21.96
O
H
N
O
O
P
OH
OH
200 190 180 170 160 150 140 130 120 110 100 90 80 70 60 50 40 30 20 10 0 -10 -20 -30 -40 -50
f1 (ppm)

^{1}H, ^{13}C and ^{31}P-NMR spectra of benzyl ((1*R*)-1-((allyloxy)(hydroxy)phosphoryl)-2-methylpropyl)carbamate (13)

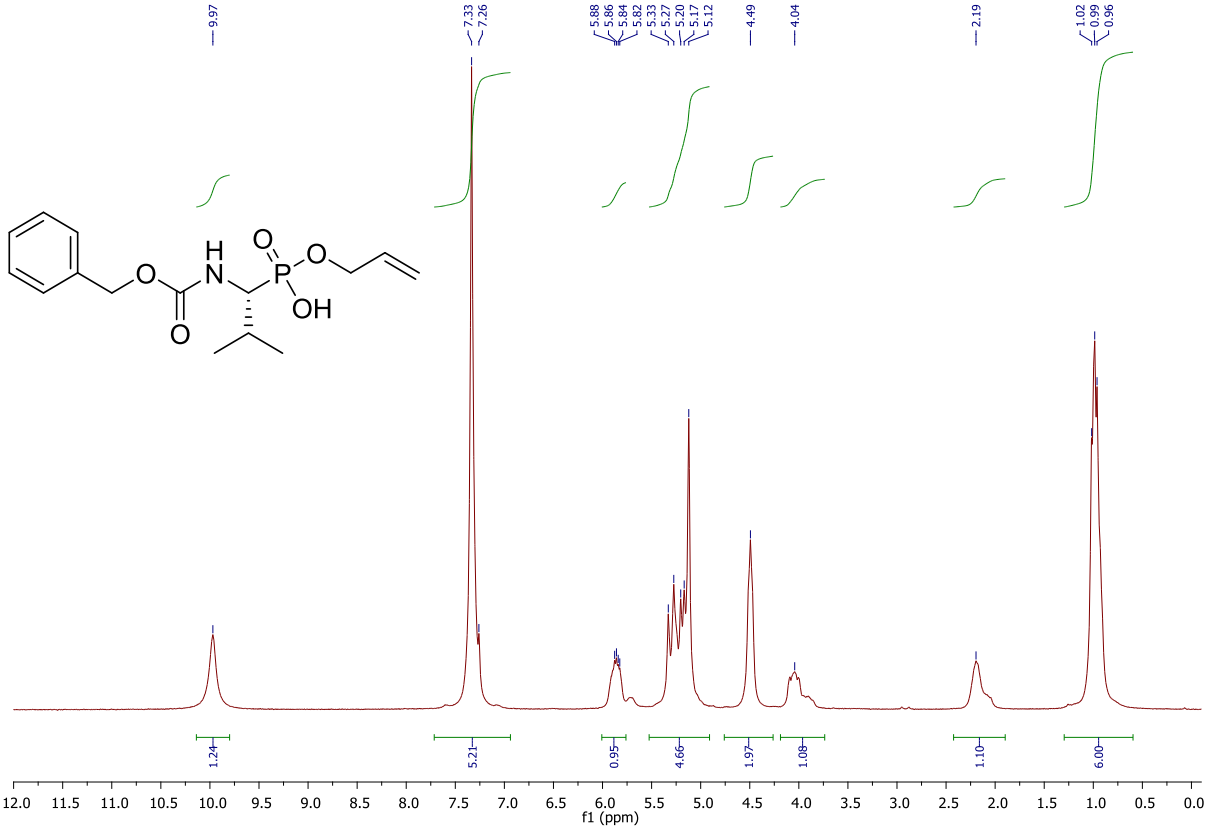

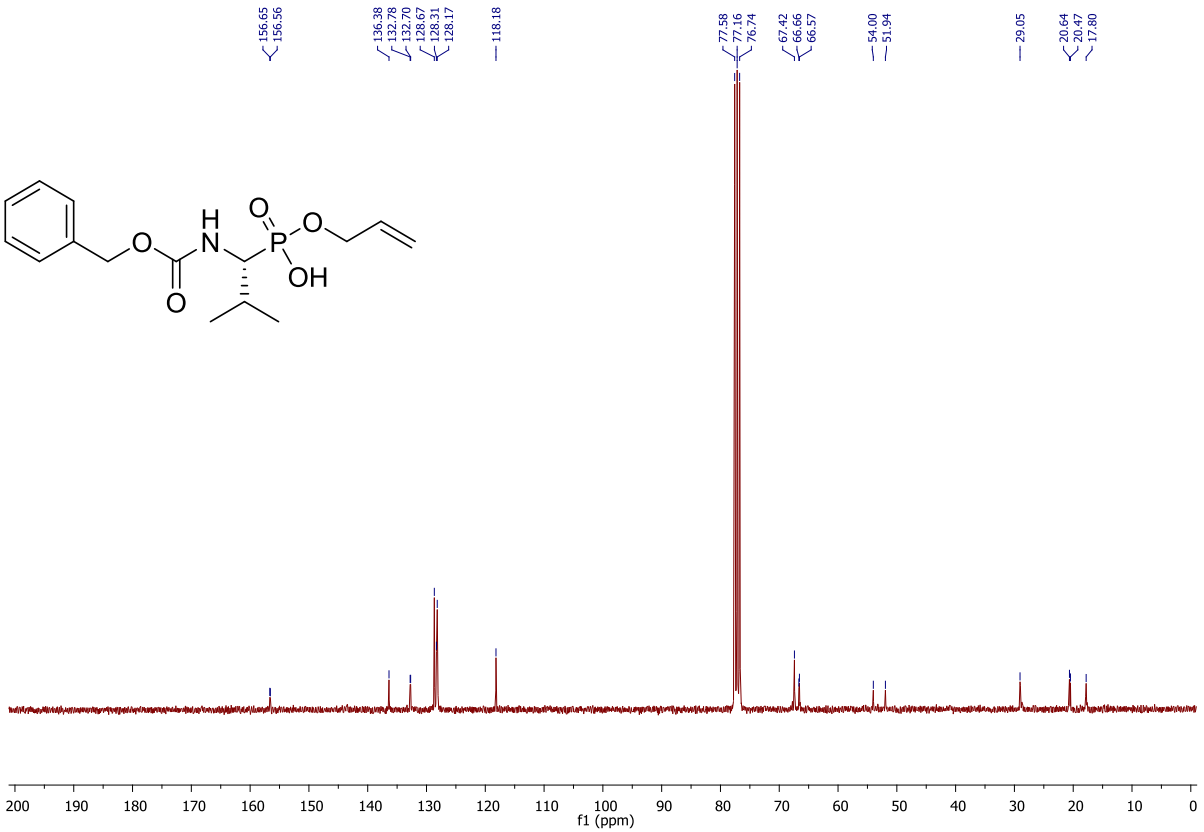

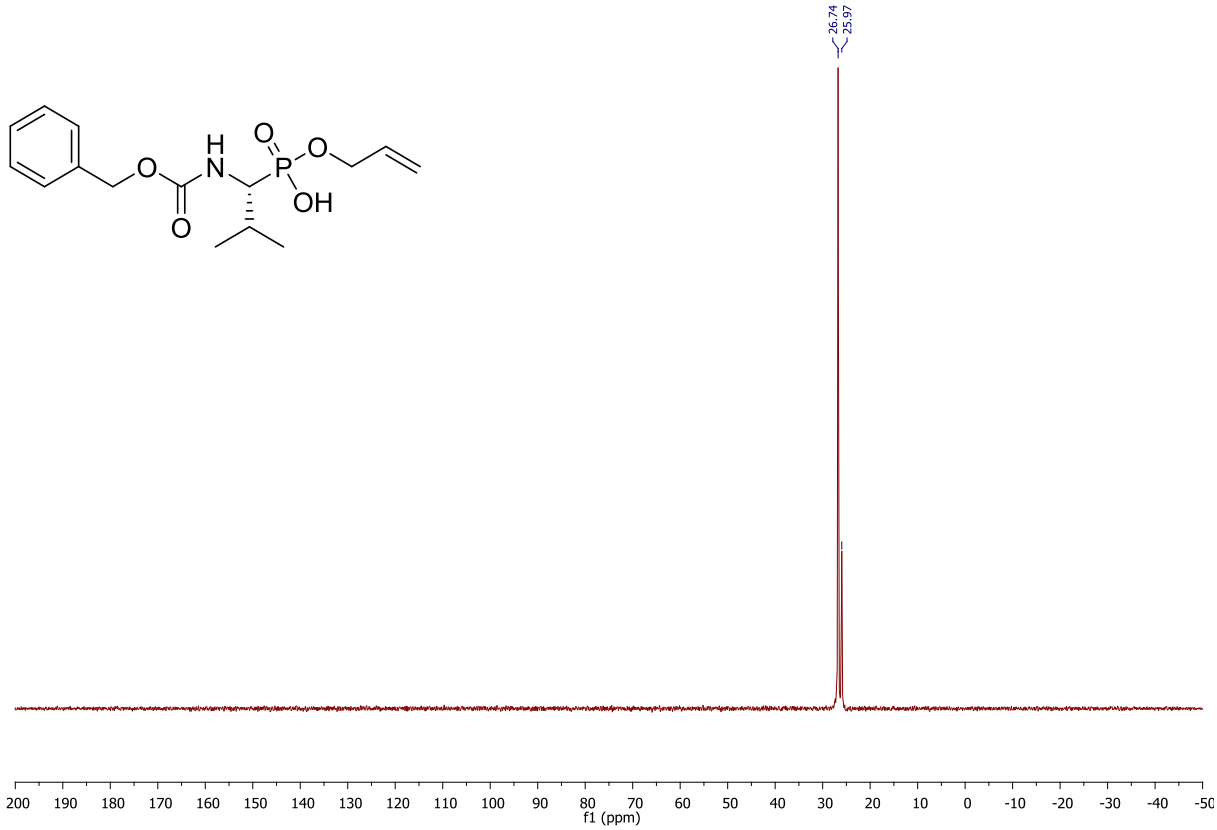
26.74
25.97
200 190 180 170 160 150 140 130 120 110 100 90 80 70 60 50 40 30 20 10 0 -10 -20 -30 -40 -50
f1 (ppm)

^{1}H, ^{13}C and ^{31}P-NMR spectra of methyl ((allyloxy)((*R*)-1-(((benzyloxy)carbonyl)amino)-2-methylpropyl)phosphoryl)-L-phenylalaninate (14)

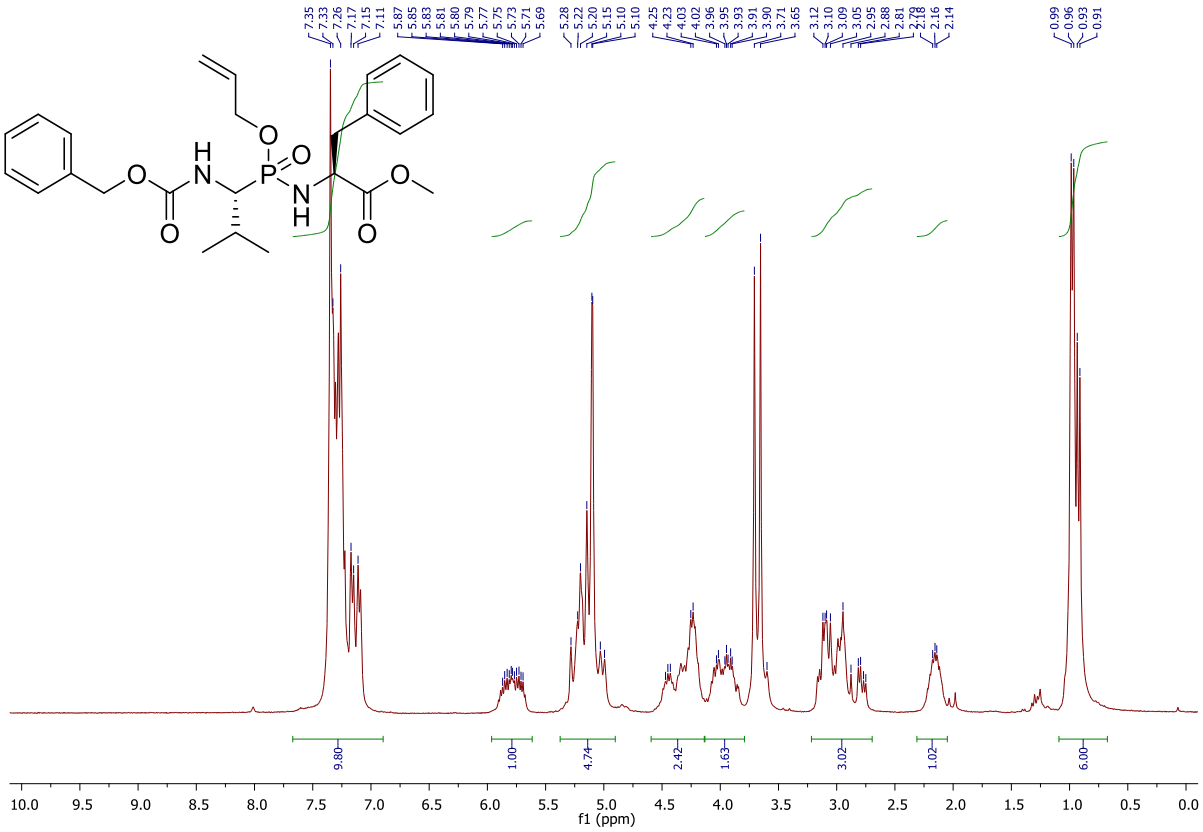

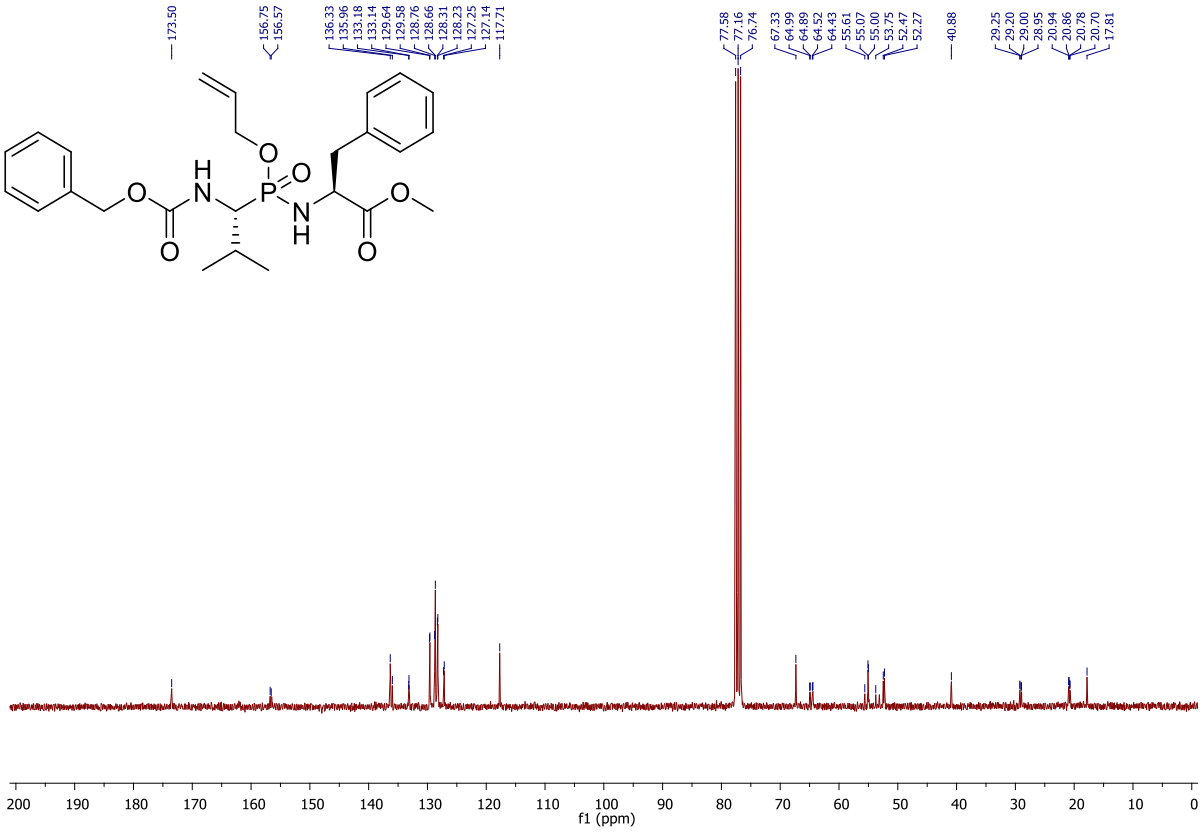

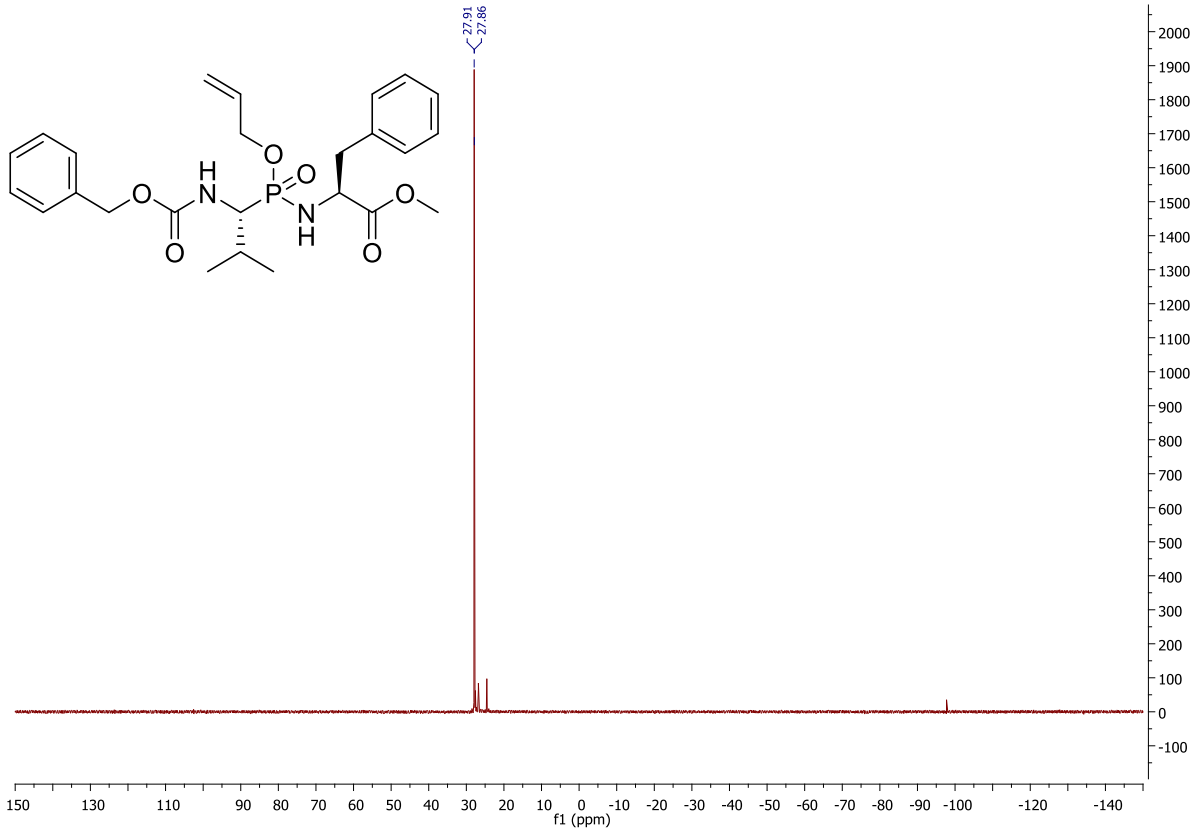
27.91
27.86
f1 (ppm)

^{1}H, ^{13}C and ^{31}P-NMR spectra of 2-(trimethylsilyl)ethyl ((allyloxy)((*R*)-1-(((benzyloxy)carbonyl)amino)-2-methylpropyl)phosphoryl)-L-phenylalaninate (15)

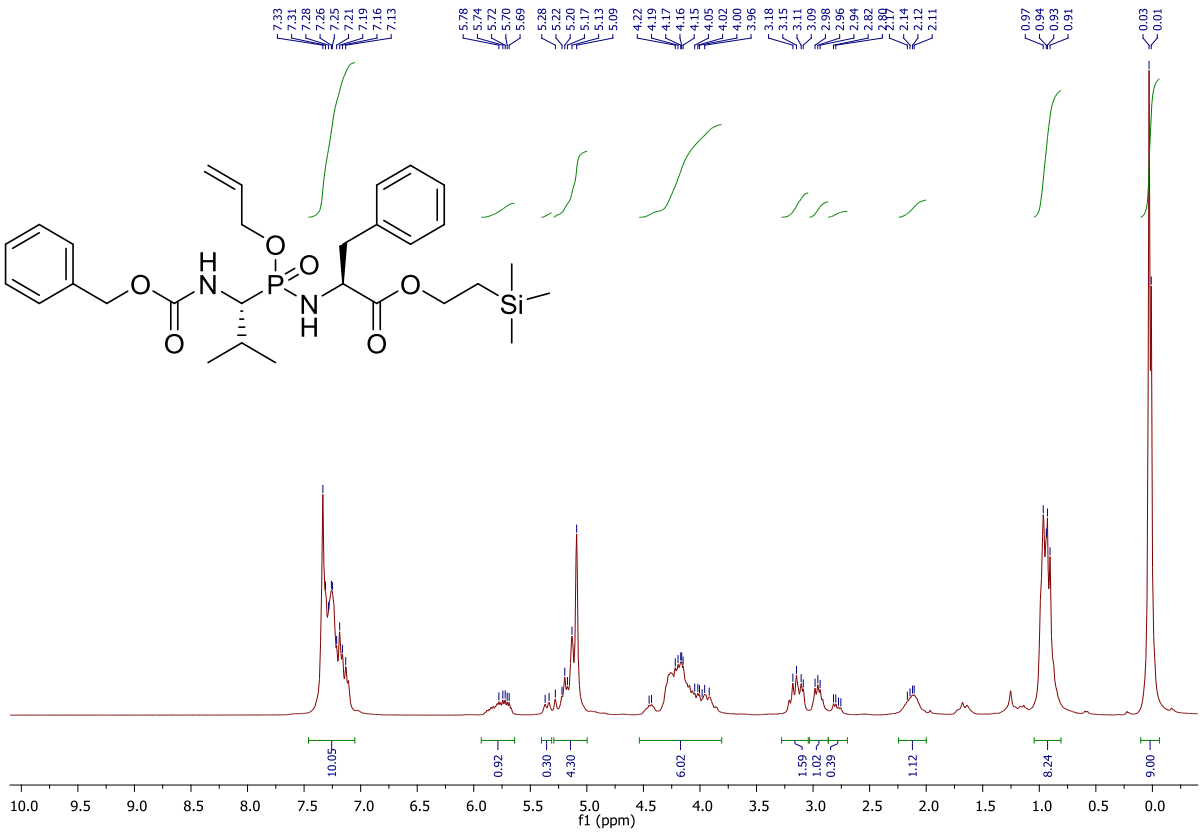

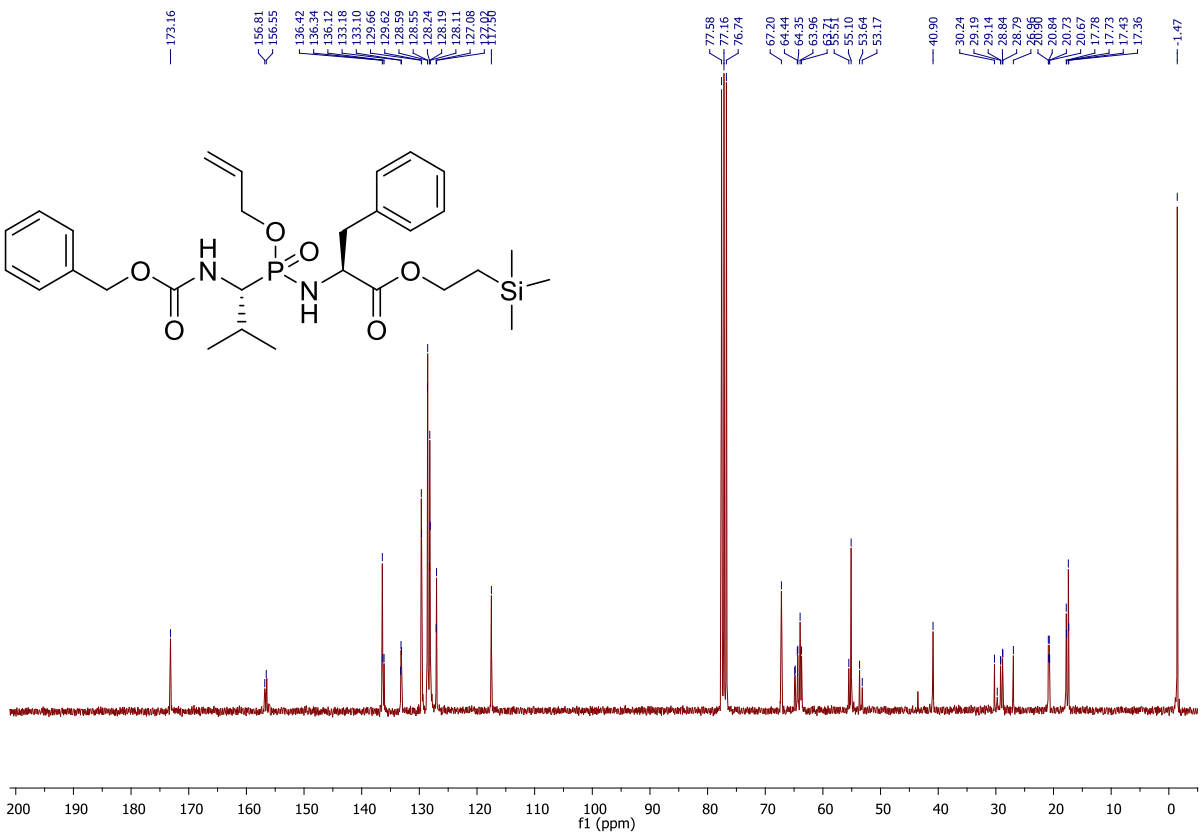

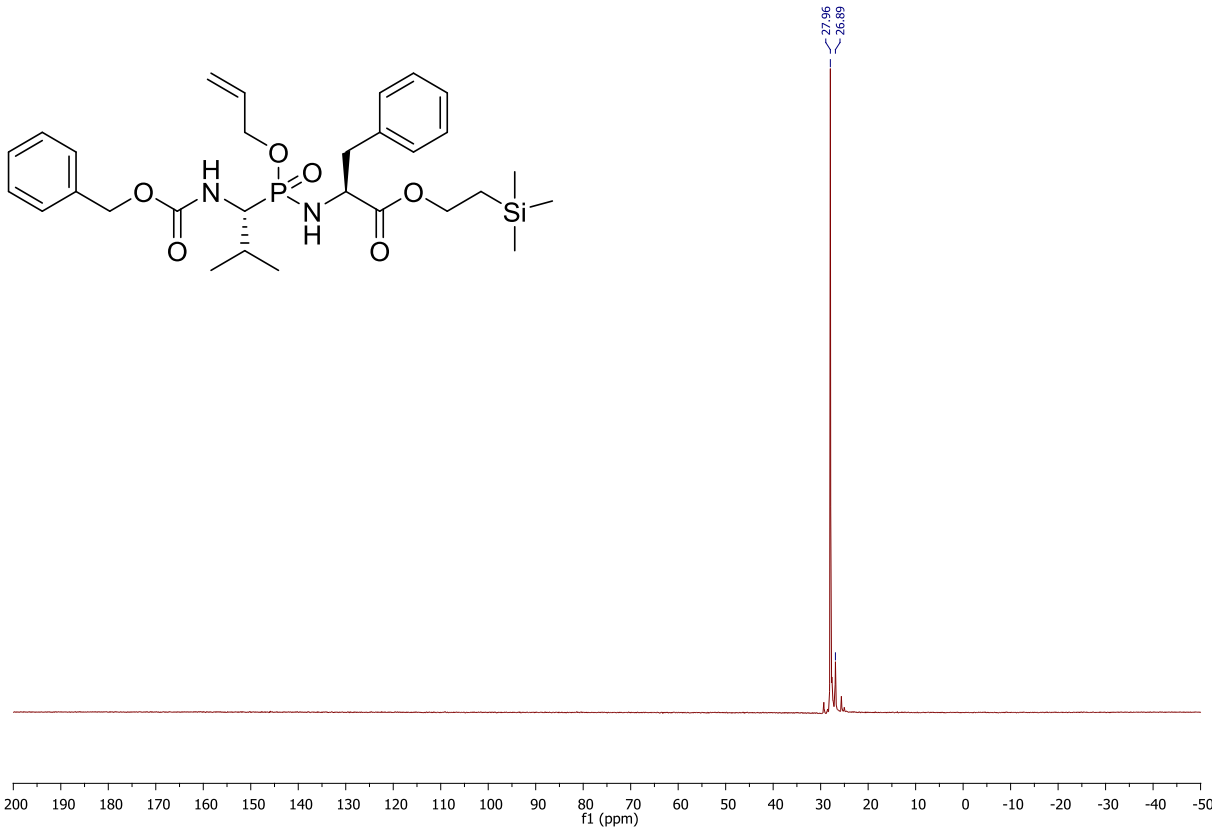
27.96
26.89
200 190 180 170 160 150 140 130 120 110 100 90 80 70 60 50 40 30 20 10 0 -10 -20 -30 -40 -50
f1 (ppm)

^{1}H and ^{13}C-NMR spectra of methyl (tert-butoxycarbonyl)-L-phenylalanyl-L-prolyl-L-tryptophanate (16)

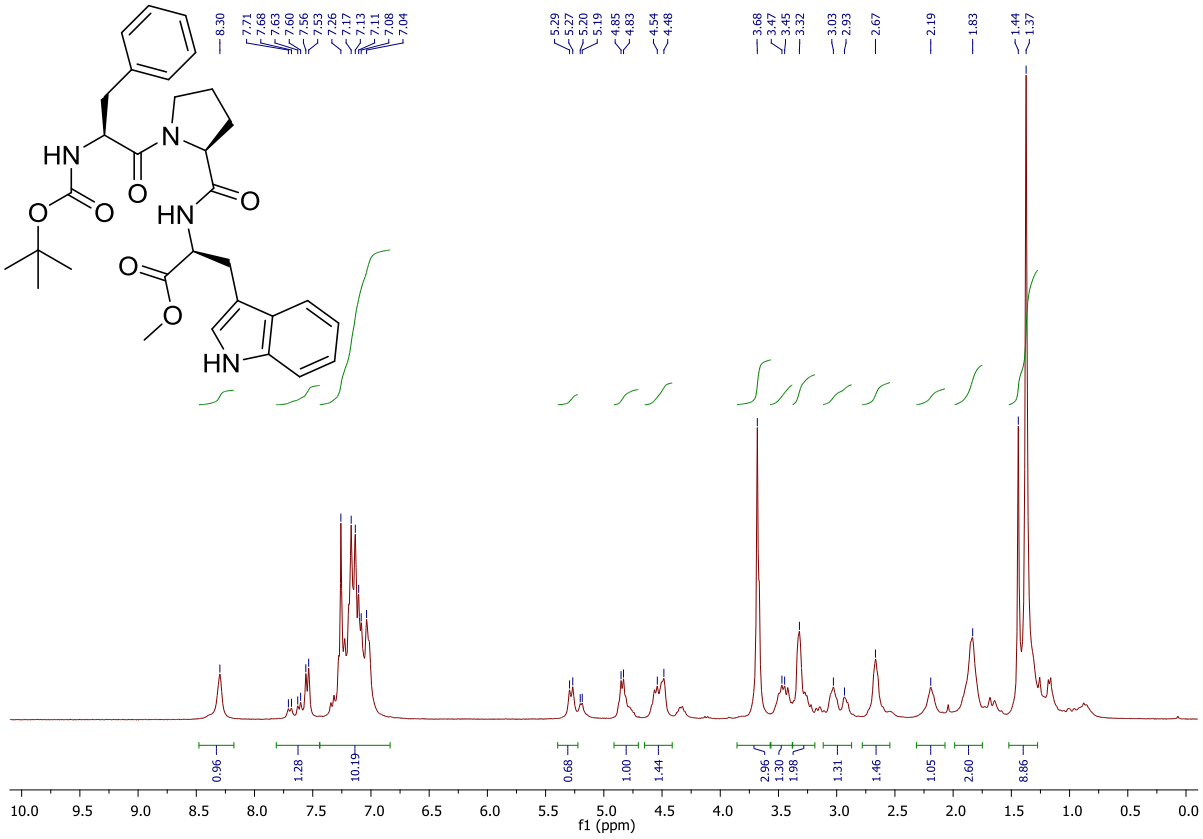

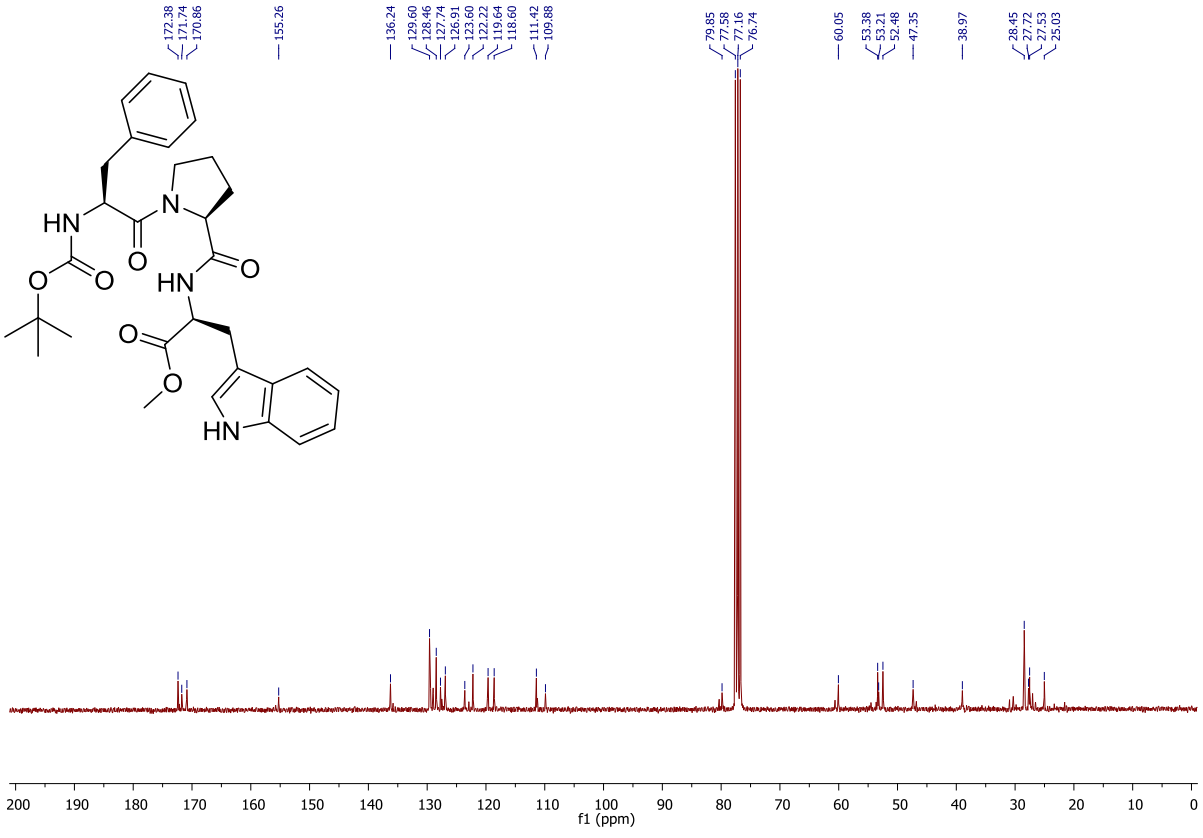

^{1}H, ^{13}C and ^{31}P-NMR spectra of methyl ((allyloxy)((*R*)-1(((benzyloxy)carbonyl)amino) 2-methylpropyl)phosphoryl)-L-phenylalanyl-L-prolyl-L-tryptophanate (17)

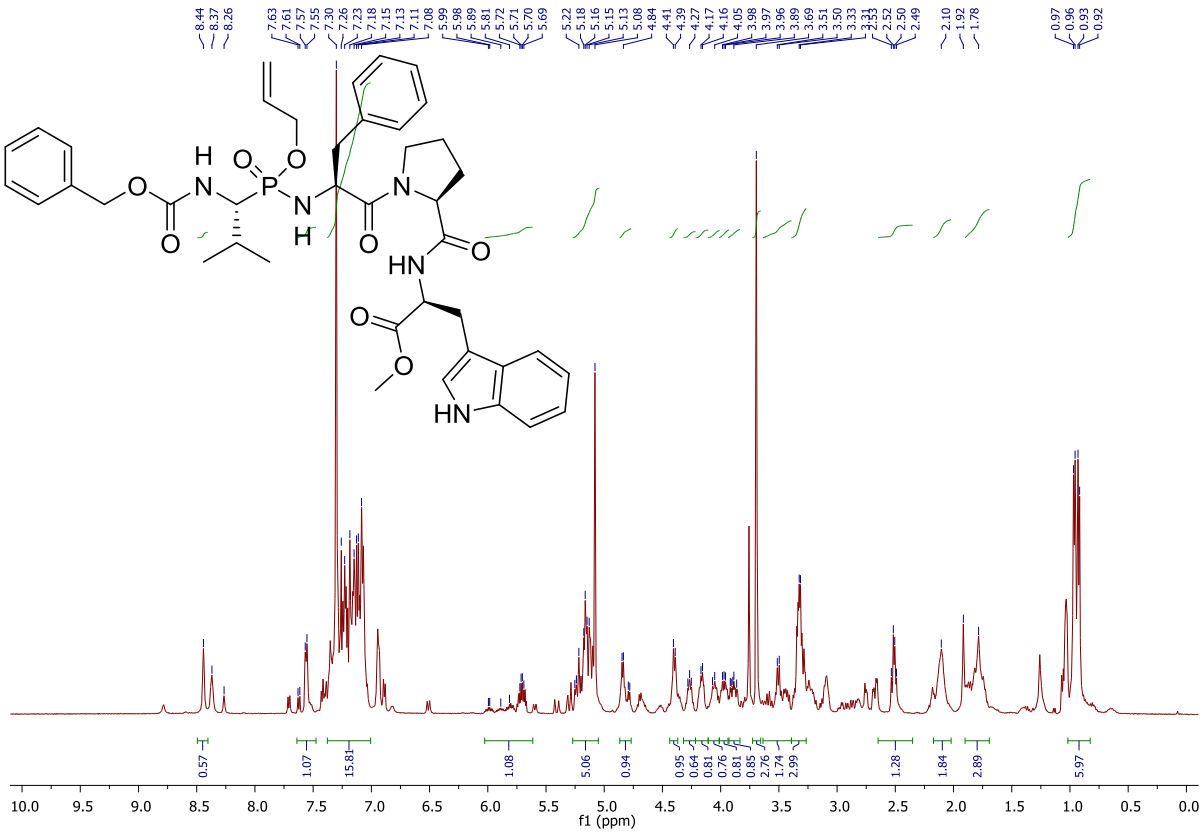

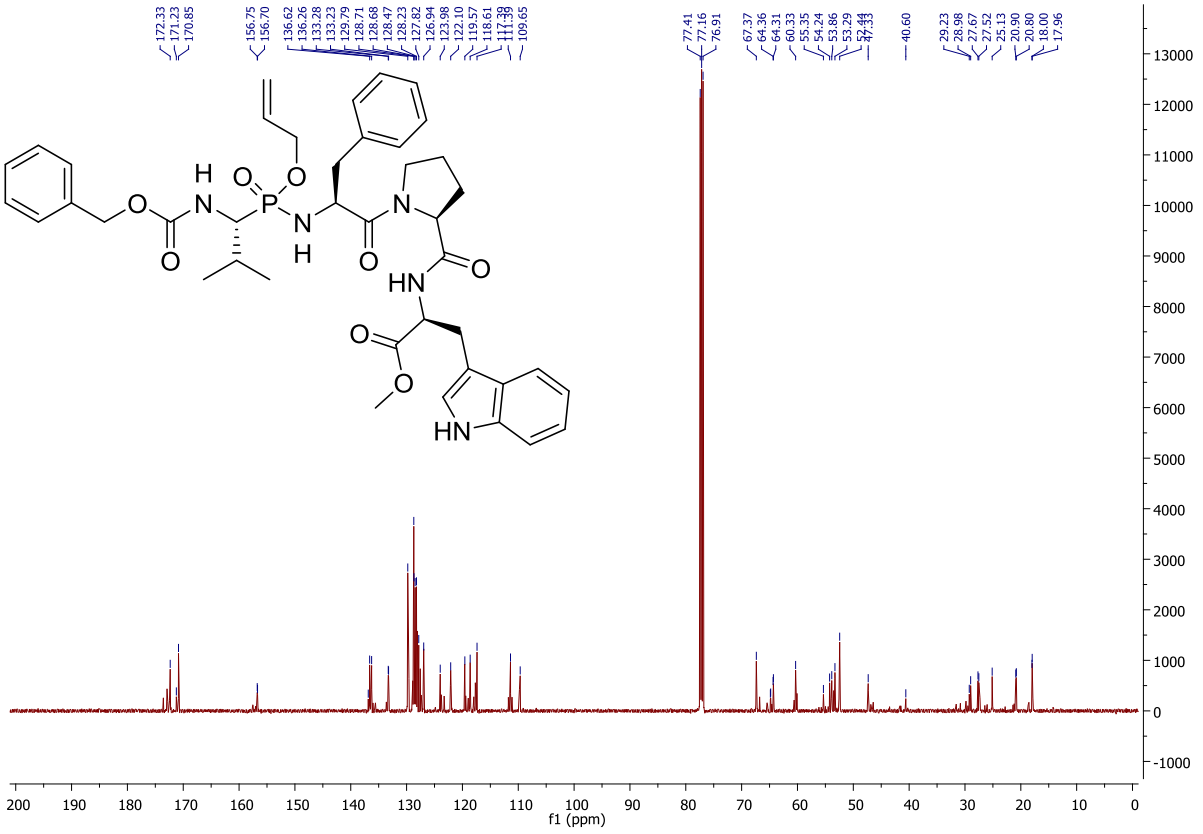

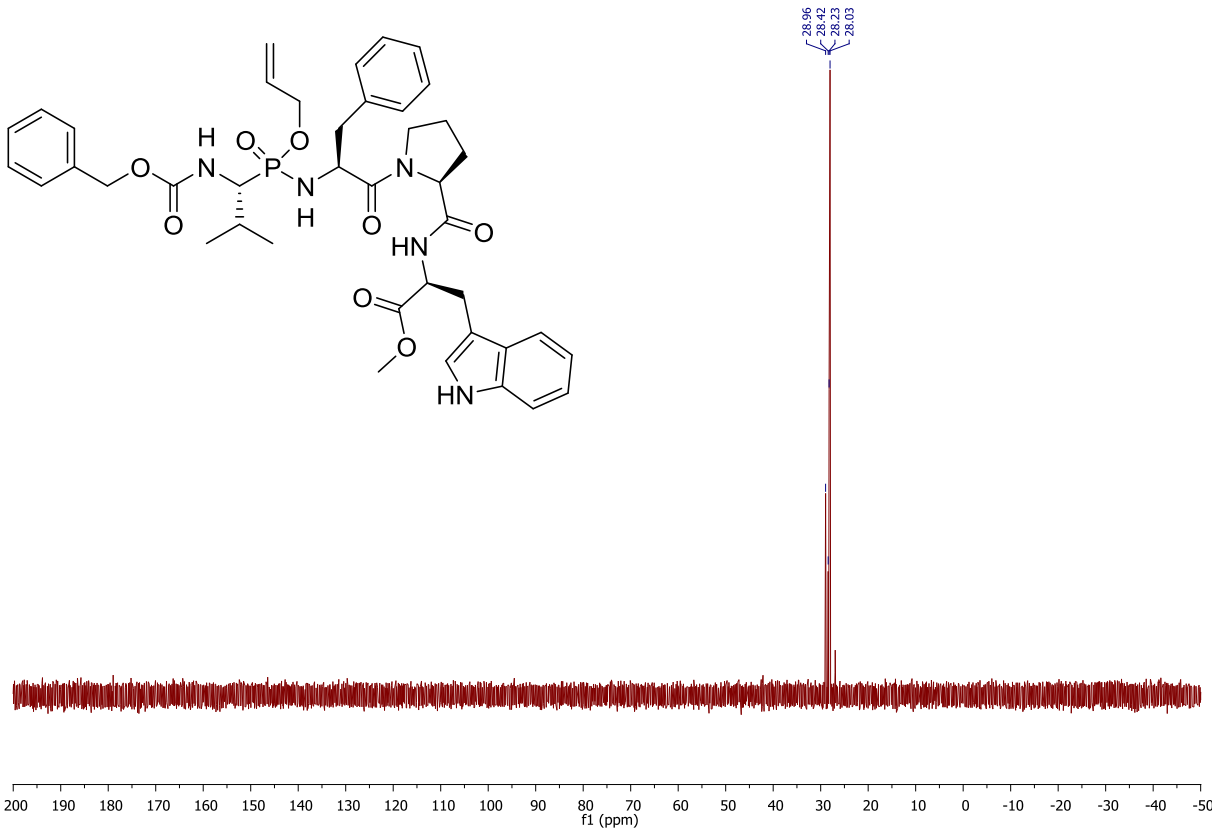
28.96
28.42
28.23
28.03
200 190 180 170 160 150 140 130 120 110 100 90 80 70 60 50 40 30 20 10 0 -10 -20 -30 -40 -50
f1 (ppm)

^{1}H, ^{13}C-NMR spectra of *P*-((*R*)-1-(((benzyloxy)carbonyl)amino)-2-methylpropyl)-*N*-((*S*)-1-oxo-3-phenyl-1-(2-(trimethylsilyl)ethoxy)propan-2-yl)phosphonamidate diethylammonium (18)

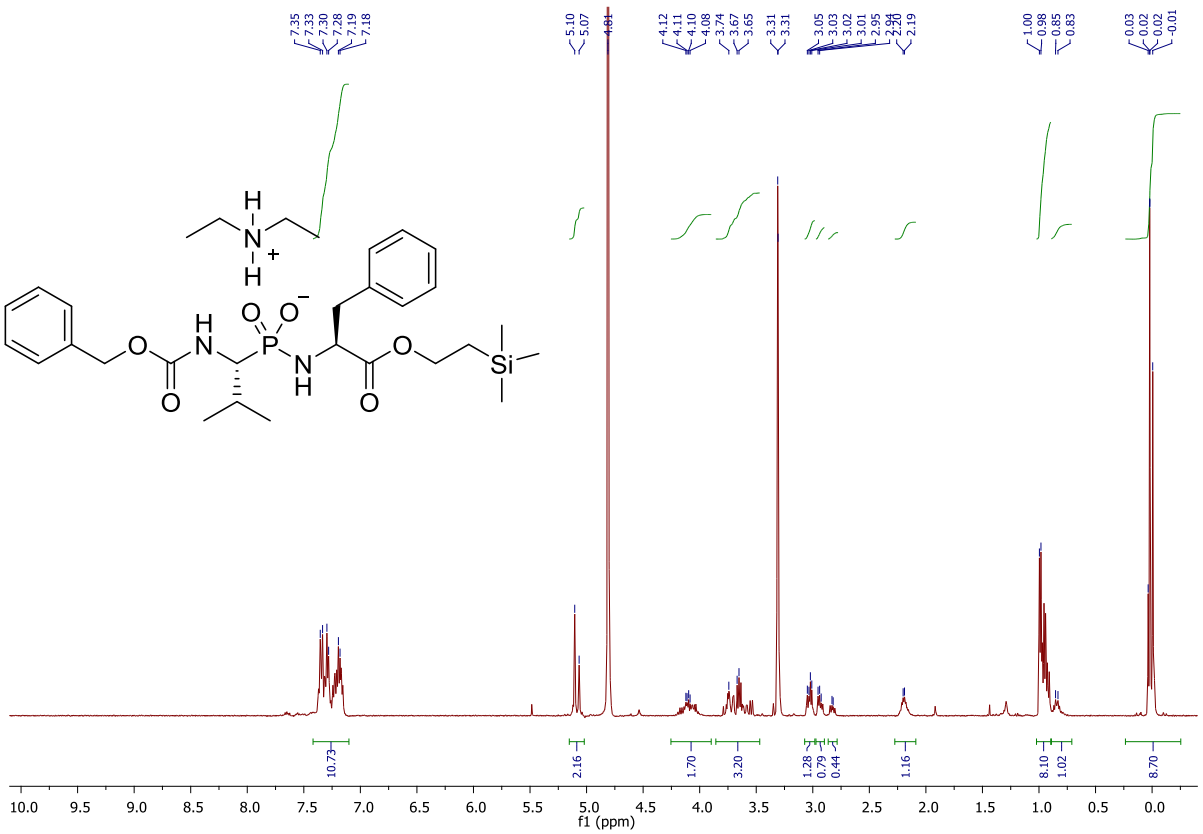

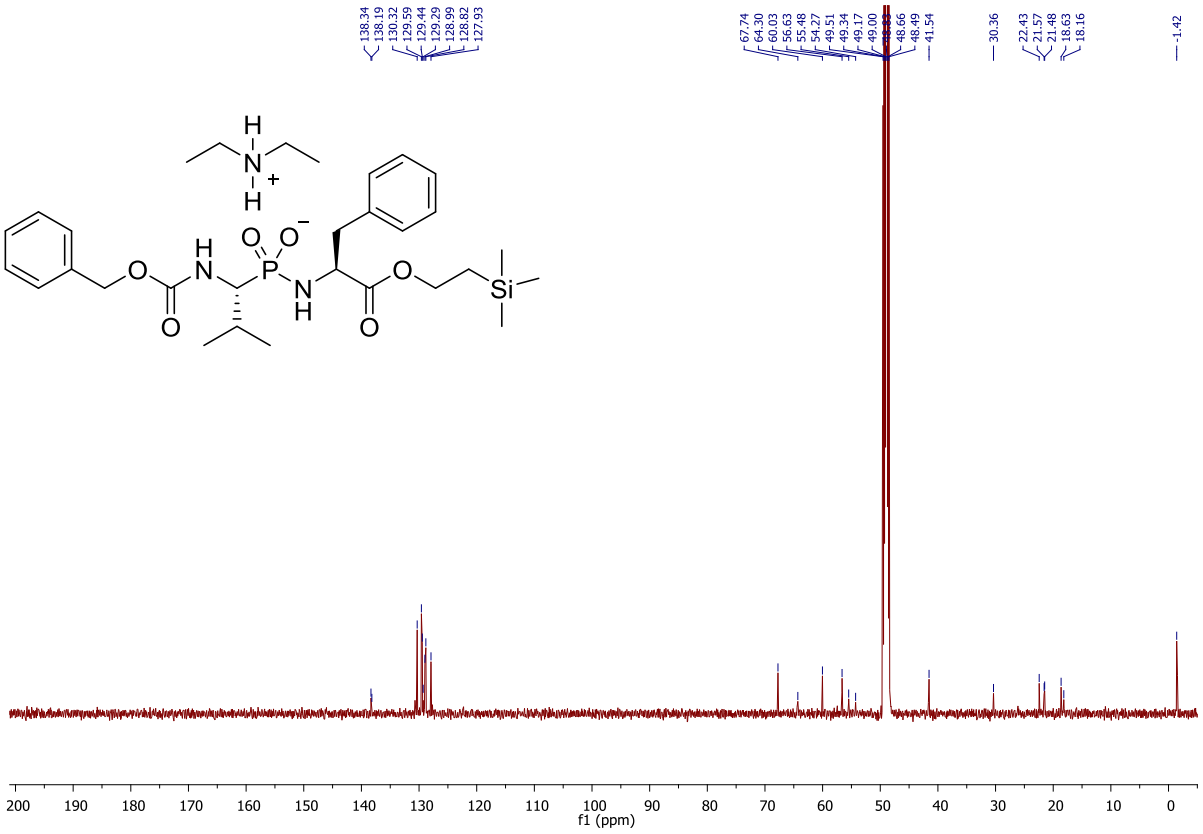

^{31}P and ^{29}Si-NMR spectra of *P*-((*R*)-1-(((benzyloxy)carbonyl)amino)-2-methylpropyl)-*N*-((*S*)-1-oxo-3-phenyl-1-(2-(trimethylsilyl)ethoxy)propan-2-yl)phosphonamidate diethylammonium (18)

^{31}P-NMR

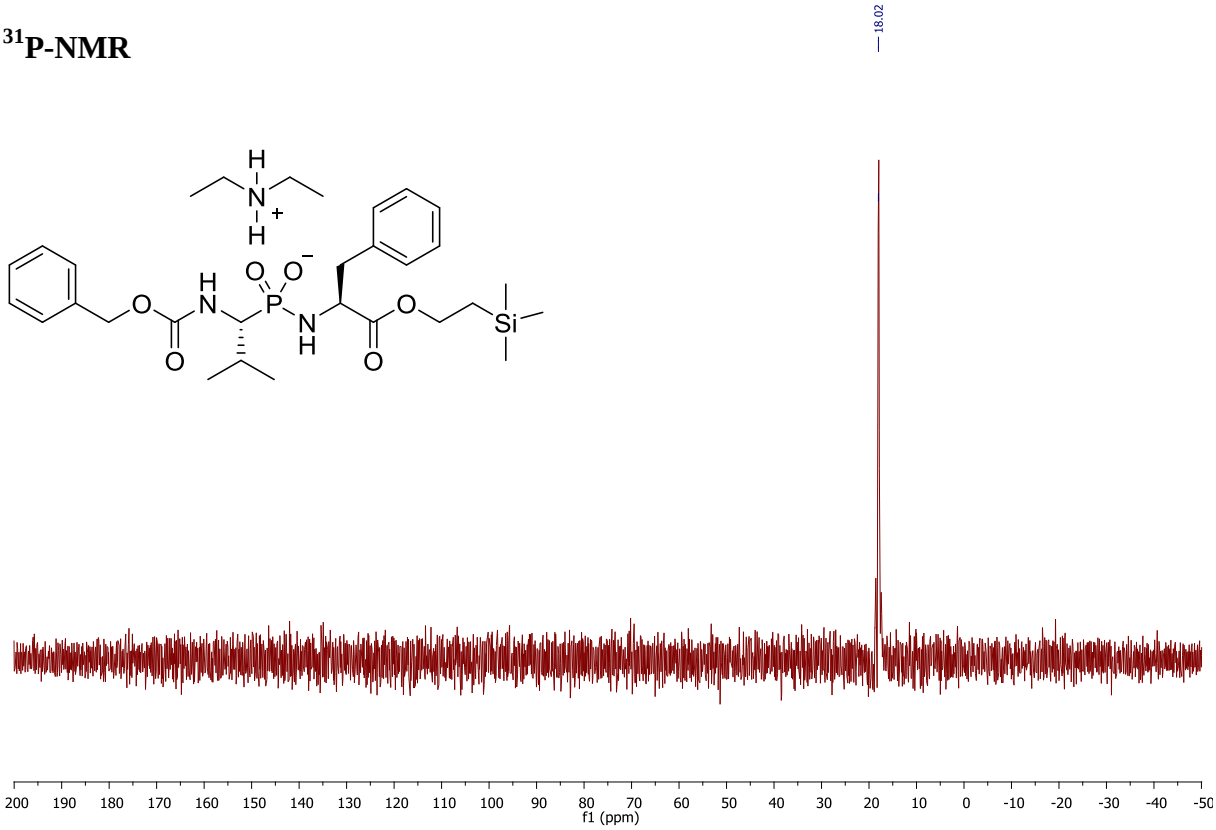

^{29}Si-NMR